الحمد لله رب العالمين

(كن في الدنيا كغريب أو كعابر سبيل) حديث

(احبب من شئت فإنك مفارقه، و عش ما شئت فإنك ميت) عبرة

(Be in this world like a stranger or as a passer by)

Haddith

(Whomever you love one day you'll leave. How long you live one day you'll die)

Proverb

To my mother, father, the rest of my family,
To my dear friends whom I lost in the war in Lebanon (Khodor, Fadi, Ibtisam and Abed), to Mawlana Al-Habashi and to Samar.

α-TUBULIN TYROSINATION AND ~~THE BEHAVIOUR OF~~ MICROTUBULES~~&~~ BEHAVIOUR *IN VITRO*.

A Thesis Submitted for the Degree

of Doctor of Philosophy

in the University of London

By

HAITHAM TALAAT IDRISS

Biophysics Section

Blackett Laboratory

Imperial College

University of London.

February 1990.

ABSTRACT

The α-tubulin subunit is modified post-translationally by the cyclic addition and removal of tyrosine at the C-terminus, through the action of the two enzymes :- the ATP requiring Tubulin Tyrosine Ligase (TTL), and Tubulin Tyrosine Carboxypeptidase (TTCP), respectively.

TTL has been purified from the brains of day-old chicks and characterised as having a m.wt. of about 43,000 and a Km of 27 μM and 8.7 μM for tyrosine and ATP respectively and has then been used to probe the possible function of tyrosination. The extent of chick brain tubulin has been experimentally increased by challenging with TTL, ATP and Tyrosine, or decreased by Carboxypeptidase A digestion.

Chick brain tubulin resolves into 8 α- and 12 β-tubulin isoforms, a number that cannot be accounted for by the expression of the multi-tubulin genes in the chick (6 α- and 7 β-tubulin genes), indicating that post-translational modifications are involved in generating some of the observed heterogeneity. All of the α-tubulin isoforms are substrates for TTL, indicating that the reported TTL tubulin non-substrate is not related to the tubulin primary sequence.

In vivo studies have demonstrated that detyrosinated microtubules are more stable than tyrosinated ones, whilst tyrosination has no apparent influence on the *in vitro* assembly kinetics of tubulin. The *in vitro* properties have been examined in greater detail by altering the level of tubulin tyrosination and monitoring the rate of length re-distribution of sheared microtubules. No effects on the length redistribution has been found indicating that tyrosination has no effect on the kinetic parameters governing dynamic instability indicating that tyrosination does not influence the kinetics of microtubule assembly *in vitro*.

The depressed lability of detyrosinated microtubules *in vivo* may be due to additional stabilising proteins. This has been examined by extracting proteins from the cold pellet and assaying their effects on nocodazole-induced disassembly of detyrosinated microtubules. These proteins, stabilised the microtubules, and this supports the possibility that detyrosinated microtubules might be stabilised by a capping protein preventing endwise disassembly of microtubules.

Acknowledgement

The writer of this thesis is greatly indebted and grateful for the patient supervision, support and guidance of Dr. Roy Burns who offered more than what was required of him as a Ph.D. supervisor. I would also like to thank Dr. Dave Stammers of the Wellcome Laboratories, for his help and support during the work at Beckenham. I am also grateful for the support and friendship of Dr. Colin McInnes during the earlier course of this work and also for that of Martyn Symmons *during the later course of this work. My thanks also go to all the members of the Biophysics section especially John Akins and Leslie Lloyd for their help and Bill Lieb for friendly company during those late hours of work in the section. I am also obliged to Mr. Nick Jackson for photographic work.*

My gratitude also goes to all the members of my family for providing me with moral and financial support especially in times when this was greatly needed.

Finally, I am indebted and shall be for the rest of my life for Mawlana Abdullah Al-Habashi, for teaching me at young age how to survive periods of enormous strain, grieve and pain.

This work has been supported by the Science and Engineering Research Council and the Wellcome Laboratories.

CONTENTS†

Contents (cont....)

† page numbers between [].

Table of Figures†

† page number betwwen [].

Table of Figures (cont...)

Table of Figures (cont...)

Table of Tables†

† page number between [].

Table of Tables (cont...)

Chapter 1

General Introduction

Maintainance of the structure and replication of eukaryotic cells depends largely on the preservation of their cytoskeleton: a fibrillar network consisting of three highly dynamic protein polymers termed microtubules, microfilaments and intermediate filaments. Elements of the cytoskeleton interact with each other and with other organelles to perform functions that vary from maintenance of cellular asymmetry to intracellular movement and the separation of chromosomes during mitosis[15].

Microtubules are a major component of the cytoskeleton, universally present in all eukaryotic cells. These hollow rod-like cylinders have a diameter of 25 nm and a wall that is 5 nm thick. Each microtubule usually has 13 protofilaments, each made of linearly arranged tubulin subunits[15]. Tubulin, is a heterodimer made of two subunits α- and β-tubulin. The β-tubulin subunit binds a GTP molecule, which is hydrolysed to GDP upon tubulin polymerisation[84]. Microtubules show both structural and kinetic polarity, resulting from the linear arrangement of the asymmetric tubulin molecules in the protofilaments[15], such that the assembly kinetics differ at the two ends, with one end [termed the plus (+) end] being more dynamic than the other [termed the minus (-) end][16]. Most microtubules, except those present in stable assemblies are highly labile, rapidly depolymerising when subjected to cold temperature, high pressure, in the presence of calcium ions or antimitotic drugs[15].

Microtubules can either be stable or dynamic *in vivo,* with the stable microtubules being present in structures such as cilia, flagella, and the complex cross-linked structures found in various protozoa. Cytoplasmic microtubules on the other hand, are generally highly dynamic, with half-times of about 10 min.[126,127]

Microtubules are not randomly organised in the cell, but are rather nucleated by and radiate from specialised structures termed microtubule organising centres (MTOC)[15,19,66]. These organising centres are discrete entities that are duplicated and transmitted to newly formed cells during mitosis[19]. In the cytoplasm of most cells the major MTOC is the centrosome, consisting of the centrioles and the surrounding pericentriolar material[19]. Most cells display a single centrosome near the nucleus which duplicates in the mid S-phase of the cell cycle[19], while in certain cells however, such as neuroblastoma N-115, multiple centrosomes have been identified[19].

A major property of centrosomes (and MTOCs in general) is their ability to nucleate microtubule growth both *in vitro* and *in vivo*[19,66]. Nucleation of microtubules *in vivo* has been demonstrated by regrowth of the microtubule network of cultured mammalian cells following drug induced depolymerisation. One characteristic of MTOCs is that this nucleation occurs at tubulin concentrations below the steady state critical concentration (Co), which will be defined later, with the (-) end being capped by the centrosome and the (+) end radiating away from it. In permeabilised 3T3 fibroblasts, centrosomes nucleate microtubule assembly at only 3 μM tubulin[19] and isolated centrosomes nucleate the assembly of 3-4 μM phosphocellulose purified tubulin, these values compare with an *in vitro* Co of 15 μM tubulin[95].

In addition to initiating microtubule growth, centrosomes also control the number of nucleated microtubules with a maximum of about 50 microtubules nucleated per centrosome at about 20 μM tubulin *in vitro*[95]. The centrosomes also stabilise anchored microtubules. Enucleated mammalian cytoplasts, whose microtubule network had been depolymerised by nocodazole, only regrew few microtubules when centrosomes were absent in the presence of moderate concentrations of nocodazole. By contrast an extensive array of microtubules was observed when centrosomes were present that was stable against moderate nocodazole concentrations[59].

Although the centrosome is the major MTOC in the cytoplasm, several other structures, such as basal bodies and kinetochores, are capable of nucleating microtubules *in vitro and in vivo*. Some of these MTOCs possess unique properties. For instance, the kinetochore is able to capture the (+) end of a microtubule radiating from centrosomes, as well as nucleating microtubule growth. Centrosomal microtubules capped by a kinetochore at their (+) end, a situation similar to that of kinetochore microtubules in the metaphase spindle, have been shown to be stable against dilution induced disassembly[93]. However, contradictory results were obtained when microtubules were nucleated by a stable cross-linked microtubule seed. Such microtubules, capped at their plus ends with kinetochores, were seen to depolymerise upon dilution[93].

Kinetics of Microtubule Assembly *In Vitro*:

Microtubule assembly can be monitored *in vitro* by following increase in turbidity at 350 nm since microtubules are rod-like structures that scatter light[47]. After warming up a tubulin solution to 37 °C, there is a lag preceding the increase turbidity[64]. This lag phase is due to the formation of microtubule nuclei onto which further addition of subunits can take place and this nucleation event is the rate limiting step in the polymerisation process. The nucleation reaction can be eliminated by addition of pre-formed microtubules that have been sheared to act as microtubule seeds[64].

Tubulin adds onto the ends of pre-formed microtubules following a condensation polymerisation mechanism according to the following equation[64]:

$$S + M \underset{k_{-1}}{\overset{k_{+1}}{\rightleftharpoons}} M$$

According to the above equation tubulin of concentration [S] adds onto the ends of microtubules of number concentration [M] in a forward reaction with an association rate constant k_{+1} and are lost from microtubule ends in a reverse reaction with a dissociation rate constant of k_{-1}. The forward reaction has been analysed in terms of pseudo-first order kinetics whilst the reverse reaction fits first order kinetics. As the net rate of polymerisation equals the rate of the forward reaction minus that of the reverse one, the overall rate of tubulin assembly can be described in terms of the following equation:

$$-d[S]/d[t] = k_{+1}[M][S] - k_{-1}[M] \qquad (1)$$

Subunit addition onto the ends of microtubules continues until the rate of the forward reaction equals that of the reverse reaction and the microtubules are said to have attained a steady state. At steady state therefore, equation (1) becomes:

$$k_{+1}[M][S] = k_{-1}[M]$$

and so a free tubulin concentration remains which is called the critical concentration or Co; and which equals the ratio of dissociation to the association rate constants[64,151]:

$$[S] = k_{-1}/k_{+1} = Co$$

Equation (1) can be re-written as:

$$-d[S]/dt = k_{+1}[M][S] - Co\ (k_{+1})[M]$$

$$= k_{+1}[M]\ ([S] - Co)$$

and therefore, a plot of the instantaneous rate of microtubule assembly against ([S]–Co) enables the determination of the value of $k_{+1}[M]$. Furthermore, if the

assembly was seeded, such that the value of [M] is known, then the value of k_{+1} can be determined. Moreover, assembly of various concentrations of tubulin enables a plot of dimer concentration versus polymer mass to be obtained and this can be used to estimate Co which can then be used for an indirect estimation of k_{-1}. Direct estimation of the dissociation rate constant can be obtained by following the rate of microtubule depolymerisation induced by dilution of the microtubules, to destabilise the polymer[64] or by depletion of GTP using a hydrolytic system such as fructose-6-phosphate and phospho-fructo kinase, enabling the estimation of k_{-1} from a first-order logarithmic plot (R.G. Burns-unpublished).

Models of Steady State Kinetics of Microtubules:

Two behaviours of microtubules at steady state have been described. In the first, termed treadmilling, the two ends of a microtubule are assumed to have different Co, consistent with the intrinsic polarity of the microtubule[90]. Tubulin subunits add at one end of a microtubule, hydrolyse the bound GTP molecule and then dissociate from the other end of the microtubule. The model suggests that net addition of tubulin occurs at one end of a microtubule termed the assembly or A-end and net loss occur at the other end termed the disassembly or D-end. Therefore, in treadmilling system, head-to-tail polymerisation of tubulin occurs leading to the flux of subunits along the microtubules. This assumes two possible values of Co, that of the A- and D-ends, with Co (A) < Co (D)[90].

Treadmilling has been demonstrated *in vitro* indirectly using pulse-chase experiments with ^{3}H-GTP[42,90,154]. Steady state microtubules pulsed with ^{3}H-GTP incorporate the nucleotide apparently in a linear fashion and such incorporation is blocked by podophyllotoxin which causes "poisoning" of the microtubule ends[90], such a pattern of incorporation does not fit with a simple linear condensation model, where diffusional exchange of subunits at the two ends would be predicted. Similarly,

steady state microtubules pulsed with ^{3}H–GTP and then chased with unlabelled nucleotide show a delay in the loss of ^{3}H–GTP indicating subunit flux on the microtubules[154]. Recent evidence for subunit flux on microtubules has been demonstrated using tubulin subunits tagged with a carboxyfluorescein derivative that can be induced to fluoresce upon photoactivation[94]. Such tagged tubulin when microinjected into cultured epithelial cells assemble into the mitotic spindle and its movement can be readily monitored by optical microscopy after photoactivation by irradiation with light at 365 nm. Results from such studies directly demonstrated poleward flux of tubulin subunits on kinetochore microtubules, with the subunits assembling at the kinetochore end and disassembling at the spindle pole end, but does not necessarily prove that the observed flux is due to the treadmilling process.

The second model is termed dynamic instability, and is the outcome of a variety of observations. First, a simple equilibrium state described by equation (1) would predict that a plot of the assembly rate d[S]/dt versus subunit concentration [S] would be linear, both above and below Co. However, several experiments *in vitro* whereby pre–assembled microtubules have been diluted to a concentration above and below the Co suggested that such a plot is linear above the Co, but is non–linear below Co with rapid depolymerisation of microtubules being observed[70]. Furthermore, experiments whereby microtubules were induced to assemble at a high tubulin concentration showed that GTP hydrolysis lags behind tubulin assembly, even though the hydrolysis occurred with a stoichiometry of 1 mole.mole^{-1}[27].

Furthermore, when microtubules were nucleated with centrosomes, assembled to steady state and then diluted, there was a decrease in the number of microtubules but an increase in the mean length of the population, indicating that some microtubules were depolymerising whilst others were elongating[95]. Similarly, microtubules assembled *in vitro* to steady state and then sheared showed an increase in mean length and a decrease in number concentration[96]. Those observations led to the proposal that microtubules at steady state exist in two populations: a small

population of slowly growing microtubules and a large population of rapidly shrinking ones, that interconvert infrequently. This model is consistent with the reported differences in the kinetics of subunit addition and GTP hydrolysis. Growing microtubules may have a "cap" of tubulin subunits containing unhydrolysed GTP, with the length decreasing as steady state is approached due to the slowing rate of subunit addition[70]. Dynamic instability therefore, is governed by several kinetic parameters: it is dependent on the rate of subunit addition and loss from the two microtubule populations, the transition probabilities from the growing to the shrinking phase and vice versa which in turn is dependent on the rate of the GTP hydrolysis and the rate of recapping of GDP microtubules[96]. In the dynamic instability model there are two Co, a low Co for GTP microtubules and a high Co for GDP microtubules. The bulk Co is therefore an average of the two Co for shrinking and growing microtubules[73], and the situation is further complicated by considering the events at the two microtubule ends.

Dynamic instability of individual microtubules has been demonstrated in real-time using dark field microscopy to visualise elongation and shortening of microtubules *in vitro*. The two ends of a microtubule elongated at different rates before stopping to grow independently and in a stochastic manner and converting to rapid depolymerisation[62].

Several *in vitro* experiments demonstrated microtubule turnover by dynamic instability. In one such experiment biotinylated tubulin was injected into BSC1 (fibroblasts) cells and the pattern and kinetics of incorporation onto pre-existing microtubules was determined[70,127]. The biotinylated tubulin was incorporated at the ends of pre-existing interphase microtubules or were nucleated by the centrosomes to assemble new microtubules. Furthermore, the unlabelled microtubules disappeared with a half-life of less than 10 min[73,127]. These results therefore suggest that a continuous cycle of microtubule growth, followed by depolymerisation exists in the cell and such a pattern of subunit incorporation and loss is only

explainable in terms of the dynamic instability model.

Microtubule Associated Proteins (MAPs):

Microtubules are often associated with accessory proteins termed microtubule associated proteins (MAPs) which bind to the wall of microtubules and regulate their properties. Functional diversity of these MAPs vary from stabilising the assembled polymer to facilitating its interaction with other cytoskeletal elements or as transporters of various components along a microtubule 'track'[15]. MAPs can roughly be divided into two groups according to their molecular weight: high molecular weight proteins and tau factor[152]. These MAPs colocalise with microtubules in the cell and co-purify with tubulin prepared by cycles of assembly and disassembly.

High molecular weight (HMW) MAPs are generally flexible rod-like structures, approximately 100-200 nm long and form arm like projections when attached to the microtubule lattice. This group of MAPs consist of MAP1 A & B, MAP2, and the motors MAP1C (cytoplasmic dynein)[50] and kinesin[61].

Brain MAP2 is the best characterised of all of the HMW MAPs. On high percentage SDS-PAGE the protein migrates as a single polypeptide of molecular weight about 280,000, but with a sequence molecular weight of 198,978[82]. On low percentage SDS-PAGE MAP2 is resolved into two polypeptides termed MAP2A and MAP2B which are the products of differential gene splicing. MAP2 is a thermostable protein, capable of withstanding temperatures of up to 100 °C. Length estimate of the molecule using electron microscopy vary between 90-185 nm in solution with up to 90 nm forming the sidearm projection from the microtubule surface[152]. Map-2 binds to microtubules *in vitro* with a stoichiometry of 1:12, and can be extensively phosphorylated: phosphorylation is to 12 moles.mole^{-1} of the tubulin-binding domain by a cAMP-activated protein kinase which leads to weakening of the MAP2:tubulin interaction[23].

Tau proteins are composed of 4-5 polypeptides of molecular weight 50,000-65,000 as judged by one dimensional electrophoresis and these proteins resolve into more than 20 components by two dimensional electrophoresis[60]. Like MAP2 these proteins are heat stable and are able to bind calcium calmodulin complex. However, in contrast to MAP2 which is localised in dendrites and cell bodies, tau proteins are mainly localised in the axons of nerve cells. Structurally, tau proteins are rod-like molecules about 50 nm long and bind to microtubules with arm like projections of about 18.7 ± 4.8 nm, protruding from the wall of the microtubule[60]. The arm-like projections of the tau protein have been implicated in cross-linking microtubules *in vitro*. Tau proteins bind tubulin with a stoichiometry of 1:5 mole.mole^{-1} and the tau binding site on microtubules might partially overlap with that for MAP1A[60]. Both MAP-2 and Tau promote microtubule assembly, and in particular lower the steady state Co, probably by altering the conformational change of the tubulin lattice associated with assembly-dependent GTP hydrolysis[17].

Drugs Affecting The Polymerisation of Microtubules:

A number of drugs are known to bind to tubulin and inhibit microtubule assembly. Colchicine, a drug extracted from the meadow saffron *Colchicum autumnale*, is the oldest known microtubule inhibitor[85]. It is a tropolone derivative consisting of three rings termed A-B, that binds to tubulin to form a tight complex in a temperature dependent manner (Kd= 3-9.1 x 10^{-7} M), with negligible binding occurring at 0 °C. The tubulin Colchicine binding site is subject to decay, in an exponential manner following first-order kinetics and a half-life of 5-7.5 h for mammalian tubulin[85]. Binding of Colchicine to tubulin is thought to induce conformational change in the tubulin subunit as it activates the tubulin GTPase activity, possibly by mimicking the tubulin conformation occurring during assembly[85]. Colchicine induces microtubule depolymerisation probably through an end "poisoning mechanism" whereby a colchicine tubulin complex is thought to add to the end of a microtubule and hinder further addition of subunits[154]. Ultra-Violet irradiation of

Colchicine generates the analogue lumicolchicine which does not bind to tubulin, whilst another colchicine analogue, colcemid, seems to bind tighter to the tubulin subunit[85].

Podophyllotoxin is another microtubule inhibitor that shares part of its binding site on the tubulin molecule with colchicine. The binding characteristics of this alkaloid drug however, are different from those of colchicine in that it binds rapidly, at 0 °C and reversibly[85].

Nocodazole is an important anti-mitotic drug acting as a microtubule inhibitor both *in vivo* and *in vitro*. *In vivo* studies showed that cultured mammalian cells treated with 0.04–10 $\mu g.ml^{-1}$ of the drug lost their appearance and became rounded within 10–20 min. of the treatment. This change in morphology was also associated with loss of directional movement and gradual disappearance of microtubules[35].

The binding of nocodazole to tubulin is rapid and reversible and causes inhibition of microtubule assembly *in vitro*[80]. The drug acts on tubulin rather than on MAPs as it inhibits the assembly of phosphocellulose purified tubulin, under conditions where pure tubulin normally assembles, and increases the Co in a dose-dependent manner. Thus, at 5 μM of nocodazole the Co for bovine tubulin assembly was 2 $mg.ml^{-1}$ compared to 0.2 $mg.ml^{-1}$ in its absence and this increase in Co was not due to tubulin self-aggregation induced by the drug. Physical studies have shown that the binding of nocodazole to tubulin induces a conformational change in the protein, resulting in an increased exposure of the SH- groups and possibly of tyrosine residues, but no perturbation of the tryptophan environment was observed[80]. However, the exact mechanism through which nocodazole acts is still not apparent.

Vinblastine, an alkaloid derived from the periwinkle *Vinca rosea* binds to tubulin reversibly at a site distinct from that of colchicine or podophyllotoxin[86].

Vinblastine has two high affinity binding sites per tubulin dimer and there might be several other low affinity binding sites present (about 20–30 for chick brain tubulin). The binding of vinblastine to tubulin induces the formation of tubulin crystals in the cell and such property has been exploited as a method for tubulin purification. The binding of vinblastine and its analogue vincristine are competitively inhibited by maytansine, a drug that binds readily and reversibly to tubulin at the two vinblastine binding sites[86].

Taxol is an anti-mitotic drug which is a potent inhibitor of cell replication[63]. Incubation of cells with this drug results in stabilisation of the microtubule array against drug and cold induced depolymerisation. Furthermore, taxol treated cells develop prominent bundles consisting of parallel arrays of microtubules. Taxol seems to enhance microtubule polymerisation *in vitro,* unlike other anti-mitotic drugs which inhibit tubulin assembly. Taxol enhances the rate and the yield of microtubules probably by lowering the critical concentration for assembly. Indeed, tubulin assembled in the presence of taxol has a Co of 0.01 $mg.ml^{-1}$ compared to a Co of 0.1 $mg.ml^{-1}$ in its absence. Furthermore, microtubules formed with taxol are normally shorter than microtubules formed in its absence, indicating that taxol enhances the nucleation event and as this leads to a higher number of microtubule ends, it would explain the enhanced rate of assembly in the presence of the drug. Taxol also promotes microtubule assembly under conditions where polymerisation does not normally proceed eg. in the absence of MAPs, GTP or at 0 °C. Furthermore, microtubules assembled with taxol are cold stable and are resistant to calcium depolymerisation. Maximal effects of the drug seem to occur when it is added in stoichiometric amounts with tubulin. The stability of taxol microtubules has been exploited for the purification of MAPs *in vitro*[63].

Tubulin:The Building Block of Microtubules:

Microtubules are assembled from a basic protein molecule called tubulin, which is a heterodimer made of two closely related polypeptides termed the α- and β-tubulin subunits each having a molecular weight of about 50,000. These subunits are associated together by non-covalent (hydrophobic) interactions, with an equilibrium dissociation constant (Kd) of 8×10^{-7} M at 4.6 °C[39].

The tubulin dimer has binding sites for numerous ligands. Tubulin binds one molecule of GTP at a site on the α-subunit termed the non-exchangeable site and another GTP molecule at a site on the β-subunit termed the exchangeable site which is readily exchangeable with free GTP and GDP in the medium[15,84]. Hydrolysis of the GTP on the exchangeable site is associated with tubulin polymerisation. Tubulin also binds ATP weakly (Kd = 2×10^{-4} M) on a site on the α-subunit[156,157]. ATP binding to tubulin can induce tubulin polymerisation[156,24].

The tubulin dimer has binding sites for ions such as Mg^{++} and Ca^{++}. Magnesium seems to be necessary for the assembly of tubulin and probably binds to tubulin as part of a GTP-Mg++ complex (Kd=1.56-1.11 $\times 10^{-8}$ M)[31]. In contrast to the effect of magnesium, calcium binds to tubulin and causes depolymerisation of the assembled microtubules or inhibition of microtubule assembly[155]. Calcium sensitivity increases by lowering the temperature or in the presence of the calcium binding protein calmodulin[155]. The intrinsic calcium effect (i.e. that not requiring the presence of calmodulin), is thought to occur by binding the ligand to the C-terminus of the tubulin heterodimer, as such sensitivity is dependent on the presence of the C-termini of the α- and β-subunits (see below).

Studies on the domain structure of tubulin has indicated that both subunits consist of two structural domains[72,116] and one regulatory domain[119] located at the

C-terminus. The two structural domains are connected by peptide linkage and other non-covalent interactions, as they remain associated together after cleavage with proteolytic enzymes[116]. Chymotrypsin cleaves the β-subunit at Tyr 281 into two fragments of molecular weight of 34,000 and 21,000 representing the N-terminal and the C-terminal domains, respectively[116]. Furthermore, trypsin cleaves the α-tubulin subunit at Arg 339 to yield two fragments of molecular weight 38,000 and 14,000 representing the N- and C-terminus domains respectively[116]. The chymotrypsin and trypsin sites are masked upon assembly suggesting that the conformation of the subunits changes upon polymerisation, causing the proteolytic site to be buried in the wall of the protofilament[116]. Moreover, based on such studies the inter-dimer bond in a protofilament is said to be formed between the large N-terminal domain of the α-subunit and the small C-terminal domain of the β-subunit[72].

The regulatory C-terminal domain of the tubulin subunits is highly charged and can be removed as a 4 Kd fragment by limited subtilisin digestion[116,119] and seems to consist of two sub-domains: a large sub-domain involved in MAP binding[51,87] (see below) and a smaller one involved in the binding of Ca^{++} ions[15]. The large C-terminus sub-domain seems to hinder tubulin-tubulin interaction, since subtilisin digestion of the C-terminus is able to relieve this hindering effect. Thus, subtilisin digested pure tubulin is able to assemble *in vitro* in the absence of MAPs, with a Co similar to those obtained for non-treated but MAP containing tubulin[119]. The smaller C-terminus sub-domain has been implicated in the binding of Ca^{++} ions. Treatment of tubulin with Carpboxypeptidase Y, to remove a 1 Kd fragment from the C-terminus, generated tubulin which upon polymerisation was resistant to Ca^{++} induced disassembly, indicating that the calcium binding site is very close to the C-terminus[139].

Tubulin consists of a set of closely related polypeptides that constitute the tubulin microheterogeneity. This heterogeneity results from the expression of multi-tubulin genes and from post-translational modifications of the encoded protein.

Post-translational Modifications of Tubulin:

Tubulin is subject to numerous post-translational modifications on both subunits, most characterised of which are tyrosinylation (hereafter referred to as tyrosination) and acetylation of the α-subunit and phosphorylation of the β-subunit.

Using rat brain supernatant obtained at 100,000 xg Barra *et al* showed that this supernatant was able to incorporate ^{14}C-tyrosine, upon the addition of ATP, KCl and Mg++ ions onto a TCA insoluble protein[13]. This incorporation of tyrosine was shown to be RNAase insensitive and was not dependent on the presence of Tyr-tRNA, indicating that the amino acid was added post-translationally by an enzymic reaction[13]. This enzymic activity was also catalysed the addition of phenylalanine and Dopa[13]. Characterisation of the labelled species showed that it was a single component, shown to be α-tubulin on the basis of its molecular weight, and co-elution with colchicine-tubulin complex on Sephadex chromatography, and precipitation with vinblastine sulphate[11].

Tyrosine incorporation is the result of the formation of a peptide bond to the C-terminal glutamate residue of the α-tubulin subunit and is catalysed by the enzyme Tubulin Tyrosine Ligase (TTL)[10,136]. This uses dimeric tubulin as the substrate, as demonstrated by the lack of inhibition of the tyrosination reaction in the presence of colchicine or podophyllotoxin[5,10]. The properties of TTL will be considered in Chapter 3.

The incorporated tyrosine can be removed by an endogeneous Tubulin Tyrosinyl Carboxypeptidase (TTCP) that preferentially detyrosinates tubulin in the polymeric form, as the detyrosination reaction increases upon enhancement of tubulin assembly by taxol[3,4]. TTCP has been partially purified from chicken brain extract using a procedure that utilises pH fractionation, ammonium sulphate precipitation and carboxymethyl anion exchange chromatography to obtain an enzyme with an apparent

molecular weight of 90,000[6]. The enzyme was also capable of catalysing the release of phenylalanine from the C-terminus of α-tubulin[6]. TTCP is activated by numerous co-factors including Mg++ and various polyamines such as spermine and spermidine[12]. Furthermore, it is inhibited by proteoglycans, soluble RNA and several polyanions, although these probably inhibit the detyrosination reaction through denaturation of the tubulin substrate[7].

It is not known with certainity whether the post-translational modification is the addition or removal of the tyrosine residue since α-tubulin, at least in vertebrates, is encoded as multiple isoforms some of which end with a C-terminal tyrosine, whilst others end with a C-terminus glutamate[131]. Furthermore, several lower eukaryotes such as *Trypanosoma rhodesiense*[71], *Physarum polycephalum*[53] and *Crithidia fasiculata*[28] have an encoded tyrosine at the C-terminus of the β-tubulin subunit. This residue however, is not involved in the tyrosination/detyrosination cycle observed for the α-tubulin subunit.

Post-translational tyrosination of tubulin has been directly demonstrated *in vivo* using cultured muscle cells[136,137]. Such cells, pulsed with ^{3}H-tyrosine under conditions inhibiting protein synthesis, showed incorporation of the amino acid onto the α-tubulin subunit. Such incorporation required the presence of intact microtubules as it was prevented in the presence of colchicine. Moreover, pulse-chase experiments showed that the half-life for tyrosine turnover in these cells was 37 min. compared to a half-life of tubulin turnover of over 45 hours[137]. This has led to the cyclic model of tubulin tyrosination and detyrosination in the cells. According to this model, a pool of free tubulin dimer in the cell exists in equilibrium with assembled microtubules. This free tubulin is tyrosinated prior to its incorporation onto microtubules where it gets detyrosinated by TTCP and is subsequently lost from the other end of the microtubule and is retyrosinated by the TTL[136]. Such a model fits well with the proposed treadmilling behaviour of microtubules at steady state. Furthermore, as the turnover of tyrosine occurs with a half-life of 37 min., this

model predicts that half of the free dimer pool should be incorporated into microtubules at least once every 37 min. to enable continuation of the tyrosination cycle.

The cyclic model of tubulin tyrosination has been recently supported through experiments using cultured epithelial cells demonstrating that detyrosination is a post-polymerisation event[57,148]. In one experiment the microtubule network of cultured TC-7 cells was completely depolymerised by nocodazole treatment and allowed to regrow after drug removal the tyrosinated microtubule array was formed within 7 min. of drug removal, whilst it took 30 min. for detyrosinated microtubules to be observed, indicating post-polymerisation detyrosination of tubulin[57]. Furthermore, analysis of the fractional composition of tubulin in the cell indicated that tyrosinated tubulin was the predominant species in the cellular free dimer pool. Post-polymerisation detyrosination has also been demonstrated in lower eukaryotes such as the protozoan *Trypanosoma brucei*, whereby the microtubules of the nascent daughter flagellum obtained during cell division are first constructed from tyrosinated tubulin, that becomes detyrosinated with time[123,124].

Instrumental in the analysis of the tyrosination status of microtubules *in vivo* is the production of several antibodies specific for tubulin with and without a C-terminus tyrosine. One such antibody is YL 1/2, a monoclonal antibody raised against yeast tubulin[69] which ends up with a C-terminus phenylalanine. As well as the original epitope, the antibody recognises the tyrosinated form of α-tubulin. Analysis of the epitope requirement of this antibody showed that it binds to peptides whose C-terminus residue is a Phe derivative, that carries a free carboxylate group and which has a penultimate residue with a negatively charged side chain[147]. Strongest binding of YL 1/2 was for a synthetic peptide with the sequence EEY, although it was capable of binding to similar peptides with a C-terminus Phe and Dopa[147].

Gundersen *et al* raised two polyclonal antibodies against the two synthetic peptide sequences $^{+}{}_{3}$HN–GEEEGEE–COO^{-} and $^{+}{}_{3}$HN–GEEEGEEY–COO^{-} that recognised detyrosinated and tyrosinated tubulin respectively[56]. These two antibodies were used in immunofluoresence studies to show that in cultured monkey kidney cells two populations of microtubules existed: those that stained preferentially with the Tyr antibody and those staining preferentially with the Glu antibody. Tyr antibodies stained basically the whole interphase microtubule network[56] of these cells which seemed to be centrosomally nucleated. Glu antibodies on the other hand reacted only with a small subpopulation of microtubules that were sinous in appearance and were constricted to the cell centre, in contrast to microtubules staining with the Tyr antibody which often extended to the cell periphery. In mitotic cells however, both antibodies stained microtubules of the metaphase spindle with the same intensity, but only Tyr antibodies immunostained the astral microtubule network. These findings were confirmed by ultrastructural studies using immunogold staining of the microtubule network of CV_1 and PtK_2 cells with the two antibodies[49], where the interphase microtubules were heavily labelled with the Tyr antibody and sparsely with the Glu antibody. However, examination of the stained microtubules by electron microscopy showed that all microtubules possessed a certain degree of staining with both antibodies, indicating that all of these microtubules are copolymers of tyrosinated and detyrosinated tubulin in varying proportions[49].

Examination of the distribution of tyrosinated and detyrosinated microtubules in proliferating Ptk_2 cells indicated that detyrosinated tubulin is the predominant form in the microtubules of stable assemblies in the cell such as centrioles and primary cilia[54]. Furthermore, stable microtubules present in differentiated cells such as those present in axonemes and basal bodies of sperm and tracheal cells, and marginal bands of platelets and erythrocytes contained elevated levels of detyrosinated tubulin[54]. Such observations indicate a possible relationship between detyrosination and the stability of microtubules, yet the marginal band of toad erythrocyte contains only tyrosinated tubulin[54] whilst the dynamic microtubules of the mitotic spindle of

Trypanosoma brucei are constructed from detyrosinated tubulin[118]. Therefore, detyrosination does not appear to be obligatory for stability. Several *in vivo* studies have correlated detyrosination with microtubule stability[18,20,55,71,75,122,145]. Many of these experiments have demonstrated enhanced resistance of microtubules enriched in detyrosinated tubulin against nocodazole and dilution induced disassembly[71]. However, the microtubules of certain cell lines such as the human fibroblast 356 show no reactivity with the Glu antibody, yet still possess a subset of microtubules that is resistant to nocodazole disassembly, indicating that detyrosination is not a prerequisite for microtubule stabilisation. Nevertheless, no specific function has yet been assigned to this post-translational modification.

Acetylation is another post-translational modification that occurs on the α-tubulin subunit. This post-translational modification was first identified in *Chlamydomonas* as a chemical modification of the tubulin constituting flagellar microtubules[83]. In this organism, a cytoplasmic tubulin precursor pool can be utilised, under protein synthesis inhibiting conditions, to regenerate the resorbed flagella to half their original length[83]. Electrophoretic studies showed that the precursor tubulin pool is enriched in a tubulin isoform termed α_1, distinct from the more basic flagellar isoform α_3. Pulse-chase experiments showed that α_3 is a post-translational modification of α_1 and further studies utilising ^{3}H-acetate showed that such modification is probably acetylation of α-tubulin[83]. Later studies confirmed that *Chlamydomonas* α-tubulin is acetylated at ε-amino group of Lys-40[79] by an acetylase activity located at the flagellar-cytoplasm membrane matrix[83]. Furthermore, flagellar tubulin seems to be deacetylated upon flagellar resorption, prior to entering the cytoplasmic tubulin pool, by a de-acetylase activity located in the cytoplasm[130]. This has led to the suggestion that the acetylation/de-acetylation cycle might be related to the assembly and disassembly of flagellar microtubules.

Several antibodies have been raised against acetylated tubulin. One of these is the monoclonal antibody 6-11-B-1 raised against sea urchin sperm axonemal tubulin

and that binds to axonemal α–tubulin from several organisms[104]. This antibody has a binding site at or near the Lys–40 residue of α–tubulin[78]. The epitope for this antibody is not restricted to axonemal tubulin as it recognises cytoplasmic microtubules of mammalian cells[105]. However, the antibody does not recognise soluble cytoplasmic α–tubulin from various sources indicating that acetylated tubulin might be present preferentially in the polymeric form[78].

Tubulin acetyl transferase (TAT) has been partially purified from *Chlamydomonas* flagellar axonemes using extraction with non–ionic detergent, followed by salt treatment and ionic exchange chromatography[91]. TAT has a molecular weight of 130,000 as estimated by gel filtration, and is a homodimer since, SDS–PAGE studies have yielded a molecular weight of about 67,000. The enzyme has a Km for acetyl CoA of about 2 μM, whilst CoA is a competitive inhibitor with a Ki of about 8 μM. *In Vitro* studies of the enzyme catalysed acetylation of α–tubulin has shown that the protein is acetylated with a stoichiometry of about 1.1 mole.mole^{-1}. Furthermore, Ca++ ions were shown to inhibit TAT activity through direct binding to the enzyme. The enzyme is capable of acetylating tubulin in either the dimeric or polymeric form, although polymerised tubulin appears to be the preferred substrate for the reaction. A tubulin de–acetylating activity, termed tubulin de–acetylase, also been identified in the cell body extract of *Chlamydomonas*, which also seems to contain an inhibitor of the TAT[91].

Acetylation has been shown to have no influence on the assembly of mammalian tubulin *in vitro*. Thus, the kinetics of temperature dependent assembly of twice cycled calf brain tubulin *in vitro*, were similar for the acetylated and non–acetylated species. Acetylated and de–acetylated microtubules also had the same disassembly profile *in vitro*[91]. However, *in vivo*, acetylation has been generally associated with stable microtubule arrays[105].

Various kinases have been shown to phosphorylate tubulin *in vitro* and two of

these enzymes: a Ca–calmodulin dependent activity and a casein–kinase II like activity, appear to be associated with microtubule preparations *in vitro*[8]. Ca–calmodulin dependent kinase activity capable of phosphorylating tubulin has been isolated from porcine brain and has been shown to consist of a major polypeptide of 50,000 molecular weight and a minor one of 60,000 molecular weight[142]. This enzymic activity was capable of phosphorylating tubulin *in vitro* with a stoichiometry of 2.6 mole.mole^{-1} with 60 % of the phosphate being ligated onto the β–subunit and 40 % onto the α–subunit[142]. Phosphorylation occurred mainly on serine residues, although some threonine residues were also modified[8,142]. Such a post–translational modification was shown to alter the confirmation of the tubulin subunit as judged by chymotryptic digestion of tubulin before and after phosphorylation, and this probably accounts for the observed inhibition of tubulin assembly *in vitro* upon phosphorylation by this enzyme[142].

Tubulin phosphorylation was also demonstrated *in vitro* by the enzyme casein–kinase II[120]. This enzyme phosphorylated pig brain tubulin only at the β–subunit on serine 423 and the incorporated phosphate is removable by phosphatase treatment. In contrast to phosphorylation by Ca–calmodulin dependent kinase, tubulin phosphorylation by casein kinase II has no effect on its assembly capability. Moreover, a casein–kinase II like activity has been shown to be associated with microtubules assembled *in vitro* and to be inhibited by heparin, indicating that this enzymic activity may be operational *in vivo*. Indeed, comparison of V8 protease digestion pattern of β–tubulin phosphorylated *in vitro* with that phosphorylated *in vivo*, through the differentiation of cultured neuroblastoma cells in a phosphate containing medium, showed that the two species were identical. This may suggests that casein kinase II might be responsible for the *in vivo* phosphorylation of β–tubulin, first reported by Gard and Kirschner, in neuroblastoma cells induced to differentiate by serum deprivation[46].

Insulin receptor kinase has also been reported to phosphorylate mammalian α-tubulin on tyrosine residues[141]. An interesting aspect of this phosphorylation reaction is the exclusive phosphorylation of α-tubulin on the C-terminus tyrosine and the prevention of incorporation of the labelled tubulin dimer into microtubules. In the case of tubulin where the C-terminus tyrosine has been removed by exogenous Carboxpeptidase activity, phosphorylation occurred at the other tyrosine residues in the subunit and no effect on polymerisation was observed.

Recently, a new post-translational modification has been described involving the progressive glutamylation of the α-tubulin subunit[41]. During such a modification glutamyl units are added unit by unit to α-tubulin, probably by an amide bond to the γ-carboxyl group of glutamate 445. The significance of such a modification is yet to be determined, but since it occurs at the C-terminus, it could play a role in regulating the binding of MAPs.

Tubulin Microheterogeneity:

One of the most striking aspects of microtubules is the diversity of cellular functions they fulfil. The same structural polymers are responsible for chromosomal segregation during mitosis and meiosis, maintaining cellular integrity through the extensive cytoskeletal network formed by interactions with other components of the cytoskeleton[15]. Clearly, a microtubule that is a part of the mitotic spindle is envisaged to be different from one which is a part of the flagellar axoneme. There must be a cellular mechanism operating on the molecular level to allocate such diverse roles to various microtubule populations. The question is then: are microtubules constructed from identical tubulin subunits or is each class of microtubules unique in its composition such that a cell possesses a structurally and functionally distinct tubulin pool for each functionally diverse subset of microtubules? Fulton and Simpson proposed such a "Multi-Tubulin Hypotheses" some time before

there was any definitive proof of tubulin heterogeneity[45]. Such microheterogeneity has since been demonstrated by isoelectric focusing[34,40,43,48,52,97,134,140] peptide mapping[46,99], immunologically[21,45] and by gene dissection using recombinant DNA techniques[29,30,108,128,131–133].

Biochemical Demonstration of Microheterogeneity:

Tubulin resolves on SDS-PAGE into two polypeptides termed α and β both of which have an apparent m.wt. of 50 kd. Early evidence that the α and β-tubulin subunits represent a set of closely related but non-identical polypeptides emerged from experiments utilising lower eukaryotic tubulin. Comparison of the α and β-tubulin subunits from the A-subfibre with those extracted from the B-subfibre of sea urchin sperm axonemes, suggested differences in the primary sequence of the proteins as demonstrated by tryptic peptide analysis[45]. Similarly, antibodies raised against flagellar tubulin from the flagellate *Naegleria gruberii* showed little reactivity with the cytoplasmic tubulin from the amoeboid cell[45]. A third member of the tubulin superfamily, termed γ-tubulin has been recently proposed however, based on sequence homology between α- and β-tubulin and a cloned gene of microtubule interacting protein (mipA) in *Aspergillus nidulans*, which shows about 33% homology to tubulin from various sources[101].

Direct biochemical demonstration of tubulin microheterogeneity has been most fully documented for vertebrate brain tissue[34,40,43,48,52,134,140]. Tubulin from vertebrate neuronal tissue separates into a minimum of 6 α and 10–14 β-tubulin bands on isoelectric focusing (IEF) gels, over a pH range of 5.3–5.8. All vertebrate brain tubulin examined has a similar IEF pattern, although the isoform complexity increases post-natally both in number and relative intensity of the resolved bands[34,52,134,140]. For instance, chick brain tubulin (from 17-day old chicks) has been shown to focus into a minimum of 6–7 α (basic) and 10 β (acidic) variants on IEF gels and as development progresses from 13-days embryo to 17-days old adult,

the overall level of the minor β-tubulin variants (most acidic) increases with respect to the major ones, accompanied by reversal of the relative proportions of the two major β-tubulins[134]. Only minor changes are observed for α-tubulin isoforms during development. However, a new α-tubulin variant is generated in the chick brain tubulin pool post-hatching. Furthermore, no difference in the isoelectric composition of tubulin isolated by one, two or three cycles of assembly is observed, indicating that the multiple tubulin isoforms have a similar capacity to assemble into microtubules *in vitro*[134].

This isoform complexity is probably due to the heterogeneity of the protein rather than the cellular heterogeneity of brain tissue, in that cultured neuronal cells exhibit the same heterogeneity as the intact brain, although the complexity is less in glial cells[40,97].

A variation from the IEF properties of brain tubulin is that of the chick erythrocyte tubulin. The β-tubulin isolated from the marginal band of chicken erythrocyte microtubules has a pI of 5.4 and in contrast to tubulin from chick brain, is more alkaline than the α-tubulin[99]. Furthermore, although the α-tubulin from both sources is more or less identical, peptide maps of α-chymotrypsin digests showed that erythrocyte β-tubulin shares only 60 % of the proteolytic fragments with brain β-tubulin, suggesting a divergent primary structure of the two subunits. This variation in β-tubulin primary structure might be responsible for the altered assembly kinetic properties of erythrocyte marginal band tubulin. Erythrocyte mtp, which has a lower Co than chick brain mtp, nucleates less efficiently, leading to slower assembly kinetics and greater microtubule mean length than brain mtp[98,99].

Genetic Characterisation of Tubulin Heterogeneity:

Much of the tubulin heterogeneity is due to the expression of multiple α- and β- tubulin genes, with the number of transcribed genes increasing in higher eukaryotes. In the budding yeast *S.cerevisae*, tubulin is encoded by two α- and one β-genes[30], while four α- and four β-tubulin genes are present in *Drosophila melanogaster*[30,110]. In vertebrates, including mammals, six functional β-tubulin genes and about seven α-tubulin genes have been identified so far, even though the mammalian genome has numerous untranscribed tubulin pseudogenes[29,30,131]. Extensive analysis of the chick tubulin genes by Cleveland and co-workers showed that the seven dispersed genes each encode a distinct β-tubulin polypeptide[29,30,131], whilst a set of five to six dispersed genes encode a similar number of α-tubulin polypeptides[29,30,107,108,131].

Using cDNA and gene sequencing techniques, the complete sequence and pattern of expression of the seven chick β-tubulin genes is now available, these β-tubulin genes, termed as cβ1-cβ7 show the same basic structure. Thus, each gene consists of four exons interrupted by three introns. In addition, the genes are flanked by a transcriptional control sequence TATATAA and an unusual polyadenylation signal ATTAAA[131]. The predicted sequence of the seven chick β-tubulin polypeptides show regions of extreme homology and clustered regions of heterogeneity, the most significant of which is region of 15 or so C-terminus amino acid, and other less heterogeneous regions at the N-terminus between residues 33-57 and 80-95[30,131,133]. Other than these two regions of clustered heterogeneity and few other minor regions, the amino acid sequence for the β-tubulin polypeptides is conserved. The seven β-tubulin genes encode six distinct tubulin polypeptides, as cβ1 and cβ2 encode two polypeptides differing by two residues only[132].

The chick β-tubulin genes are subjected to differential programs of expression during development and differentiation[132,133]. Sullivan *et al* have proposed that the hypervariable C-terminal region of the β-tubulin polypeptides, which has been conserved amongst vertebrates, can be used to classify the β-tubulin polypeptides into six distinct isotypic classes, designated ClassI-VI[133]. These classes correlate, in part, with the pattern of expression in that,class I isotype defines a β-tubulin, such as that encoded by cβ7, which is ubiquitously expressed, while cβ1 and cβ2 belong to isotypic class II and are expressed in many tissues and are the major neuronal β-tubulins[59,131,132]. Class III, to which cβ4 belongs is expressed weakly in neurones, but is neurone specific[59,131,132]. Class IVb isotype is encoded in the chick by cβ3, and is the major testis β-tubulin that is weakly expressed in other tissues[59,107,132,133]. Isotypic class V defines cβ5, an isotype expressed in low amounts in various tissues and cell types but which is not detectable in neurones[59,132,133]. Finally, Class VI comprises the highly divergent hematopoitic tissue β-tubulin encoded in the chick by cβ6. This β-tubulin isotype is the major constituent of the erythrocyte marginal band[59,131,132].

Vertebrate α-tubulin is encoded by at least seven genes, the properties of these genes are similar to those of the vertebrate β-tubulin ones, encoding polypeptides with the major region of heterogeneity being located at the C-terminus[132]. As for β-tubulin, mammalian α-tubulins seem to possess consensus C-terminus sequences defining distinct α-tubulin isotypic classes[132]. For example the mouse, for which most extensive data is available, possesses at least seven genes encoding six distinct tubulin isotypes. For five of these isotypes (encoded by the genes mα1, mα2, mα3/α7, mα4 and mα6), at least one mammalian counterpart has been identified that correlates with one of these isotypes in terms of the c-terminus sequence and the pattern of expression. The sixth mouse isotype is encoded by a highly divergent and testes specific gene[132].

The chick α-tubulin genes show heterogeneity amongst themselves and also amongst mammalian sequences[132]. These genes, termed cα1-cα6 and cα8 encode polypeptides with hypervariable regions at the C-terminus[108,132]. The C-terminal sequence of these polypeptides however, is different from that of mammalian α-tubulins and therefore, chick α-tubulins do not fall into obvious mammalian isotypic classes. The only exception to this phenomenon is cα1 which is the only chicken α-tubulin gene that has a mammalian counterpart (the mouse gene mα1), in terms of C-terminus sequence and pattern of expression[132].

Blot hybridisation experiments of total RNA from various chick tissues with oligonucleotides complementary to sequences from the various chick α-tubulin genes showed that these genes have complex patterns of expression in many tissues and cell types[132]. Thus, cα1 encodes the major brain tubulin isoform being also expressed in other tissues[132], cα2 is testis specific[107] whilst cα3 is a minor constitutive gene[132]. Cα5 and cα6 encode identical polypeptides and are said to be alleles of the same gene, and both of these alleles are expressed in various tissues in minor amounts[132]. Cα8 is expressed ubiquitously at low levels, but mainly in brain and lymphocytes[132]. Expression of cα4 has not been detected in the tissues examined so far even though it represents a functional gene[108]. Finally, cα7 originally thought to be an α-tubulin gene, has now been shown to be a pseudogene[108].

Only two of the α-tubulin genes, cα1 and cα8 encode a polypeptide with a C-terminus tyrosine[108,132] unlike the mammalian α-tubulin genes where all apart from two encode proteins with a C-terminus tyrosine[132]. Cα1 encodes a polypeptide with a C-terminal sequence of DYEEVGVDSVEGEGEEEGEEY, whilst cα8 encodes a tubulin with DYEEVGTDSMDGEDEGEEY as the C-terminal sequence[108,132]. It is possible that all or some of the remaining α-tubulin genes encode polypeptides that do not participate in the usual tyrosination/detyrosination cycle and thus do not act as substrates for the enzyme TTLase.

Post-translational Modifications and Tubulin Heterogeneity:

The tubulin microheterogeneity observed by IEF cannot be accounted for solely by the expression of variable number of tubulin genes, as the number of bands observed, especially that of β-tubulin, exceeds the number of tubulin genes in vertebrates[44]. Clearly, other mechanism(s) must be in operation to generate the isoform complexity, and three post-translational modifications have been identified: the tyrosination of the α-tubulin C-terminus, acetylation of the α-tubulin Lys 40 and phosphorylation of β-tubulin and possibly α-tubulin.

As the pKa for the aromatic tyrosine side chain is 9.7[33] and as the pH range used for focusing is 4-7[134], there should be no significant ionisation of the tyrosine residue, and therefore, the contribution of the C-terminus tyrosine to the overall pI of the protein is negligible under the IEF conditions employed. By contrast, addition of an acetate moiety on the protein is expected to affect the overall pI of the protein causing an acid shift. Indeed, in the slime mould *Physarum polycephalum*, the flagellate-dominant α-tubulin isoform (α3) is an acetylation product of the myxoamoebal-dominant α-tubulin isoform (α1)[117]. Similarly, phosphorylation of tubulin is also expected to generate isoform complexity causing an acid shift in the modified protein, and a β-tubulin isoform selectively phosphorylated during differentiation of cultured neuroblastoma cells (β2-tubulin) is probably a phosphorylation product of a more basic β-tubulin isoform (β3)[40,46].

Functional Significance of Multi-tubulin Polypeptides:

Experiments addressing a function for multitubulins have been mostly done in relation to the function or distribution of β-tubulins. Two hypothesis have attempted to explain the function of the closely related but significantly variable tubulin polypeptides[29]. The earliest, "Multi-Tubulin Hypothesis" advanced by Fulton and Simpson after immunological work on the flagellar tubulin of the protozoan

Naegleria gruberii, argued that isotypically distinct tubulin pools must exist in the cell to construct biochemically and functionally distinct microtubules[45]. Thus, according to this hypothesis multiple tubulin isoforms are functionally unequivalent. An alternative hypothesis explaining the function of multitubulins advocates that the various tubulin genes encode functionally equivalent polypeptides. However, multiple genes exist to serve for alternate regulation of tubulin expression in different cells or tissues[110]. In such a case, the expression of the various tubulin genes would be subjected to differential transcriptional regulation depending on a cell's unique program of development and differentiation. Such a mechanism therefore postulates, that it is the sequence heterogeneity of the untranscribed gene segments, rather than the heterogeneity of the encoded tubulins that is of significance.

Lewis et al [81], using mouse isotype specific monoclonal antibodies have shown that all β-isoforms present in one cell are assembled into all classes of microtubules observed. Similarly, the product of a chimeric gene comprising 75% of chick class II gene at the N-terminus and 25% yeast β-tubulin gene at the C-terminus, after transfection into mouse 3T3 cells was incorporated into all classes of microtubules and the cells divided normally[132]. Moreover, tubulin from the slime mould *Physarum polycephalum*, when injected into ptk2 cells, assembles into cytoplasmic and mitotic spindle microtubules[109]. Indeed, there is no direct evidence of subcellular sorting of tubulin isotypes into distinct microtubules, although indirect evidence of subcellular localisation of β-tubulin isoforms in the squid giant axon has recently been proposed[2]. Recently, non-uniform distribution of the rat neuron specific β-tubulin isotype (typeIII), along the length of individual microtubules has been reported[65]. Using immunogold electron microscopy, this isoform has been shown to be distributed in "patches" along individual microtubules of cultured neutrites and microtubules assembled *in vitro*. This would suggest preferential association of certain isoforms during tubulin assembly.

Examples of the expression of a tubulin isoform being restricted to a certain tissue or cell type do not necessarily imply restriction of function. Thus, brain tubulin was shown to substitute for the haemopoeitic β-tubulin (β6) in the *in vitro* reconstruction of marginal band microtubules in chicken erythrocyte[132]. Moreover, mutation of a locus in the *Drosophila* genome that encodes a β-tubulin specific for developing spermatocytes (β2-isoform) showed that tubulin to be multifunctional, participating in the assembly of all classes of spermatocyte microtubules[110,132]. In this metazoan microtubules are involved in four main processes during spermatogenesis: mitosis, meiosis, assembly of the sperm tail axoneme and shaping of the nucleus into needle like head of mature sperm. β2 is expressed in the testis during spermatogenesis only and, at first, it was thought that it was uniquely utilised for the construction of the doublet containing sperm flagellar axoneme, a structure not constructed anywhere else in *Drosophila*. As expression of β2 is unique to male testis, mutations in the β2-tubulin gene lead only to male sterility, with no effect on the viability of the insect. Demonstration that β2-tubulin was not unique to the assembly of the sperm flagellar axoneme, but was also involved in the construction of the meiotic spindle and cytoplasmic microtubules came by isolation of dominant mutations exhibiting male sterility and showing altered electrophoretic mobility of the β2-tubulin polypeptide (termed $\beta 2t^{D}$). Males expressing the mutated subunit had defective spermatid differentiation in which the assembly of the axoneme was disrupted, but also in which drastic meiotic abnormalities were observed, including failure to assemble proper spindle. Such multifunctionality of the β2-tubulin subunit was further demonstrated by isolation of recessive mutants in β2-tubulin genes. Expression of the defective subunits in homozygote males in one class of mutants showed failure of all microtubule mediated processes during the spermatogenesis stages subsequent to β2-expression. All of this seems to suggest that the various tubulin isotypes are functionally equivalent, supporting a regulatory function for multi-tubulin genes.

Such examples strongly imply that different tubulin isoforms have identical interactions, yet the mere fact that the C-terminus β-tubulin isotype defining sequence has been conserved in all vertebrates examined indicates that such a sequence is required to fulfil an important function. The C-terminus of α and β-tubulin has been implicate in MAP binding[51,87] calcium depolymerisation[138] and as a regulator of microtubule assembly[119]. Clearly then, variation in this C-terminus sequence might lead to differential regulation of the above processes. Indeed, distinct co-localisation of certain β-isoforms and MAPs have been demonstrated, with the mouse mβ2 isoform co-localising with MAP3 in rat cerebellum, whilst the localisation of mβ6 is similar to that of MAP1A[21].

The prospect of isoform specific MAPs as regulators of microtubule function is quite plausible. Indeed, one can imagine the expression in any particular cell of multi-tubulins all of which can assemble in different classes of microtubules, but sorting of the MAPs into different cellular compartments, conferring specific properties on the microtubules they interact with. Moreover, differential expression of various isotypes in different cells[132], together with the observation that the chick haemopoeitic β6 is kinetically different *in vitro* than brain tubulin[98,99] argues for functional non-equality amongst various β-tubulins. Finally, the report by Gard and Kirschner of a certain β-tubulin isoform selectively phosphorylated upon cellular differentiation suggests a cellular mechanism capable of distinguishing between various tubulin isoforms[46].

CHAPTER 2

General Methods

Preparation of Microtubule Protein:

Microtubule Protein (mtp) was prepared from 2 days-old-chick brains by two cycles of temperature dependent assembly and disassembly. One hundred chicks were decapitated and their brains were dropped immediately into 100 ml of pre-chilled MEM buffer pH 6.4 containing 0.1 mM DTT and 10 μg ml^{-1} leupeptin. After cooling on ice for 10 minutes, the brains were homogenised by three strokes in a blender, three strokes with Dounce 'A' homogeniser, and two strokes in Dounce 'B' homogeniser. The homogenate was spun at 17,600 xg in a Beckman centrifuge (JA-20 rotor) maintained at 4°C. The supernatant was then assembled at 37 °C for 7 minutes by adding solid ATP to 1 mM. The assembled microtubules were collected by centrifugation for 30 minutes (17,600 xg) at 30°C. The supernatant was discarded and the microtubule pellet was re-suspended in 6 ml of MEM buffer, homogenised through 12 passages in a 10 ml glass homogeniser and left to cold dissociate on ice for 20 minutes. The cold stable pellet was removed by centrifugation at 65,000 xg in an MSE centrifuge (10x10 rotor) maintained at 4°C for 30 minutes. The supernatant obtained was assembled at 37°C for 20 minutes in 100 μM GTP, 1 μM Phospho-enol Pyruvate (PEP) and 1 unit/ml Pyruvate Kinase. The assembled microtubules were collected by centrifugation at 65,000 xg (30°C) for 30 minutes and the microtubule pellet obtained was re-suspended in 3-4 ml of MEM buffer and cold dissociated on ice for 2 hours. After clarifying the cold dissociated mtp by centrifugation at 65,000 xg (4°C) for 30 minutes, the supernatant was adjusted to 67 mM NaCl using a 5 M stock solution and stored in aliquots in liquid nitrogen until used.

Preparation of Detyrosinated Microtubule Protein:

The first cycle microtubule pellet was re-suspended in MM buffer, cold dissociated on ice, and centrifuged (17,600 xg). The supernatant was supplemented with 100 mM GTP, 1 mM PEP, 1 unit/ml pyruvate kinase and 5 $\mu g.ml^{-1}$ Carboxypeptidase A (CPA- bovine pancreas- Sigma), and incubated at 37°C for 20 minutes. The CPA was then inhibited by addition of DTT to 20 mM, using a 1 M stock and further incubation for 10 minutes. After collecting microtubules by centrifugation (65,000 xg, 30 min., 4 °C), the microtubule pellet was re-suspended in MEM buffer and treated as described earlier.

Preparation of Maximally Tyrosinated Tubulin:

Tubulin was enriched for tyrosinated α-tubulin by incubation of mtp with TTL (see next chapter for preparation), tyrosine (0.28 mM), ATP (2.5-5 mM), KCl (150 mM), and $MgCl_2$ (1 mM). A typical incubation mixture contained:

MTP (5 mg ml^{-1})	500 μl
ATP (100 mM)	16 μl
Tyrosine (10 mM)	17 μl
KCl (2 M)	48 μl
$MgCl_2$ (1 M)	3 μl
TTL (65 U/ml)	60 μl

and was incubated for 40 min. at 37 °C.

The extent of tyrosination was determined by including 10 μl of ^{14}C-Tyr (50 μCi / ml), dried under a stream of $N_{2(g)}$, in an assay containing one tenth of the stated volumes. Following incubation, a 50 μl aliquot was pipetted onto a Whatman

3 MM filter disc (2.1 cm), washed with 10 % and 5 % TCA, and counted in 6 ml of scintillant. Such incorporation studies show that the tyrosination state of α-tubulin is increased by about 40 %. When the tyrosinated mtp was to be subsequently used for assembly studies, the amount of TTL was reduced to minimise the inhibition of assembly by the enzyme (Chapter 3) and the mtp was incubated on ice for 20 minutes after the end of the warm incubation, to disassemble any microtubules that might have polymerised, and then desalted on a Sephadex column.

Buffers for MTP preparations:

MEM buffer:

MES-KOH pH 6.4	100 mM
EGTA	2.5 mM
EDTA	0.1 mM
$MgCl_2$	0.5 mM
DTT	1 mM

MM Buffer:

MES-KOH pH 6.8	100 mM
$MgCl_2$	0.5 mM

Assembly of Microtubule Protein:

Prior to assembly, the GTP and GDP component of the mtp were removed by gel filtration chromatography. Typically, 500 μl of about 12 mg.ml^{-1} mtp were eluted through a Sephadex G-50 (Pharmacia) column (250 x 9 mm), pre-equilibrated with MEM buffer containing 67 mM NaCl. Protein concentration was estimated by A_{280} and fractions of highest protein concentration were pooled and supplemented immediately with GTP.

This nucleotide-depleted mtp was assembled with 100 μM GTP and a regenerating system consisting of 1 mM PEP and 1 U/ml pyruvate kinase in a final assay volume of 500 μl. Polymerisation was initiated by placing the assembly mixture in a glass cuvette, pre-warmed to 37 $^{\circ}$C in a Beckman DU-8 spectrophotometer. Kinetics of polymerisation were followed by monitoring the light scattering at A350 nm.

On occasions the mtp was assembled without fractionation on Sephadex G-50. In such cases the mtp would be diluted to the desired concentration with MEM/NaCl buffer and then supplemented with GTP, PEP and pyruvate kinase, before inducing assembly by raising the temperature. In either case, polymer formation was confirmed by electron microscopy.

Electron Microscopy of Microtubules:

Preparation of Grids:

Copper grids (0.5 μm-Taab) were coated with Formvar according to the following scheme. A 3 % Formvar solution in Chloroform was prepared by gentle agitation over a period of 30 min. and then poured into a slide jar. A clean glass slide was immersed in chloroform and once dry, into the Formvar solution for 10

seconds. The slide was taken out of the Formvar solution and excess liquid drained by blotting one edge of the slide with absorbant tissue. After allowing to air dry, the slide was scored on its edges with a sharp razor blade and the Formvar film was pinched off the glass slide in a large Petri dish filled with distilled water and allowed to float onto the water's surface. Grids were placed on the Formvar film which was then adhered to a piece of good quality paper. The grids were allowed to air dry overnight prior to carbon coating at a pressure of 10^{-4} torr. The carbon coated grids were irradiated with UV light for few seconds prior to use.

Sample Preparation:

Microtubules were fixed in glutaraldehyde and negatively stained with uranyl acetate. Typically, 10 μl of assembled microtubules were fixed in 90 μl of 0.1 % glutaraldehyde made in MEM buffer, to give a final protein concentration of 0.1-0.2 $mg.ml^{-1}$. The fixed microtubules were incubated at 37 °C for 30 min. after which a drop was placed on a piece of parafilm using a Pasteur pipette. A grid was then placed on top of the sample drop (carbon side on liquid) and allowed to stand for 1 min., before being consecutively placed on three drops of 1 % uranyl acetate (freshly prepared in dH_2O), for 1 min. each. Excess stain was blotted with a piece of filter paper and the grids were placed in a grid storage box. Microtubules were normally viewed and photographed at a magnification of x10,000.

Polyacrylamide Gel Electrophoresis (PAGE) of Proteins:

Electrophoresis of proteins was performed in slab polyacrylamide gels containing sodium dodecyl sulphate (SDS-Fisons) under denaturing conditions in a discontinuous buffer system. Two types of gel systems were used. For quick separation, "Mighty Small II" (Hoeffer scientific instruments) gel was used, otherwise, a gradient gel system was utilised.

Rapid protein separation:

Below is the recipe for making two 100 x 83 x 1.5 mm gels consisting of a 10 % resolving gel and 4 % stacking gel. Acrylgel and Bis-acryl gel are the commercial name for acrylamide and bis-acrylamide used by 'National Diagnostics'.

Resolving gel:

Acrylgel (30 % w/v)	6.50 ml
Bis acrylgel (2 % w/v)	2.30 ml
3M Tris-HCl buffer pH 8.8	2.50 ml
SDS (10 % solution)	0.20 ml
Distilled water	8.00 ml
Ammonium persulphate (10 %)	0.10 ml
TEMED	7 μl

Stacking Gel:

Acrylgel (30 % w/v)	1.30 ml
Bis-acrylgel (2 % w/v)	0.54 ml
0.5 M Tris-HCl pH 6.5	2.50 ml
SDS (10 %)	0.05 ml
Distilled water	5.60 ml
Ammonium Persulphate (10 %)	30 μl
TEMED	25 μl

The resolving gel was prepared and immediately poured between glass plates. Water-saturated butan-1-ol was layered on top to ensure an even surface. The gel was allowed to polymerise for 1-2 hours at room temperature after which the butan-1-ol was then drained and the stacking gel was poured and allowed to polymerise for one hour.

Gradient SDS-PAGE:

Linear 15 % to 4 % gradient gels were prepared by pouring 15 % and 4 % acrylamide solutions between two 160x180x1.5 mm glass plates (Bio-Rad gel casting system), after mixing in a two well gradient former. The recipe for making one gradient gel is given below:

Resolving Gel:

4 % Solution:

Acrylgel (30 % w/v)	2 ml
Bis-Acrylgel (2 % w/v)	0.8 ml
Tris-HCl (3 M) pH 8.8	1.80 ml
SDS (10 % w/v)	0.15 ml
d H_2O	10.25 ml
Ammonium Persulphate (10 %)	40 μl
TEMED	15 μl

15 % Solution:

Acrylgel (30 % w/v)	7.5 ml
Bis-Acrylgel (2 % w/v)	3.0 ml
Tris-HCl (3 M) pH 8.8	1.80 ml
SDS (10 % w/v)	0.15 ml
d H_2O	2.60 ml
Ammonium persulphate (10 %)	40 μl
TEMED	15 μl

Stacking Gel:

Acrylgel	1	ml
Bis-Acrylgel	0.4	ml
Tris-HCl (0.5 M) pH 6.8	2.5	ml
SDS (10 %)	30	μl
d H_2O	6	ml
Ammonium persulphate (10 %)	30	μl
TEMED	25	μl

Gels were processed as described above.

Electrophoretic Conditions:

Samples for SDS–PAGE were prepared by mixing protein solutions with equal volume of sample buffer:

Tris–HCl pH 6.8	25mM
SDS	4 %
Glycerol	20 %
β–mercaptoethanol	10 %
Bromophenol blue	trace amounts.

After boiling for 2 min., protein aliquots were loaded into the wells at 10 μg per major protein band. The gel was then transferred to the electrophoretic tank, filled with SDS–PAGE tank buffer:

Tris	25 mM
Glycine	192 mM
SDS	0.1 %

Small gels were run at 150 volts for 90 min. For gradient gels, samples were first stacked at 100 volts for 30 min. and the gel was then run at 55 volts

overnight. Alternatively, gradient gels were run at 150 volts for about 6 hours. In all cases electrophoresis was stopped when the tracking dye was about 10 mm from the bottom of the gel. At the end of the run the gels were disassembled, the stacking gel discarded and the resolving gel stained overnight in Coomassie blue staining solution:

Coomassie Blue G-50 (Sigma)	0.025 %
Acetic Acid	15 %
Iso-propanol	25 %

The stained gel was differentiated in several changes of 10 % acetic acid for at least 6 hours (usually overnight). Staining and destaining were carried out at room temp. on a rocker platform.

Electroblot Transfer of Proteins From SDS-Gels (Western Blotting):

Western blotting of proteins onto nitrocellulose (NC) was essentially as described by Towbin *et al*[138]. At the end of electrophoresis the gel was disassembled, the stacking gel removed and the resolving gel placed in Transfer Buffer (TB) for 5 min. with gentle agitation. Meanwhile, a piece of NC (Schleicher and Schull, BA 85 pore diameter 0.45 μm) was cut slightly larger than the gel and soaked in distilled water for 5 min. Blotting was carried out in a Bio-Rad 'Trans Blot Cell' and the blotting 'sandwich' was assembled by laying the gel over the NC sheet (taking care not to trap air bubbles between the gel and the NC), and enclosing them between Scotch Brite and 3MM filter sheets, pre-soaked in Transfer Buffer:

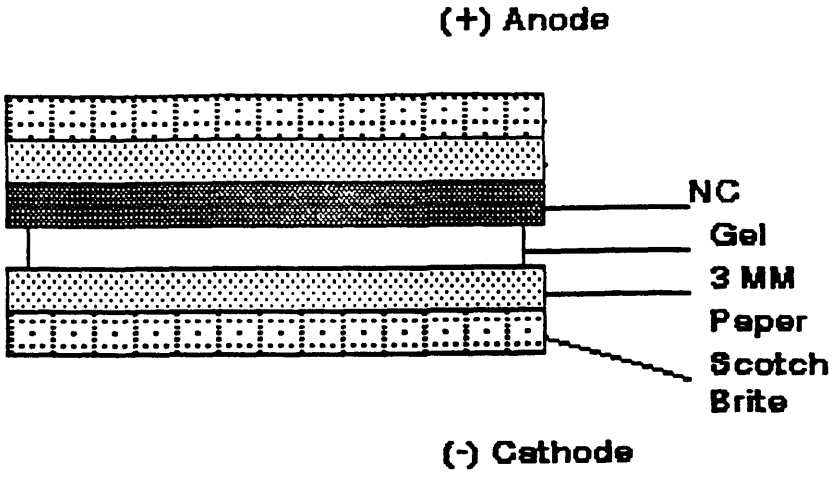

The sandwich was transferred to the blotting cell, with the NC sheet placed on facing the anode. Blotting was carried out at 300 mA for 4 hours or 100 mA overnight. At the end of the run the sandwich was disassembled, the NC was cut around the periphery of the gel with a sharp razor blade and the NC sheet was carefully lifted off the gel and washed in distilled water for 5 min. Protein on the NC sheet was visualised by staining with 0.2 % Ponceau 'S' in 3 % TCA and 3 % Sulphosalicyclic acid (Sigma Ponceau 'S' concentrate) for 2 min. and differentiating in distilled water. Distinct bands were marked with a pencil and the NC sheet was cut into strips. The NC sheets were either placed in TBS-Tween buffer if they were to be immunostained or dried and stored until needed.

Immunostaining of Western Blots:

Proteins immobilised on NC can be visualised by probing with various specific antibodies followed by secondary antibodies to which an enzyme such as Horse Radish Peroxidase is conjugated. The immunostaining regime described below does not require quenching of the NC sheet with BSA or any other protein, provided that the non-ionic detergent Tween-20 (Sigma) is included in all of the washing steps. However, on occasions NC sheets were quenched in Tris-buffered saline (TBS)

containing 1 % skimmed milk (Marvel) and 0.5 % Tween-20 for 1 hour at room temperature.

To immunostain proteins, NC strips that have been stained with Ponceau 'S' were incubated with HST buffer for 15 min., followed by 2 x 5 min. washes in TBS-Tween. The strips were then incubated with the primary antibody (diluted appropriately in TBS-Tween), for 1-2 hours at room temperature, in volumes sufficient to wash over the NC strips during rapid agitation on a rocker platform (5 ml per 80 mm petri dish and 10 ml per 140 mm petri dish). At the end of the incubation, the antibody was removed and the NC strip subjected to 5 x 5 min. washes with TBS-Tween. The NC strip was then incubated with the secondary antibody (peroxidase conjugated), diluted appropriately with TBS-Tween for 1 hour at room temperature. At the end of the incubation the strip was washed with TBS-Tween (5 x 5 min.) and with TBS (1 x 5 min.) prior to incubation with the substrate solution. The peroxidase reaction yields a purple colour which develops over a period of 30 min. The reaction was stopped by washing the NC strip with several changes of distilled water over a period of 10 min. The strip was then allowed to air dry and was stored in the dark.

Buffers for Western Blotting and Immunostaining:

Transfer Buffer:

Tris	25 mM
Glycine	192 mM
Methanol	20 %

Tris-Buffered Saline (TBS):

Tris-HCl pH 7.4	10 mM
NaCl	140 mM

TBS-Tween:

TBS containing 0.1 % (w/v) Tween-20 (sigma).

HST Buffer:

Tris-HCl pH 7.4	10 mM
NaCl	1 M
Tween-20	0.5 % (w/v)

Substrate Solution:

40 mg of 4-Chloro-1-Napthol (Sigma) were dissolved in 6 ml of Methanol, and 94 ml of TBS added, followed by 25 μl of 30 % hydrogen peroxide.

Fractionation of Tubulin by YL1/2 Immunoaffinity Chromatography:

The anti-tubulin monoclonal antibody YL1/2, originally raised against yeast tubulin, is known to bind specifically to α-tubulin with a C-terminus tyrosine, from a variety of eukaryotes[69]. Because of its specificity to tyrosinated or phenylalaninated α-tubulin, such antibody can be utilised to separate tyrosinated α-tubulin from non-tyrosinated tubulin by affinity chromatography.

Preparation of YL1/2 Immunoaffinity Column:

Cyanogen Bromide (CNBr) activated Sepharose-4B (2 g; Sigma) was swollen in 1 mM cold HCl at 4 °C for 1 hour. Meanwhile, 0.5 ml of YL1/2 ascites fluid (Serotec) were run through a Sepharose G-25 column (PD-10; Pharmacia) pre-equilibrated with 0.1 M sodium bicarbonate ($NaHCO_3$) pH 8.3, containing 0.5 M NaCl. The final volume of the eluted antibody was 3.5 ml with a protein concentration of about 4.8 $mg.ml^{-1}$ (as estimated by A_{280}). The swollen gel was then washed with the bicarbonate buffer (100 ml) on a sintered glass funnel, prior to incubation with the antibody at a protein concentration of 0.83 $mg.ml^{-1}$ in a final volume of 20 ml with the bicarbonate buffer. The antibody was coupled to the Sepharose overnight by gentle mixing on a rotatory wheel at 4 °C. The Sepharose was then collected on a sintered glass funnel and further washed with 25 ml of blocking buffer (0.5 M glycine pH 8.0 with 1 M Tris). The A_{280} of the effluent was determined to estimate the amount of YL1/2 coupled to the Sepharose, approximately 90 % of the protein was bound. The gel was further washed with 100 ml of blocking buffer for 45 min. at room temp. to block the excess active groups on the Sepharose. The gel was finally washed with MEM buffer (100 ml), loaded into a column (190 x 20 mm) to give a final bed volume of 5 ml, and equilibrated with 50 ml of Elution Buffer (EB) [0.1 M Mes pH 6.8. 0.1 mM GTP, 2.5 mM EGTA, 0.1 mM EDTA and 0.5 mM $MgCl_2$], and left at 4 °C until used (2 hours).

Preparation of Microtubule protein for Chromatography:

Detyrosinated mtp prepared as previously described was tyrosinated by incubation with TTL (prepared as described in Chapter 3), ATP and tyrosine essentially as will be described in Chapter 3. The incubation mixture consisted of:

Mtp (15 mg.ml^{-1})	0.4 ml
ATP (20 mM)	0.2 ml
Tyrosine (10 mM)	10 μl
^{14}C-tyrosine(50 mci/ml)	90 μl
KCl (2 M)	60 μl
$MgCl_2$	4 μl
TTL (65 U/ml)	40 μl

The above mixture was incubated at 37 °C for 45 min. and then a 30 μl aliquot was applied to a 3 MM filter disc which was processed for scintillation counting to estimate the extent of tyrosination. The mtp was cooled on ice for 30 min. to disassemble any microtubules that might have formed during the incubation at 37 °C and then passed through a Sephadex G-25 column pre-equilibrated with EB. The protein containing G-25 void fraction was subsequently loaded onto the YL1/2 Immunoaffinity column, saving a small aliquot for protein and radioactivity estimation.

Chromatography Conditions:

Tyrosinated mtp (3.5 ml) was loaded onto a YL1/2 column at a rate of 6 ml.hr^{-1}, using a peristaltic pump and the column was subsequently washed with 10 ml of EB at the same rate. Non-specifically and weakly-bound protein was eluted with EB containing 0.1 M KCl (25 ml) at a flow rate of 12 ml.hr^{-1} and

tyrosinated tubulin was then eluted with EB containing 1 M KCl. The A_{280} of each fraction (3.5 ml) was measured against an EB blank and its ^{14}C-Tyr content estimated by counting 100 μl aliquots in a Beckman Scintillation Counter (LS 1808). These counts from liquid samples were confirmed by filter assay of 100 μl aliquots on filter discs (Chapter 3), as free ^{14}C-Tyr present in the fractions could result in artificially high count rate.

A typical YL1/2 column elution profile, for mtp tyrosinated to 30 % and fractionated as described above, is given in Fig. 2.1. The major protein peak eluting in the void volume comprises the non-tyrosinated tubulin (Glu-Tu) and MAPs. The 1 M KCl peak consists of the tyrosinated α-tubulin (Tyr-Tu) which represents 24 % of the total mtp. Note that some activity is recovered with the 0.1 M KCl wash, probably representing tyrosinated tubulin weakly bound to the column.

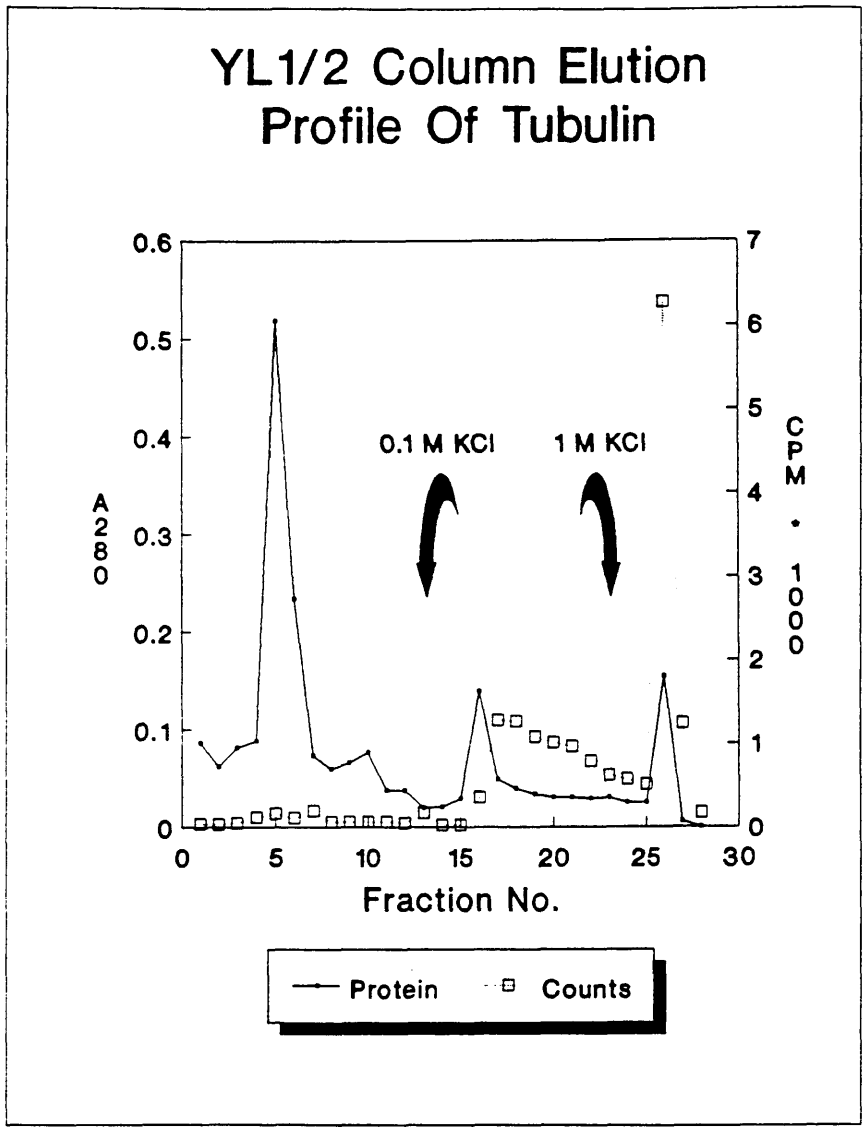

Fig. 2.1:- Separation of tyrosinated and non-tyrosinated tubulin on a YL 1/2 immunoaffinity column. Mtp tyrosinated to 30 % was fractionated on the YL1/2 Column as described in the text. The major protein peak represents Non-tyrosinated tubulin and MAPs. The small peak eluted with 1 M KCl represents tyrosinated tubulin (Tyr-Tu), where most of the ^{14}C-Tyr activity lies.

Phosphocellulose Chromatography of Tubulin:

Microtubule protein was fractionated into tubulin and the microtubule associated proteins (MAPs) using the cation exchanger phosphocellulose. In this case, tubulin elutes in the void volume while the MAPs remain bound and can be eluted with high salt. The dry cellulose phosphate was precycled by gently stirring a pre-weighed amount with 25 volumes of 20 % ethanol, was washed with distilled water for 5 min. and was resuspended after filtering on a sintered glass funnel, and resuspended in 25 volumes of 0.5 M NaOH. The alkali was decanted off after 5 min. and the slurry was washed with several changes of distilled water (5 min. each) until the pH of the supernatant was below 10. The slurry was then resuspended in 0.5 M HCl for 5 min., followed by several washes with distilled water until the pH was above 3. The slurry was then taken up into MEM buffer and titrated to pH 6.4 with KOH. After allowing the slurry to settle for 5 min., the supernatant was decanted off to remove fines. The swollen gel was poured into a 110 x 10 mm column to give a final bed volume of about 6 ml. After equilibrating the column with MEM buffer, the mtp was loaded (maximum 2 mg protein per 1 ml of swollen cellulose) and eluted with MEM and MEM containing 0.7 M KCl. The purity of the tubulin was confirmed by SDS-PAGE.

MicroHartree Assay For Protein Determination:

Chemical estimation of protein was done using the method of Hartree[58] scaled down for use with small sample volumes containing about 10 μg protein. Basically, ten tubes were set up containing 2-20 μg of BSA using a 1 mg.ml^{-1} stock solution, tubes of unknown samples contained about 10 μg protein. Tubes were set up containing 360 μl of Folin 'A' solution (diluted 1:1 with water), and about 10 μg of the sample protein or 0-20 μl of 1 mg.ml^{-1} BSA. The tubes were incubated at 50 $^{\circ}$C for 10 min., cooled on ice for 5 min., after which 20 μl of Folin 'B' was

added and mixed by vortexing. Exactly 10 min. after the addition of Folin 'B', 600 μl of Folin 'C' were added followed by vortexing for 10 seconds. The tubes were then incubated at 50 °C for 10 min., followed by cooling on ice for 5 min., prior to reading the absorbance at 650 nm against the blank assay that contained no protein.

Solutions For MicroHartree:

Folin 'A':

K,Na tartrate	2 g
Na_2CO_3 (anhydrous)	100 g

Dissolved with 500 ml of 1 M NaOH and adjusted to 1 litre with dH_2O.

Folin 'B':

K,Na tartrate	2 g
$CuSO_4.5H_2O$	1 g

Dissolved in 90 ml of water and 10 ml of 1 M NaOH.

Folin 'C':

Folin–Ciocalteau reagent (BDH) diluted 1 vol. + 15 Volumes of dH_2O immediately before use.

CHAPTER 3

The Tyrosinating Enzyme: Tubulin Tyrosine Ligase.

INTRODUCTION:

Addition of a tyrosine residue to the C-terminal of α-tubulin is carried out by the enzyme Tubulin Tyrosine Ligase (TTL)[136]. This enzyme, first demonstrated to be present in vertebrate neuronal tissue, is now known to be present in lower eukaryotes such as sea urchin[74], *Trypanosoma brucei*[118] and *Crithidia fasiculata*[28]. The enzyme is also present in many vertebrate non-neuronal tissues[1,136].

TTL is a protein with molecular weight of about 40,000[44,100,125] . It can catalyse the tubulin tyrosination reaction in the presence of tyrosine (Km=30 μM), ATP (reported Km=8.5[44,100] and 750[10] μM). The enzyme can also catalyse the addition of other aromatic amino acids and their derivatives such as phenylalanine (Km=1.20 mM)[10,5] and dopamine (Km=0.16-1.2mM)[10]. The optimal pH for the enzymic reaction is 8, with another peak of activity around pH 6.5[80]. TTL can also catalyse the removal of a tyrosine residue from the C-terminal of α-tubulin (reverse of the tyrosination reaction), although this requires high levels of ADP and free phosphate[44,136].

Tubulin Tyrosine Ligase is quite specific for tubulin. The enzyme will not tyrosinate peptides with the same C-terminus amino acid sequence as detyrosinated tubulin[149], neither will it act on decayed tubulin such as tubulin stored at pH above 7.5[136]. The specificity of the enzyme is thought to be due to a stable complex formation between TTL and the β-tubulin subunit during the course of the reaction[149]. The region of the enzyme responsible for the formation of this stable complex is distinct from the region responsible for ligating the tyrosine residue onto the C-terminus glutamic acid[149]. The tubulin substrate of TTL seems to be the

dimeric species[5,10,44], as enhancement of the microtubule assembly leads to a decline in the degree of tubulin tyrosination[5]. Specificity of TTL for dimeric tubulin rather than tubulin in a polymer is probably due to a conformational change in the β-tubulin subunit upon polymerising, preventing the formation of TTL-β-tubulin complex[149].

Furthermore, the soluble pool of cytoplasmic tubulin contains a fraction which is not a substrate for the enzyme[5,10,44], not more than 50 % of tubulin can normally be charged up with tyrosine *in vitro*, although in some organisms[24] or under conditions of cellular differentiation[136] as much as 85 % tyrosination of tubulin has been reported. The level of TTL activity, tyrosinated, potentially tyrosinable and non-substrate tubulin has been shown to vary during development *in vivo*, with the highest levels TTL activity and tyrosinated tubulin being present in embryonic stages and declining considerably during adulthood[10,114].

Purification of TTL to homogeneity (as judged by SDS-PAGE) has been achieved using three different procedures. The first purification scheme utilises one anion exchange chromatography step, followed by ATP and tubulin affinity chromatography to yield an enzyme which is 8,100 fold purified[44,100]. However, the yield from this procedure is low and the pure enzyme is very unstable with most of the activity decaying within weeks. The second purification procedure utilises, in addition to the anion exchange and ATP affinity chromatography steps, glycerol gradient centrifugation, phosphocellulose chromatography and affinity purification on a Tyrosyl-aminohexyl column to produce an enzyme which is stable upon storage at -80 °C[125]. Although the yield from such a procedure was low (1.6 %), the enzyme was used to raise monoclonal antibodies that have been used for one step immunoaffinity purification of TTL[125].

This chapter will describe purification of TTL according to the procedure described by Murofushi. Such a procedure could be repeated with fidelity up to the

ATP-Sepharose purification step. Subsequent purification on a tubulin-affinity column was not successful in this study.

METHODS:

Assay of TTL Activity:

The assay for the enzyme activity is based on the incorporation of ^{14}C-tyrosine onto the C-terminus of α-tubulin[44,100]. This is determined by incubating TTL with the necessary substrates for tyrosination and estimating the amount of acid insoluble radioactivity incorporated onto tubulin. Typically, a 60 μl assay mixture contained tubulin, Mes pH 6.8 (55 mM) ATP (2.5 mM), tyrosine (0.16 mM), KCl (150 mM), $MgCl_2$ (15 mM) and DTT (15 mM). A typical incubation mixture is given below:

Mtp (5 mg/ml)	20 μl
KMD Buffer	10 μl
ATP (15 mM)	10 μl
$^{14}C/^{12}C$-tyrosine	10 μl
TTL or Enzyme Buffer	10 μl

The assay mixture was prepared on ice and then transferred to a water bath at 37 °C, immediately after the addition of tyrosine. The sample was then incubated for 20 min. after which a 50 μl aliquot was removed with an automatic pipette and transferred to a Whatman 3MM filter disc (2.1 cm), which was dropped into a beaker of 10 % cold TCA (about 10 ml/disc). After 4 x 2min. washes with 10 % TCA and 3 x 2 min. washes with 5 % TCA the disc was air dried and counted in 6 ml of scintillant ('Ready Protein'- Beckman). The discs were allowed to incubate in the scintillant for about an hour before counting to release the protein off the filter disc. Whenever assaying for TTL activity, a control sample was incubated

containing all the components of the reaction, except for TTL, to determine the enzyme activity associated with the mtp. The specific activity of tyrosine in each assay mixture (CPM.nmole^{-1}) was determined by counting an aliquot (5 μl) on filter discs without washing, and used to calculate the molar incorporation.

Buffers for TTL Assay:

KMD Buffer:

Mes	25 mM	pH 6.8 with KOH
KCl	600 mM	
$MgCl_2$	75 mM	
DTT	60 mM	

Enzyme Buffer:

Mes	10 mM	pH 6.8 with KOH
KCl	300 mM	
$MgCl_2$	38 mM	
DTT	28 mM	

Tyrosine Solution:

Stock Tyrosine solution (10 mM) was prepared by dissolving tyrosine in 0.1 M HCl. For the assay ^{12}C-tyrosine was diluted with 10 volumes of ^{14}C-tyrosine (513 Ci/mmol) in sufficient quantities for the assay.

Purification of TTL:

Preparation of Affinity Columns:

ATP is linked to CNBr-activated Sepharose 4B (sigma) through a sebacate linker arm[44,100]. The general scheme of the reaction is outlined below:

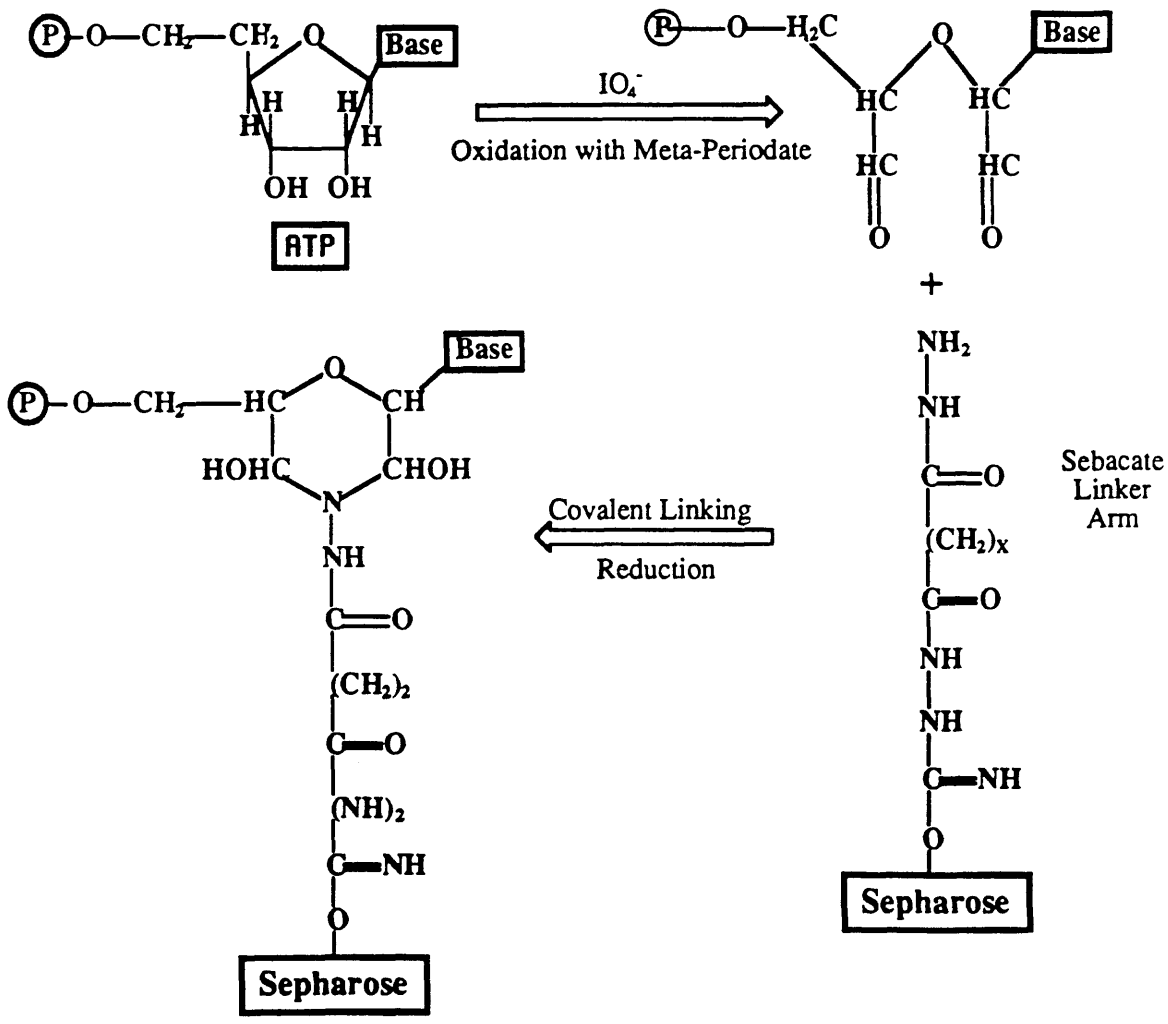

Sepharose-Sebacic-Acid-Hydrizide-ATP

Preparation of the ATP-Sepharose affinity column[44,100] comprises three main steps:

a) preparation of sebacic acid hydrazide

b) preparation of sepharose–sebacic acid hydrazide

c) linking of ATP to the sepharose–sebacic acid hydrazide arm.

a) Sebacic acid hydrazide was prepared from sebacic acid dimethyl ester (SADE) and hydrazine hydrate (85 %)[44,100]. The reaction was carried out in 1 lit. round bottom flask connected to a reflux condenser. Typically, 50 ml of SADE, 100 ml hydrazine hydrate and 100 ml of ethanol were mixed and refluxed for three hours. During the course of the reaction the mixture became cloudy with a fine layer of solid appearing at the bottom of the flask as condensation proceeded, and little liquid remained after 10 min. of the reaction. At the end of the reaction, 150 ml of ethanol were poured into the reaction flask and the solid (sebacic acid hydrazide) was collected on a Buchner funnel using negative pressure. The white slurry was then washed four times with ethanol (100 ml each) and was left standing at room temperature overnight. The slurry was then recrystallised from the minimum volume of an ethanol:water (1:1 mixture) and stored at 4 ^{0}C until used.

b) CNBr–activated Sepharose (1.5 g) was swollen in 200 ml of cold 1 mM HCl solution at 4 $^{\circ}$C, and 1 g of the recrystallised sebacic acid hydrazide was dissolved in 16 ml of glacial acetic acid at room temperature to make a saturated solution. Initially, all of the hydrazide dissolved and then re–precipitated upon further stirring, which was removed by centrifugation at 180,000 xg for 30 min. The swollen Sepharose was then collected on a Sintered class funnel and mixed with 12 ml. of the hydrazide solution. The mixture was stirred overnight in a universal bottle using a wheel rotator. The gel was then washed with 50 ml of 1 M sodium acetate pH 5.0 in acetic acid and then resuspended in 6 ml of the same buffer.

C) ATP was oxidised by stirring 2 ml of a 20 mM solution in water, with 2 ml of 18 mM sodium periodate ($NaIO_4$), freshly prepared in the dark. The mixture was stirred for 1 hour at 0 °C in the dark and then 3.6 ml were added to the Sepharose-hydrazide suspension and the whole mixture was stirred at 4 °C in the dark for a further 3 hr. The gel was consecutively washed with 75 ml of 1 M NaCl, 75 ml of 1 mM EDTA, 75 ml of distilled water, and poured in a 20 x 200 mm chromatography column. The final bed volume was about 6 ml. The amount of ATP coupled to the sepharose was estimated by measuring the A_{257nm} of the effluent obtained after the ATP coupling step, assuming that a 0.1 mM ATP solution gives A_{257nm} of 1.46. Results showed that 23.8 μmoles were coupled to the gel (approximately 4 μmoles/ml wet sepharose), equivalent to 66 % coupling.

Preparation of Tubulin Affinity Columns:

Tubulin affinity columns were made using either horse mtp or chick tubulin. To prepare horse mtp affinity column 1.5 g of CNBr-activated sepharose were swollen in 200 ml of cold 1 mM HCl solution. The gel was consecutively washed with 100 ml each of dH_2O and 10 mM Mes-1mM EGTA-0.5 mM $MgCl_2$ pH 6.8. Horse mtp (2.9 $mg.ml^{-1}$) in this buffer supplemented with 1 mM GTP was added to the swollen Sepharose and the mixture was stirred overnight on a rotator wheel at 4 °C. The gel was washed on a Sintered glass funnel with 200 ml 0.1 M Tris-0.6 M KCl-1 mM EGTA-0.5 mM $MgCl_2$ pH 7.0 for 1 hour at 4 °C, 200 ml of 25 mM Mes-0.6 M KCl-5 mM $MgCl_2$-0.5 mM DTT pH 6.8 for 30 min. and finally, with 100 ml of 25 mM Mes-5 mM $MgCl_2$ and 1 mM DTT pH 6.8. The gel was loaded into a chromatography column (10 x 145 mm) to give a final volume of about 4 ml.

Preparation of chick tubulin affinity column was carried out essentially as described earlier with the exception that the MAPs were removed by phospho-cellulose chromatography prior to coupling to Sepharose. Estimation of the protein concentration from the washed gel after coupling showed that about 85-90 % of the protein was coupled to the gel giving a protein concentration of about 6 mg protein per ml swollen Sepharose and a final bed volume of 4.5 ml.

Purification Procedure:

The TTL was purified from the warm supernatant following the last cycle of microtubule assembly[36,80]. This supernatant, stored at -20 °C in the presence of 50 % glycerol was dialysed, before use against three changes of Running Buffer 1 (RB1): 25 mM Mes-5 mM $MgCl_2$-0.5 mM EDTA-50 mM KCl-0.5 mM DTT pH 6.8, over a period of four hours. The dialysed supernatant was centrifuged at 17600 xg for 30 min. in a Beckman centrifuge (JA-20 rotor) maintained at 4°C, to remove any denatured protein. The supernatant (250 ml) was loaded onto a 330 ml Q-Sepharose cation exchange column (Pharmacia), pre-equilibrated with 1 lit. of RB1, at a rate of 20 $ml.hr^{-1}$. After washing the column with one bed volume of RB1, the bound protein was eluted with 1200 ml of 50-500 mM linear KCl gradient at a rate of 225 $ml.hr^{-1}$, collecting 9.4 ml fractions at 4 °C. The A_{280nm} of each fifth fraction was measured against RB1 blank. Every 20 fractions were pooled and assayed for TTL activity as described earlier. The elution profile from the Q-Sepharose column, shown in Fig 3.1, and the activity of the pooled fractions given in table I show that TTL elutes in a broad peak between 0.1-0.25 M KCl, with half of the activity eluting in the void volume. The exact reason for this non-binding fraction activity is unknown, but could represent a different TTL isoform with a pI different from that of the retained fraction.

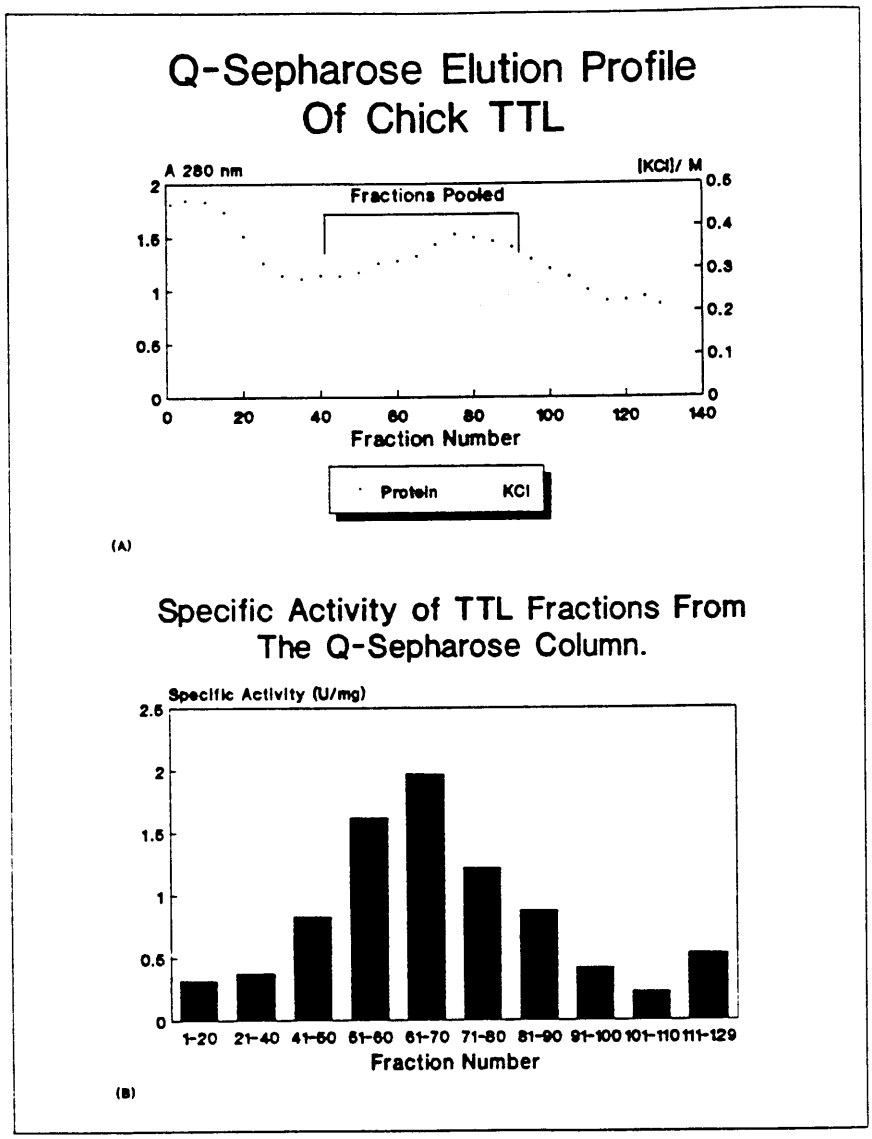

Fig. 3.1:- Elution profile from the Q-Sepharose anion exchange column during the chick TTL purification. Fractions pooled for the sebacate-ATP-Sepharose affinity purification step are bracketed (A). These fractions had the highest specific activity as can be seen from table III.I and (B).

Table *III.I*:- *Activity of TTL fractions from the Q-Sepharose Column. A unit (U) is defined as the amount of enzyme incorporating 1 nmole of tyrosine in 1 min. Fractions pooled and loaded onto the ATP affinity column are shown in bold.*

Fract. Number	Conc. (mg/ml)	Vol. (ml)	Protein (mg)	Activity (U)	Specific Activity (U/mg)
Load	7.82	530	4145	1219	0.29
Effluent	1.68	775	1294	683	0.52
1-20	1.78	178	317	102	0.32
21-40	1.21	178	215	82	0.38
41-50	1.15	91	105	88	0.83
51-60	1.24	91	113	183	1.62
61-70	1.33	91	121	238	1.97
71-80	1.49	91	136	167	1.22
81-90	1.45	91	132	116	0.88
91-100	1.29	91	117	40	0.42
101-110	1.11	91	101	23	0.23
110-129	0.92	68	155	83	0.53

Q-Sepharose fractions of highest specific activity were combined and applied directly to the Sepharose-sebacic acid hydrazide-ATP affinity column, pre-equilibrated with 50 ml of Running Buffer 2 (RB2): 25 mM Mes-5 mM $MgCl_2$-0.5 mM DTT pH 6.8, at a rate of 40 ml.hr^{-1}. After loading, the column was washed with 20 ml of RB2 followed by 100 ml of RB2 containing 0.5 M KCl to elute any non-specific binding. The column was then washed with 20 ml of RB2 containing 100 mM KCl to reduce the salt concentration, and then the enzyme was eluted with 25 mM Mes pH 6.8-25 mM $MgCl_2$-25 mM ATP-100 mM KCl-0.5 mM DTT pH 6.8, at a rate of 17 ml.hr^{-1}, collecting 6-8 ml fractions. The protein concentration of all fractions was measured using the procedure of Hartree described in Chapter 2, and the activity estimated as in Chapter 2.

The enzyme activity eluted with the first six fractions collected (Table III.II). Active fractions from the ATP column were stored overnight in liquid nitrogen and the next day pooled, diluted with equal volume of Running Buffer3 (RB3): 25 mM Mes-5 mM $MgCl_2$-1 mM DTT pH 6.8, to reduce the salt concentration to 50 mM. The fractions were then directly applied to a horse mtp column, pre-equilibrated with RB3 containing 50 mM KCl, at a rate of 25 ml.hr^{-1}. The column was then washed with 25 ml of RB3, containing 100 mM KCl, and the enzyme was eluted with RB3 containing 0.4 M KCl at a rate of 6 ml.hr^{-1}, collecting 3 ml fractions.

Most of the activity passed straight through the column with only a small fraction of the activity eluting with 0.4 M KCl (Table III.III). Although the exact reason for non-binding of the TTL to the mtp column is unknown, it could be due to a low affinity of the chick TTL to horse tubulin, or could result from mtp denaturation during the column preparation.

The effluent from the horse mtp column was stored in liquid nitrogen for 2 days and then reloaded onto a chick tubulin affinity column, under conditions identical to those described above. Some of the enzymic activity decayed upon

storage in liquid nitrogen (about 130 units were lost), probably due to very low concentration of the stored enzyme, the remaining activity (61 units) however, were sufficient fo loading on the chick affinity column. Although more activity was recovered in this case than previously (see Table III.IV), with 12 units binding to the column, it was still a small proportion of the load, i.e. complete binding of TTL to a tubulin affinity column was not attainable under our conditions.

Studies of tubulin tyrosination, used horse TTL prepared by the above procedure, with the omission of the mtp or tubulin immunoaffinity step. Hence, fractions from the ATP affinity column were pooled and concentrated by ultrafiltration using a 250 ml Amicon cell, fitted with PM-10 membrane and desalted by several washes with RB2. The enzyme fraction obtained by such a procedure is quite adequate for tyrosination experiments and is stable at -80 °C.

Samples from the first warm supernatant, Q-Sepharose column and ATP column enzyme fractions were run on an SDS-PAGE gel. The silver-stained gel [Fig. 3.2(a)] showed the ATP column enzyme fraction to consist of a major band having an approximate m.wt. of 43,500 [Fig. 3.2(b)], corresponding to the purified enzyme. In addition there are about six other minor bands corresponding to protein contaminants. It was difficult to obtain reproduceable SDS-PAGE results from the enzyme fractions purified on a tubulin affinity column, due to the low protein concentration of the fractions. Several experiments showed the enzyme fraction to be contaminated with at least two proteins of m.wt. 40-50 Kd, corresponding to similar contaminants previously reported by Schroder *et al.* These workers also reported an unsuccessful purification of TTL on an mtp affinity column.

Table III.II:- *Activity of TTL fractions from the ATP-Sepharose Column. Note that most of the protein elutes in the void volume and that additional TTL activity is lost with the 500 mM KCl wash. Protein concentration was determined by the method of Hartree as in Chapter 2. Fractions 1-6 were pooled and used for the tubulin affinity chromatography.*

Fraction Number	Conc. (mg/ml)	Vol. (ml)	Protein (mg)	Activity (U)	Specific Activity (U/mg)
Load	1.33	455	605	500	0.83
Effluent	1.11	475	527	73	0.14
KCL Wash	0.43	45	19.44	38	1.95
ATP Wash					
1	0.083	6.6	0.55	29	53
2	0.095	7.2	0.68	40	59
3	0.085	7.8	0.66	39	59
4	0.035	8.6	0.30	31	103
5	0.032	8.6	0.28	16	57
6	0.022	8.6	0.19	13	68
7	0.005	8.6	0.04	0	-

Table III.III:- *Activity of TTL fractions from the horse mtp affinity column. Protein concentration was estimated by measuring the* A_{280nm}. *The protein concentration of the load and the effluent were estimated by the method of Hartree. The protein concentration of the TTL fractions might be overestimated due to the presence of traces of ATP.*

Fraction Number	Conc. (mg/ml)	Vol. (ml)	Protein (mg)	Activity (U)	Specific Activity (U/mg)
Load	0.032	100	3.2	192	60
Effluent	0.030	100	3.0	192	64
Salt Wash					
1	0.05	3.2	0.16	2.17	13.6
2	0.28	3.2	0.89	2.54	2.8
3	0.06	3.2	0.19	0	-

Table III.IV:- *Activity of the TTL fractions from the chick tubulin affinity column. Protein concentrations were estimated by the method of Hartree. Notice that some of the activity decayed upon storage.*

Fraction Number	Conc. (mg/ml)	Vol. (ml)	Protein (mg)	Activity (U)	Specific Activity (U/mg)
Load	0.025	105	2.63	61	23.2
Effluent	N/D	105	N/D	45	N/D
Salt Wash					
1	0.0164	3.6	0.059	0	-
2	0.0232	3.6	0.035	6.12	175
3	0.0202	3.6	0.073	6.12	84

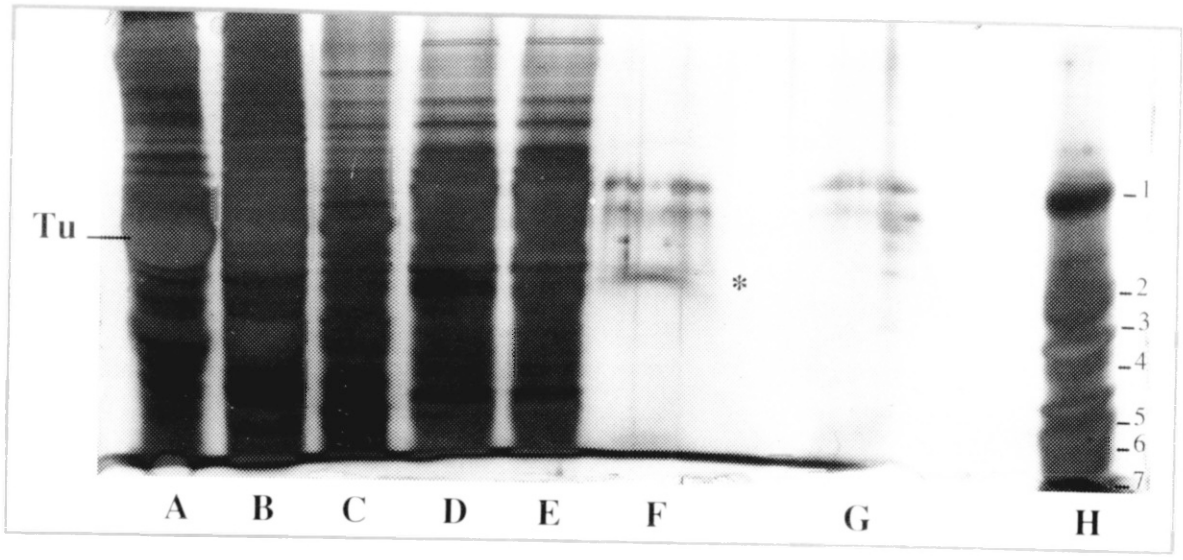

Fig. 3.2 (a):- Silver stained SDS-PAGE of protein *fractions obtained during the various purification steps of TTL. Lanes:- (A) 2x mtp (50 µg), (B) Cold supernatant (150 µg), (C) Q-Sepharose column void (100 µg), Lane (D) ATP-column load (100 µg), Lane (E) ATP column void (100 µg), (F) TTL fraction from ATP column (25 µg), (G) TTL fraction from tubulin column (20 µg), (H) m.wt standards:- Bovine albumin (1), Egg albumin (2), Glyceraldehyde-3-phosphate dehydrogenase (3), Carbonic anhydrase (4), Trypsinogen (5), Trypsin Soybean Inhibitor (6), Lacalbumin (7).*

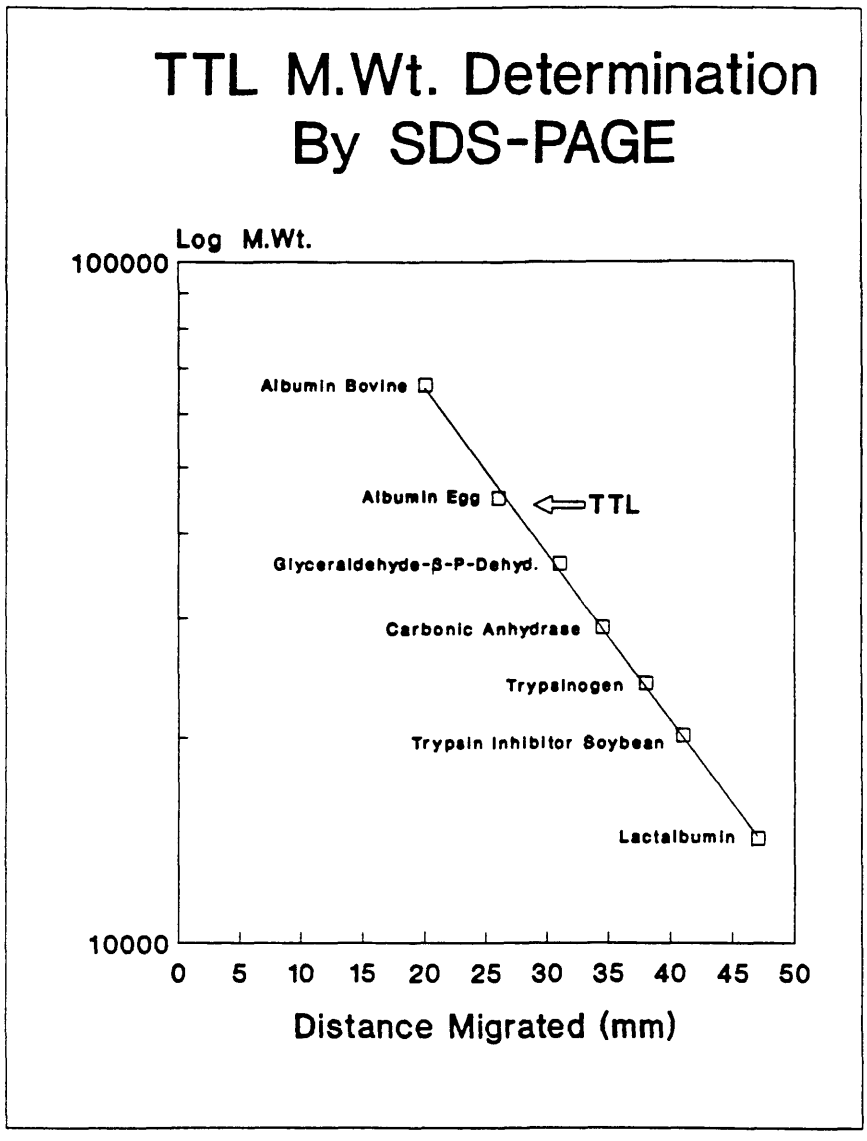

Fig. 3.2(b):- Estimation of TTL m.wt. by SDS-PAGE. Migration distance of the protein markers separated on the gel shown in Fig. 3.2(a) was measured and plotted against the Log of the respective m.wt., to obtain the calibration graph shown. Migration distance of TTL was also measured (28 mm) and this corresponded to a m.wt. of 43,560 daltons (arrow).

Determination of the Km for Tyrosine:

Detyrosinated mtp (3.83 mg.ml^{-1}) was incubated with horse TTL (20 U/ml), ATP (20 mM) and various concentrations of ^{14}C-tyrosine (97.5 μM) in a final volume of 60 μl as described in Chapter 3.

The assay mixtures were incubated at 37 °C for 30 min. immediately after the tyrosine was added, and processed as described previously (Chapter 3), counting 25 25 μl aliquots. Table V gives a summary of the results which were then used for a Lineweaver-Burk "double reciprocal plot" to estimate the Km for tyrosine. Such a plot, fitted using least squares regression analysis, is shown in Fig. 3. The straight line obtained gives a Km for tyrosine of approximately 27 μM. A Km value of 38 μM was obtained by the Direct-Linear plot of Cornish-Bowden.

Table III.V:- *Results From the tyrosine Km estimation experiment. Initial rates (vo) were expressed as nM tyrosine ligated onto tubulin per minute. Each value is an average of two.*

Assay	[Tyr] (μM)	Tyr Ligated (Pmoles/25μL)	Initial Rate (Vo) (nM.min^{-1})	1/Vo (nM^{-1}.min)	1/[Tyr] (μM^{-1})
1	4.875	8.72	17.44	0.0573	0.2051
2	9.750	12.99	25.98	0.0385	0.1026
3	14.625	19.44	38.88	0.0257	0.0684
4	19.500	28.83	47.66	0.0210	0.0513
5	24.375	25.81	51.62	0.0194	0.0416
6	29.250	37.45	74.90	0.0134	0.0342

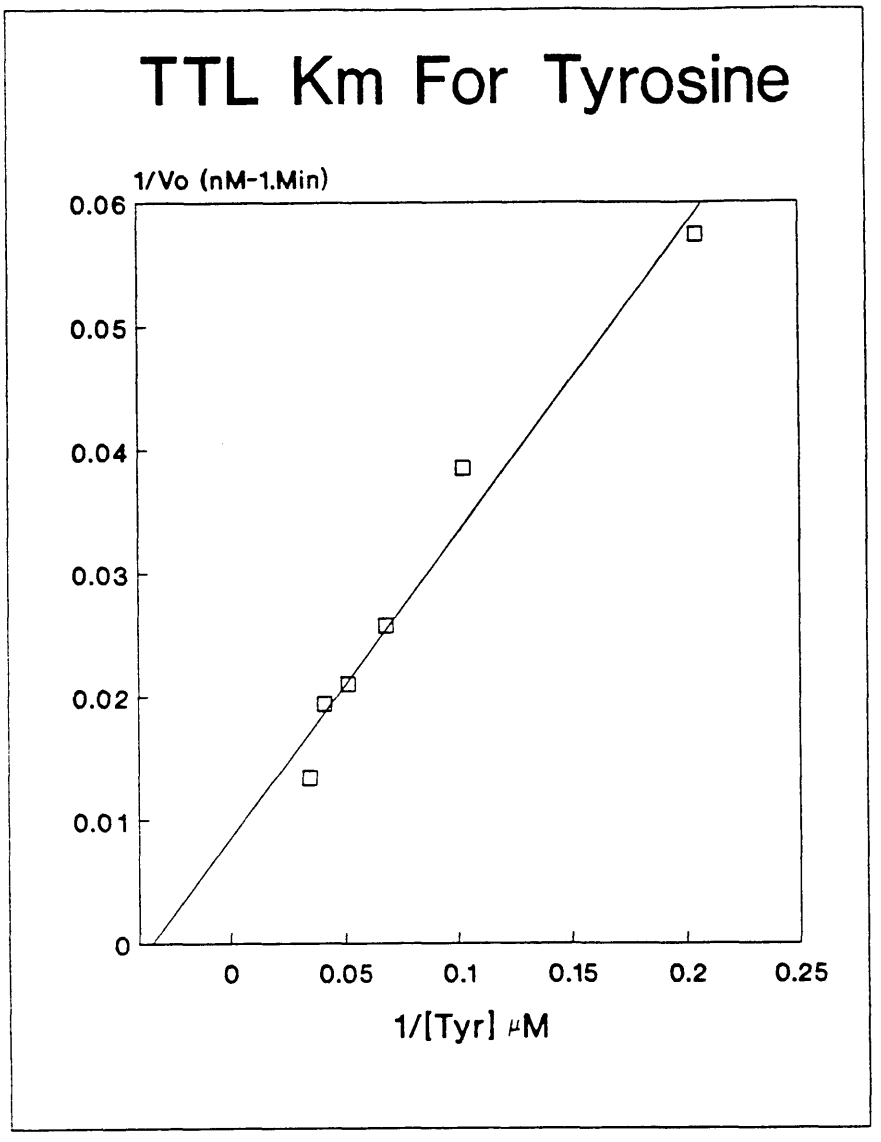

Fig. 3.3 :- ***Estimation of the TTL Km for tyrosine by a Lineweaver-Burk plot.*** *Each point is an average of two measurments. The x-axis intercept corresponds to a Km value of about 27 μM.*

Determination of the Km for ATP:

Tubulin Tyrosine Ligase that has been purified on an ATP-affinity column and concentrated in an amicon cell was used for this Km determination. This enzyme fraction was found to be contaminated with trace amounts of ATP from the ATP-affinity chromatography purification step and therefore, it was necessary to eliminate this contaminating nucleotide prior to the determination of the Km. Furthermore, it was necessary to remove any exchangeable GTP present in the tubulin fraction as this could partially replace ATP in the tyrosination reaction. Finally, it was necessary to eliminate any ATPase activity present in the twice-cycled mtp as this might lead to an overestimation of the Km value.

Removal of the ATPase activity was achieved by fractionating tubulin on a phosphocellulose column, such treatment yielded tubulin devoid of MAPs and the associated enzymic activities. Elimination of the contaminating nucleotide from the TTL fraction and tubulin was achieved by treatment with the Charcoal Norit 'A'. This was necessary as the enzyme is not stable against prolonged dialysis or repeated desalting in a Centricon cell. Below is an outline of the experimental procedure utilised for the determination of the ATP Km.

Twice-cycled mtp, detyrosinated by CPA treatment, was fractionated on phosphocellulose as described in Chapter 2 and the eluted tubulin was supplemented with $MgCl_2$ (10 mM). TTL (20 μl, 60 U/ml) and phosphocellulose purified tubulin (200 μl, 3.0 $mg.ml^{-1}$) were incubated with 50 μl of 10 % Norit 'A' (Aldrich chemicals) suspension prepared in MEM buffer. The Norit 'A' was pelleted (9,950 xg, 3 min., 4 $^{\circ}C$) and the supernatant was re-extracted with Norit 'A'. Successive re-extraction led to protein loss: a third treatment of the protein reduced the protein concentration to only 0.75 $mg.ml^{-1}$. Moreover, it was necessary to mix the TTL with tubulin prior to the Norit 'A' treatment, as treatment of TTL on its own with the charcoal leads to the complete loss of the enzymic activity.

Six assays containing tubulin/TTL mixture (0.7 mg.ml^{-1}), tyrosine (0.16 mM, 8 μCi) and varying concentrations of ATP (0.67–33.33 μM) were incubated at 37 °C for 20 min., and processed as described earlier (Chapter 3). The results of the experiment are given in Table VI and are represented graphically in Fig. 3.4 in the form of a double reciprocal plot. Linear regression analysis of the data points gave a straight line with an x-axis intercept corresponding to a Km value of 8.7 μM. A Km value of 8.4 was obtained by a Direct-Linear plot of the data. This Km value is in good agreement with that reported by Murofushi (8.5 μM)[80], but differs considerably from that reported by Barra *et al* (0.75 mM)[9]. It should be noted that the assay mixture incubated with no ATP did not give any significant count rate, indicating that the contaminating nucleotides have been successfully removed by the Norit 'A' treatment.

Table III.VI:- *Results from the ATP Km determination experiment. Initial rates (Vo) were expressed in $\mu M.min^{-1}$. The background count rate was taken to be 725 CPM corresponding to the count rate of the sample containing no ATP. This background rate was subtracted from all the other count rates. The specific activity of tyrosine in this experiment was 53182 $CPM.nmole^{-1}$.*

Assay	[ATP] (μM)	1/[ATP] (μM^{-1})	Count Rate (CPM)	Initial Rate (Vo) ($\mu M.min^{-1}$)	1/Vo ($\mu M^{-1}.min$)
1	33.33	0.03	3974	0.068	14.70
2	16.67	0.06	3306	0.056	17.86
3	6.67	0.15	2300	0.039	25.64
4	3.33	0.30	1550	0.027	37.04
5	1.67	0.60	793	0.013	76.92
6	0.67	1.50	367	0.0063	158.73

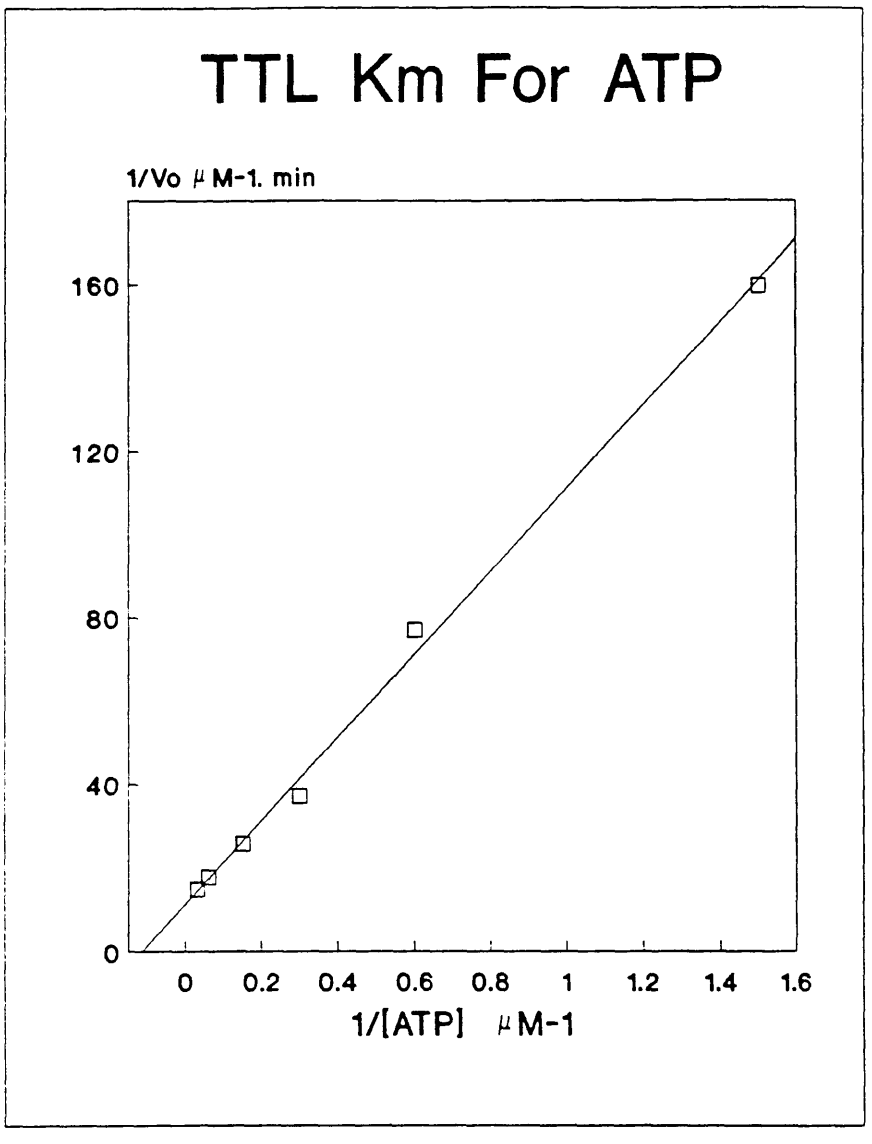

Fig. 3.4 :- Estimation of the TTL Km for ATP by a Lineweaver-Burk Plot. The x-axis intercept corresponds to a Km value of about 8.7 μM.

Utilising TTL to Maximally Tyrosinate Tubulin:

Chick brain tubulin can be maximally tyrosinated (45-55%) by exogenous TTL treatment. It has been widely reported that a fraction of the tubulin (55-45%) does not seem to participate in the tyrosination reaction[5,136]. This could be due to protein denaturation during the course of the reaction or due to polymerisation of a fraction of the subunits. To eliminate these possibilities as the source generating the tubulin non-substrate fraction, detyrosinated mtp was tyrosinated with TTL (10 U/ml) over a period of 60 min., by incubation of detyrosinated mtp (1.3 $mg.ml^{-1}$), ATP (2.5 mM), tyrosine (0.16 mM, 8 μCi/ml).

The whole mixture was incubated at 37 °C for 60 min., removing 40 μl aliquots for processing at various time intervals to follow the course of the reaction. The reaction is complete within the first 8 minutes (Fig. 3.5). Under these conditions 0.18 nmoles of tyrosine (average of 12 values) were ligated per 0.41 nmoles of tubulin, indicating that 45 % of the α-tubulin can accept a tyrosine residue and 55 % acts as a non-substrate for TTL. This non-tyrosinable fraction was observed in all of the tyrosination experiments performed. The scatter of the data in the plateau region of the graph shown in Fig. 3.5 is probably due to small variations in the pipetting volumes during the course of the experiment.

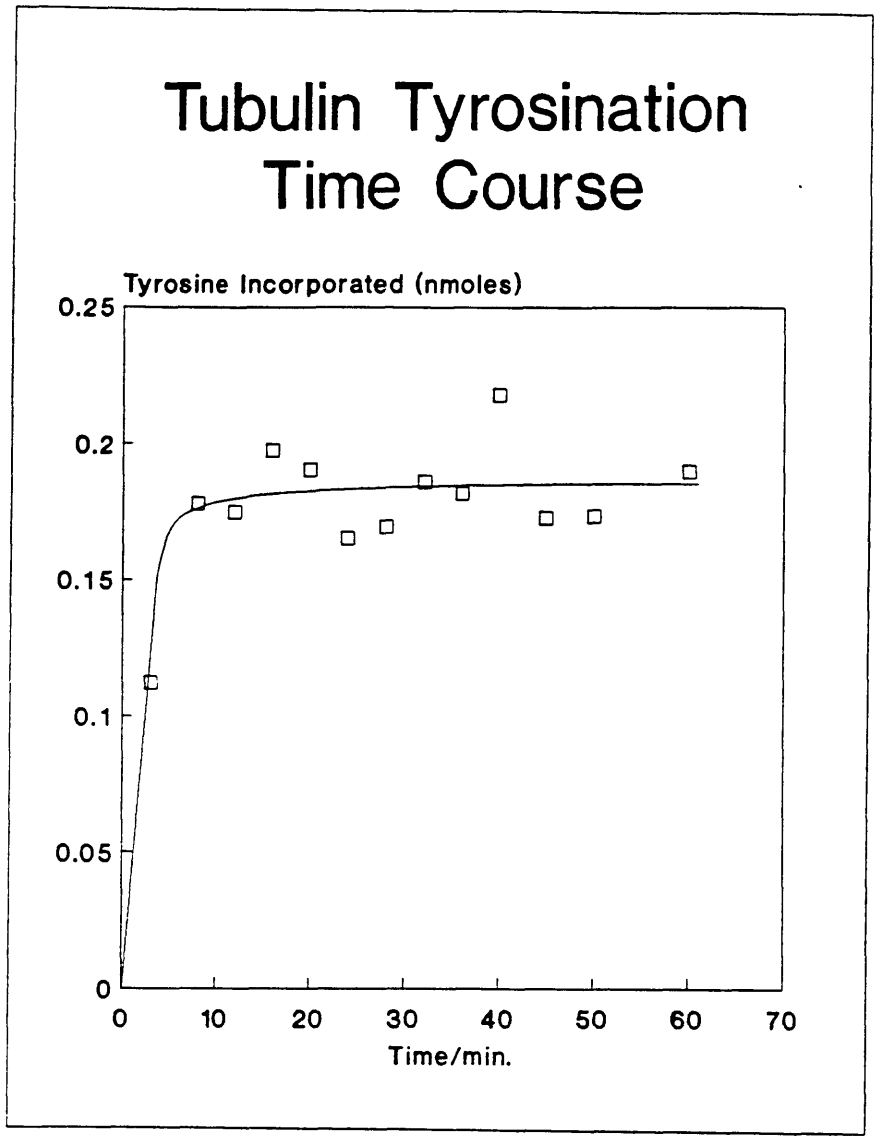

Fig. 3.5 :- Time Course of α-tubulin tyrosination. The tyrosination reaction of twice cycled mtp by TTL was followed over a period of 1 hour. The count rate obtained (CPM) was converted to nmoles of tyrosine incorporated using a specific activity for tyrosine of 84684 cpm.nmole^{-1}. The plateau region of the curve corresponds to an average tyrosine incorporation of 0.183 nmoles (mean of the 12 points in the plateau region), yielding 45 % tyrosination of α-tubulin.

DISCUSSION:

Tubulin Tyrosine Ligase was successfully purified by a repetition of the Murofushi procedure[44,100] up to the ATP-Sepharose affinity chromatography step. Subsequent purification of the enzyme on a tubulin or mtp affinity column was not successful in this study, nor has it been successful in the hands of others[125]. SDS-PAGE showed that the partially purified TTL fraction consisted of a main band of apparent m.wt. of 43,000 corresponding to the enzyme and about six other minor protein contaminants Fig. 3.2 (a). The yield of the purified enzyme was 41% and it had a specific activity of about 150 U/mg, which is higher than that reported by Murofushi for TTL purified to a similar stage (40 U/mg)[100]. Specific activities higher and lower than 150 U/mg were observed on various occasions. The partially purified TTL had a Km for ATP (8.7 μM) and tyrosine (27 μM) similar to those reported by Murofushi for the homogeneously purified enzyme (8.5 μM and 30 μM for ATP and tyrosine respectively)[100]. The measured Km for ATP was different however from that reported by Barra *et al* (0.75 mM)[10], probably due to the presence of ATPase activity in the partially purified TTL fraction used by these workers. It should be noted that any Km estimation for ATP will be slightly overestimated as it does not take into account the reported weak binding of ATP to tubulin[156,157].

The partially purified TTL fraction was utilised to maximally tyrosinate tubulin *in vitro*. The experiment given in Fig. 3.5 showed that tubulin could be tyrosinated with a stoichiometry of about 0.45 mole.mole^{-1}, with approximately 55 % of the tubulin being non-tyrosinable. This non-tyrosinable fraction cannot be attributed to denaturation of the enzyme or the substrate (tubulin) during the course of the reaction as this maximal tyrosination was achieved within the first 8 minutes of the incubation. Furthermore, it is unlikely that the non-tyrosinable tubulin represent a fraction going into polymeric form prior to tyrosination as TTL has been shown to act as inhibitor of tubulin assembly[149] and as tubulin was used in the assay at a

concentration (10 μM) less than that required to give significant assembly. Indeed, tyrosination of chick tubulin devoid of MAPs (see Chapter 4) occurs with a stoichiometry of about 0.5 mole.mole^{-1}, indicating that complete tyrosination does not occur even under non-polymerising conditions.

Recent work by Paturle *et al*[103] utilising tubulin fractionated on a YL1/2 immunoaffinity column showed that there is no relationship between assembly competency of tubulin and its ability to be tyrosinated. These workers demonstrated that tubulin that did not act as substrate for TTL was assembly competent. Moreover, by raising polyclonal antibodies against the non-tyrosinable tubulin fraction, they demonstrated that tubulin which is non-tyrosinable possesses a specific epitope not present on tyrosinable tubulin, as the latter was unreactive with the polyclonal antibodies. Therefore, it seems that non-tyrosinable tubulin defines a sub-population distinct from that acting as TTL substrate.

Tubulin which does not act as a TTL substrate could represent specific α or β-tubulin isotype(s) and could partly be due to decayed subunits that lost the capacity to be tyrosinated upon storage or during purification.

CHAPTER 4

Characterisation of The Heterogeneity of Chick Brain Tubulin.

In Chapter 1 description of the tubulin microheterogeneity in vertebrates and its possible sources were described. In this chapter, biochemical characterisation of the twice cycled chick brain tubulin will be examined using a combination of IEF and western blotting techniques. In particular, the post-translational modification status of the isoforms will be determined and the possible participation of such modifications in generating some of the heterogeneity will be addressed. Finally, the ability of TTL to tyrosinate all of the available α-tubulin isoforms will be investigated.

METHODS:

Isoelectric Focusing of tubulin:

Isoelectric focusing was carried out in vertical slab gels, consisting of 3.5% acrylamide, 0.2% bis-acrylamide, 8 M urea, 1.8% Nonidet P-40, 2.2% ampholines and 0.13 M Bicine. The improved resolution of this IEF regime comes from the utilisation of Bicine as a chemical spacer to enhance the separation of bands. A typical recipe for making one IEF gel is given below:

Urea	11 g
Acrylgel (30 % w/v)	2.70 ml
Bis-acrylgel (2% w/v)	2.30 ml
Nonidet P-40	4.00 ml
Biolyte (4-6)	0.40 ml
Biolyte (5-7)	0.10 ml
Bicine	0.50 g
Deionised Water	1.80 ml

(Biolyte is the commercial name for ampholines used by Bio-Rad).

The mixture was warmed to a temperature not exceeding 34 °C to dissolve the urea, followed degassing in a vacuum dessicator for 5–10 min. After adding 40 µl of 10 % ammonium persulphate and 20 µl of TEMED to initiate polymerisation, the gel was poured between the assembled gel cassette and left to stand at room temperature for a minimum of two hours. After the gel had set, the wells were filled with "Overlay Buffer" and the gel was prefocused at 8 watts constant power for 30–45 min. The anodic and cathodic buffers were 0.09% Phosphoric acid and 0.2 M sodium hydroxide respectively, each made up in deionised water and degassed for at least 30 min. At the end of the pre-run, protein samples were introduced to the wells using a Hamilton syringe, taking care not to disturb the overlay buffer layer. The protein was then focused for 5–6 hours at 8–10 watts constant power with a maximum voltage setting of 1700 volts. At the end of the run the gel was disassembled and either placed in staining solution if the gel was to be stained or Destain Solution II if the gel was to be blotted onto nitrocellulose. Gels at the completion of a run were often cut in half with a sharp razor blade. One half was stained and the other was processed for western blotting.

Sample Preparation:

Protein samples for IEF were prepared by dissolving 60 mg of urea in 50 µl of protein solution, followed by the addition of 100 µl of Sample Buffer. When the protein solution concentration was below 3 mg/ml, samples were prepared by adding the above amounts of urea and Sample Buffer to 500 µl of protein. Samples prepared as indicated can be frozen at −20 °C and used again.

Staining of IEF Gels:

Gels were stained in Coomassie Staining Solution on a rocker platform at room temperature for 2 hours or overnight. Gels were then destained for 1 hour in 2-3 changes of Destain Solution I and then left in Clearing Solution indefinitely. Gels stained overnight are sometimes smeared by precipitating ampholines, in such a case the gel should be destained in Destaining Solution II.

Western Blotting of Isoelectric Focusing Gels:

Tubulin was electrotransferred from IEF gels essentially as described by Otey *et al*[102]. Gels at the end of electrofocusing were placed in Destain Solution II for 1 hour or overnight. Each gel was then placed in deionised water for 1 hour, followed by soaking in Equilibration Buffer for 2 hours. After rinsing the gel in three changes of Transfer Buffer (10 min. each), the gel was layered over a piece of N.C. sheet (slightly larger than the gel) in a tray filled with Transfer Buffer. From this stage onwards, the subsequent steps are identical to those described in Chapter 2.

Autoradiography of Western Blots:

Radioactive Protein transferred to N.C. sheets was autoradiographed by exposing the dry N.C. strips to Hyperfilm-TM (Amersham) autoradiography film for an appropriate length of time at -20 °C, using an intensifying screen. Films were developed in Kodak LS24 developer for 2 min.

Buffers and Solutions for IEF and Western Blotting:

Sample Buffer:

Urea	9.5 M
Nonident P-40	2 % (w/v)
Ampholines (5-10)	2 % (v/v)
β-mercaptoethanol	5 % (v/v)

Overlay Buffer:

Sample Buffer diluted 1 in 3 with deionised water.

Coomassie Staining Solution:

Coomassie Brilliant Blue (G-50)	0.1 %
Methanol	50 %
Acetic Acid	10 %

Destain Solution I:

Methanol	50 %
Acetic Acid	10 %

Destain Solution II:

Isopropyl Alcohol	25 %
Acetic Acid	10 %

Clearing Solution:

Methanol	5 %
Acetic Acid	7 %

Equilibration Buffer:

Tris-HCl pH 8.8	0.37M
β-mercaptoethanol	5 %
SDS	0.3 %

RESULTS:

Bicine Enhances the Separation of Tubulin on IEF Gels:

Tubulin separated on IEF gels without the inclusion of Bicine focuses into a total of 16 narrowly separated bands (Fig. 4.1). Such a pattern of separation is clearly inappropriate for immunostaining studies as the bands are too close to each other. Enhancement of separation on IEF gels can be achieved in several ways such as increasing the gel length, narrowing the pH range and utilisation of chemical spacers (IEF principles and methods-pharmacia). Mixing of Biolytes pH range 5-7 and 6-4 in different proportions, to vary the slope of the pH gradient, had little effect on the band separation (results not shown). However, using Bicine to chemically separate the bands resulted in a drastic improvements in the separation pattern, as shown in Fig. 4.2(a). The bands are now more spaced and an increased number of bands is resolved, indicating that without Bicine more than one band focused in the same region. In the Bicine IEF system a minimum of 20 bands are

resolved. The basic bands (α-tubulins) resolve less sharply than the acidic ones. The reason for this is not known, but could be due to more than one band focusing in the same region.

Isoform Complexity of Tubulin on IEF Gels:

The 8 α-tubulin (basic) and 12 β-tubulin (acidic) bands [Fig. 4.2(a)] were identified by western blotting of the IEF gels as described in Chapter 2 and immunostaining with three different anti-tubulin monoclonal antibodies: YL1/2 (serotec), an antibody specific for tyrosinated α-tubulin; 6-11-B-1 (generous gift from G. Pipperno), an antibody recognising acetylated α-tubulin and KMX-1 (generous gift from K. Gull), an antibody specific for β-tubulin. [Fig. 4.2(b)]. For convenience, the α-tubulin bands will be referred to as α_1-α_8 with α_1 being the most basic variant and β-tubulin bands as β_1-β_{12} in order of increasing acidity. Immunostaining of the blotted tubulin isoforms with YL1/2 [Fig. 4.2(b) lane(1)] using a peroxidase-conjugated anti-rat secondary antibody, revealed the bands designated α_1-α_6. Pre-incubation of the N.C. strip with CPA prior to YL1/2 immunostaining (see methods), eliminated the YL1/2 immunostaining reaction [Fig. 4.2(b) lane (2)], indicating that YL1/2 recognises tyrosinated α-tubulin only. Immunostaining of the tubulin IEF blot with 6-11-B-1 revealed the bands denoted as α_3 and α_5-α_8 [Fig. 4.2(b) lane (3)], while KMX-1 immunostaining of western blots revealed the β-tubulin bands designated β_1-β_{12} [Fig. 4.2(b) lanes (4) and (5)].

Clearly then, as indicated in Table IV.I, tubulin variants α_1, α_2 and α_4 are not acetylated, whilst α_7 and α_8 do not appear to carry a C-terminus tyrosine. This raises the possibility that the two isoforms α_7 and α_8 do not participate in the usual tyrosination detyrosination cycle of α-tubulin and hence, may not function as substrates for TTL.

The pattern of separation of tubulin using this IEF regime is very similar to that reported previously for chick brain tubulin[111], with the exception of at least one more α- and two more β-tubulin isoforms (β_{11} and β_{12}) are resolved. It should be noted that α_1, α_7 and α_8 seem to relatively less abundant than the other α-tubulin variants, whilst α_5 and α_6 have very close pIs and hence are narrowly separated. Furthermore, β_4 and β_6 are the major β-tubulins in the chick brain with β_6, the most acidic of the major β-tubulin variants, being less abundant than β_4, an observation previously documented for chick brain[111]. Also, β_{11} and β_{12} seem to be present in small amounts, being hardly detectable on western blots [Fig. 4.2(a) and 8(b) lanes (4) and (5)], in other experiments however, they were observed to be more abundant. One point to be noted from Fig. 4.2(b) is that there is a minor cross-reaction of YL1/2 and 6-11-B-1 with bands in the β-tubulin region. Although the reason for this minor cross-reactivity is unknown (and could be due to a minor α-tubulin comigrating with the β-tubulin or cross-reactivity of the antibodies with β-tubulin), it is nevertheless useful in the sense that it facilitates the direct comparison of tubulin immunostaining pattern from different N.C. strips, using β_4 and β_6 as reference points. The tubulin immunostaining pattern of IEF blots is summarised in Table IV.I.

Fig.(4.1):- IEF pattern of tubulin separated on gels without the inclusion of Bicine. Twice cycled chick mtp was fractionated on phoshocellulose as in chapter 2. The eluted tubulin was processed for IEF and elctrofocused as described in the text without the inclusion of Bicine. Approximately, 49 μg were loaded onto the gel. The major β-tubulins: β_4 and β_6 are marked with arrows.

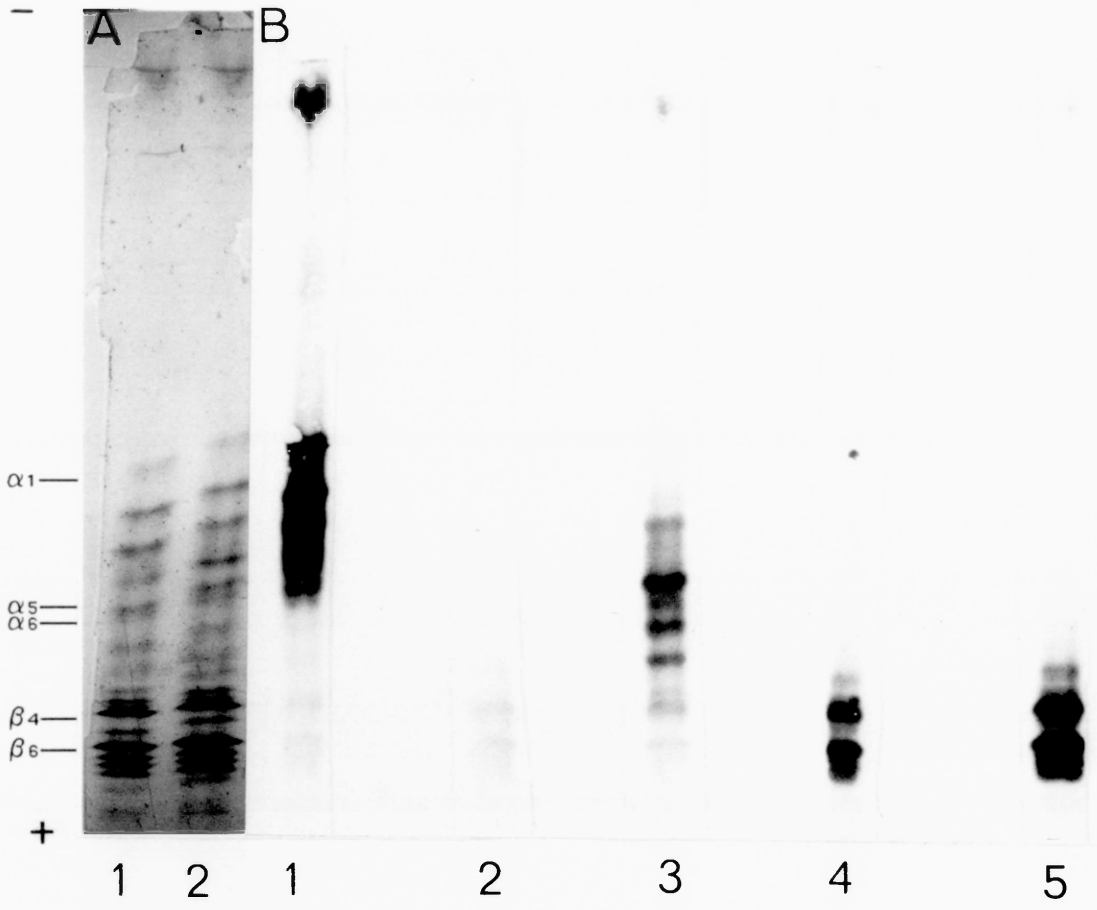

Figure 4.2:- IEF pattern of tubulin separated in the presence of Bicine and its post-transational modification status. *(A) Coomassie stained IEF gel of phosphocellulose tubulin (56 μg and 75 μg lanes 1 and 2 respectively), separated as described in text. (B) corresponding western blots of the gel shown in (A) of lanes loaded with 75 μg of tubulin, immunostained with YL1/2 (lane 1), YL1/2 after preincubation of the blot in CPA as in Chapter 2 (lane 2), 6-11-B-1 (lane 3), KMX-1 (lanes 4 and 5). Tubulin bands are designated α_1-α_8 and β_1-β_{12} in (A), with the major β-tubulins β_4 and β_6 labelled in (B) for refence. YL1/2, KMX-1 and 6-11-B-1 were used at a dilution of 1:1000, 1:500 and 1:10 respectively.*

Table IV.I:- *Staining pattern of the IEF tubulin bands with YL1/2, 6-11-B-1 and KMX-1.* (+) *designates a band positively stained with the antibody and* (−) *refers to a negative reaction with the antibody, weak cross reactions of anti-α-tubulin antibodies with β-tubulin were classified as* (−). *Immunostaining of* β_{11} *and* β_{12} *with KMX-1 was very weak due to the low amount present on the gel.*

Tubulin Band	YL1/2 Reaction	6-11-B-1 Reaction	KMX-1 Reaction
α_1	+	−	−
α_2	+	−	−
α_3	+	+	−
α_4	+	−	−
α_5	+	+	−
α_6	+	+	−
α_7	−	+	−
α_8	−	+	−
β_1	−	−	+
β_2	−	−	+
β_3	−	−	+
β_4	−	−	+
β_5	−	−	+
β_6	−	−	+
β_7	−	−	+
β_8	−	−	+
β_9	−	−	+
β_{10}	−	−	+
β_{11}	−	−	+
β_{12}	−	−	+

Although the α-tubulin staining pattern described in Table IV.I is real, on certain occasions YL1/2 and 6-11-B-1 would more or less immunostain the same bands, thus, both will react with tubulin variants α_1-α_6. The reason for this variation, which is observed between tubulin samples prepared from different batches of chicks, is not known but could be related to variations in the homogenisation regime between different preparations. Nevertheless, the results described in Table VII are reproducible and do not appear to be artifactual.

Are All of The α-Tubulin Variants Tyrosinable:

Results from the previous section showed that the IEF tubulin variants α_7 and α_8 do not react with YL1/2. These variants could represent two tubulin gene products that do not act as substrates for TTL. Two approaches were exploited to examine whether these variants can be tyrosinated. The first approach was to tyrosinate tubulin *in vitro* using TTL and examine the immunostaining of IEF blots of this tyrosinated tubulin. The second approach was to tyrosinate tubulin *in vitro*, followed by fractionation of the tyrosinated and the non-tyrosinated tubulin on YL1/2 affinity column and comparison of the IEF pattern of the two fractions.

Phosphocellulose purified tubulin was maximally tyrosinated with exogeneous TTL treatment (1.15 U/ml tubulin) at 37 °C for 40 min. as described in Chapter 2. Such treatment increased the tyrosination level of the protein by approximately 50 %. After concentrating and desalting in a Centricon PM-30 the protein was subjected to IEF as described in methods section. Results from this experiment are given in Fig.(4.3). The stained portion of the gel [Fig. 4.3(a)] clearly shows the α-tubulin variants α_1-α_6. Bands α_7 and α_8 however, are not visible on the stained gel. Fig. 4.3(b) shows immunostaining of three N.C. strips of the blotted portion of

the gel with YL1/2 [lane (1)], 6-11-B-1 [lane (2)] and YOL1/34 [lane (3)], which is a general anti-α-tubulin antibody. YL1/2 shows immunostaining of α_1-α_6, 6-11-B-1 of α_1-α_7 and YOL1/34 of α_1-α_6 and possibly α_7. Thus, although the presence of α_7 is not seen by the Coomassie staining of the gel, it is nevertheless visible by the 6-11-B-1 staining [Fig. 4.3(b) lane (2)] and weakly by YOL1/34 immunostaining. The variant α_8 was not detected by immunostaining either because it failed to resolve on the IEF or because it was present in undetectable amounts. Furthermore, α_5 and α_6 which are seen close to each other on the IEF gel, immunostain as a single band on the N.C. strips (Fig. 4.3). The immunostaining pattern observed in this experiment is one where 6-11-B-1 stain the same bands as YL1/2. Careful examination of Fig. 4.3(b) suggests at first instance that α_7 might be a non-tyrosinable tubulin isoform as it was stained with 6-11-B-1 but not YL1/2 [Fig. 4.3(b) lanes (2) and (1) respectively). However, the corresponding autoradiogram of the nitrocellulose strips shows that α_7 which was stained with 6-11-B-1 had incorporated ^{14}C-tyrosine and therefore, is tyrosinable. In fact, increased exposure of the autoradiogram shows the presence of α_7 on the N.C. strip stained with YL1/2 [Fig. 4.3(c) lane (1)].

Results from this experiment demonstrated that tyrosination does not contribute towards the isoform complexity of tubulin. Earlier, based on the pI of tyrosine, the prediction was made that this post-translational modification would not cause a shift in the pI of tubulin. The results shown in Fig. (4.3) [and also in Fig. (4.4) of the following experiment] clearly demonstrate that this is so as the same number of tubulin isoforms were observed for non-treated and *in vitro* tyrosinated tubulin.

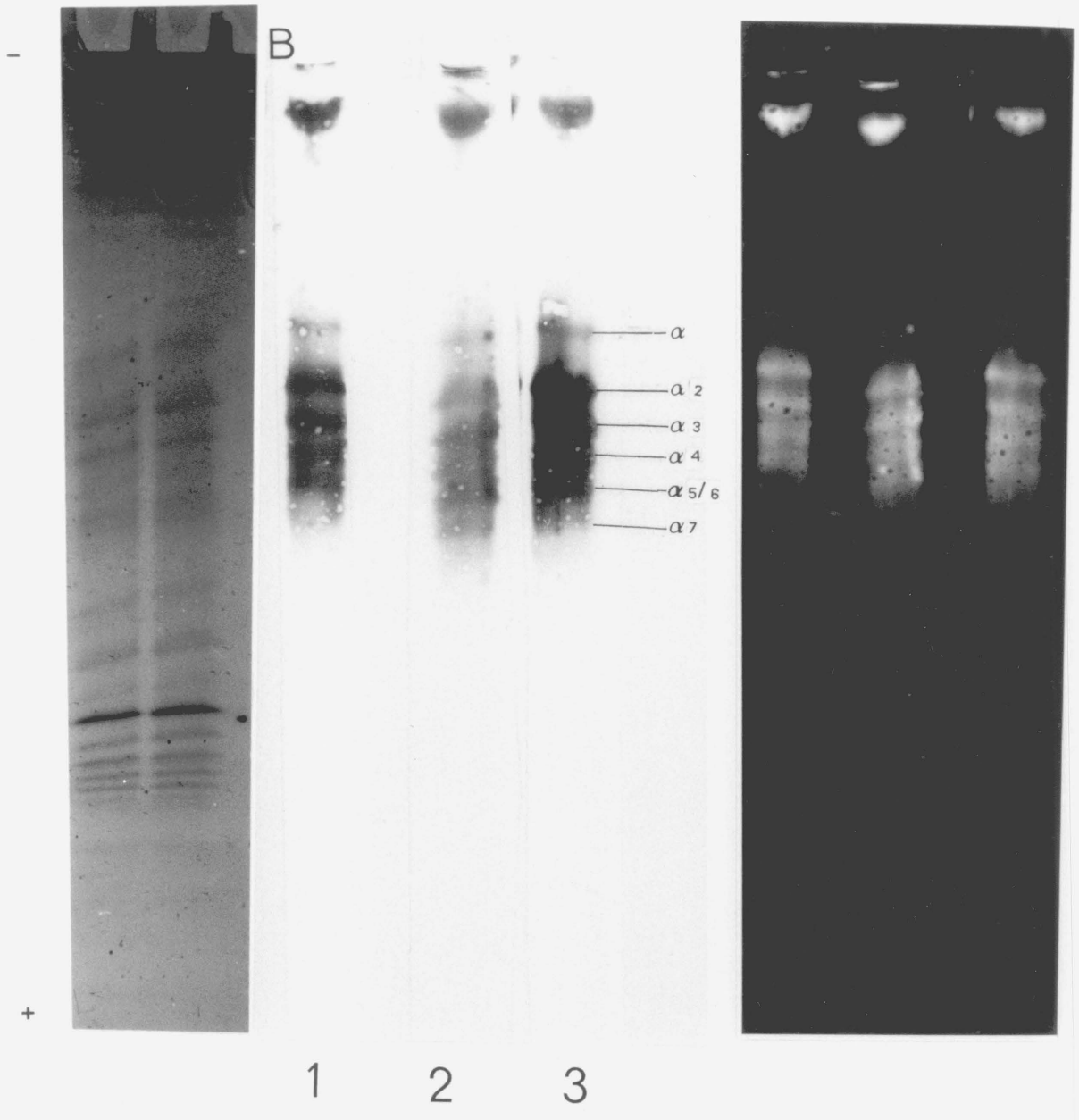

***Fig. 4.3*:- IEF pattern of maximally tyrosinated tubulin.** *Phosphocellulose tubulin was tyrosinated in the presence of ^{14}C-Tyr and processed for electrofocusing as described in the text. The Coomassie stained portion of the gel (A) shows α_1-α_6, but not α_7 or α_8. The corresponding blots (B) were immunostained with YL1/2 (lane 1), 6-11-B-1 (lane 2) and YOL1/34 (lane 3). The corresponding autoradiogram of (B) is shown in (C). Protein loading on gel was 100 μg and autoradiography was for 10 weeks. Note that α_7 is apparent by 6-11-B-1 immunostaining and by autoradiography.*

The second approach consisted of tyrosinating tubulin as described in Chapter 3, followed by fractionation on YL1/2 immunoaffinity column essentially as described in Chapter 2. For this type of experiment it was not necessary to fully charge up tubulin with tyrosine as it is the tyrosine incorporation rather the degree of the incorporation that is being tested.

Mtp fractionated onto a YL1/2 column and separated onto IEF gels after Centricon PM-30 concentration and desalting, shows the heterogeneity pattern typical of chick brain tubulin, with α_1-α_8 reasonably visible [fig. 4.4(a)]. Comparison of the IEF pattern for mtp not bound to the YL1/2 column (defined here as Glu-Tu) and tubulin eluted from the affinity column (Tyr-Tu) shows that it is identical [Fig. 4.4(a) lanes(2-3) and (1) respectively]. This in itself indicates that all of the α-tubulin variants can be tyrosinated. Immunostaining of the corresponding N.C. blots with YL1/2 does not give a significant reaction with Glu-Tu, whilst giving extensive reaction with Tyr-Tu [Fig. 4.4(b) lanes (1) and (2) respectively]. The weak YL1/2 staining of Glu-Tu is probably due to some contamination with Tyr-Tu. YL1/2 is seen to stain all of the α-tubulin variants with α_7 and α_8 staining weakly [Fig. 4.4(b) lane(2)], clearly indicating that they are tyrosinable. Further confirmation to this effect is obtained from the corresponding autoradiogram of the blots [Fig. 4.4(c)] indicating that they have incorporated ^{14}C-tyrosine.

To sum up, experiments whereby phosphocellulose tubulin had been tyrosinated and then separated on IEF gel or whereby mtp was tyrosinated, fractionated on a YL1/2 column and then separated on IEF, showed that all of the α-tubulin variants are capable of incorporating tyrosine. Assuming that the α-tubulin polypeptides expressed in brain focus into distinct bands on IEF gels, then probably a mechanism other than variation in the α-tubulin primary sequence is responsible for the generation of the TTL non-substrate species.

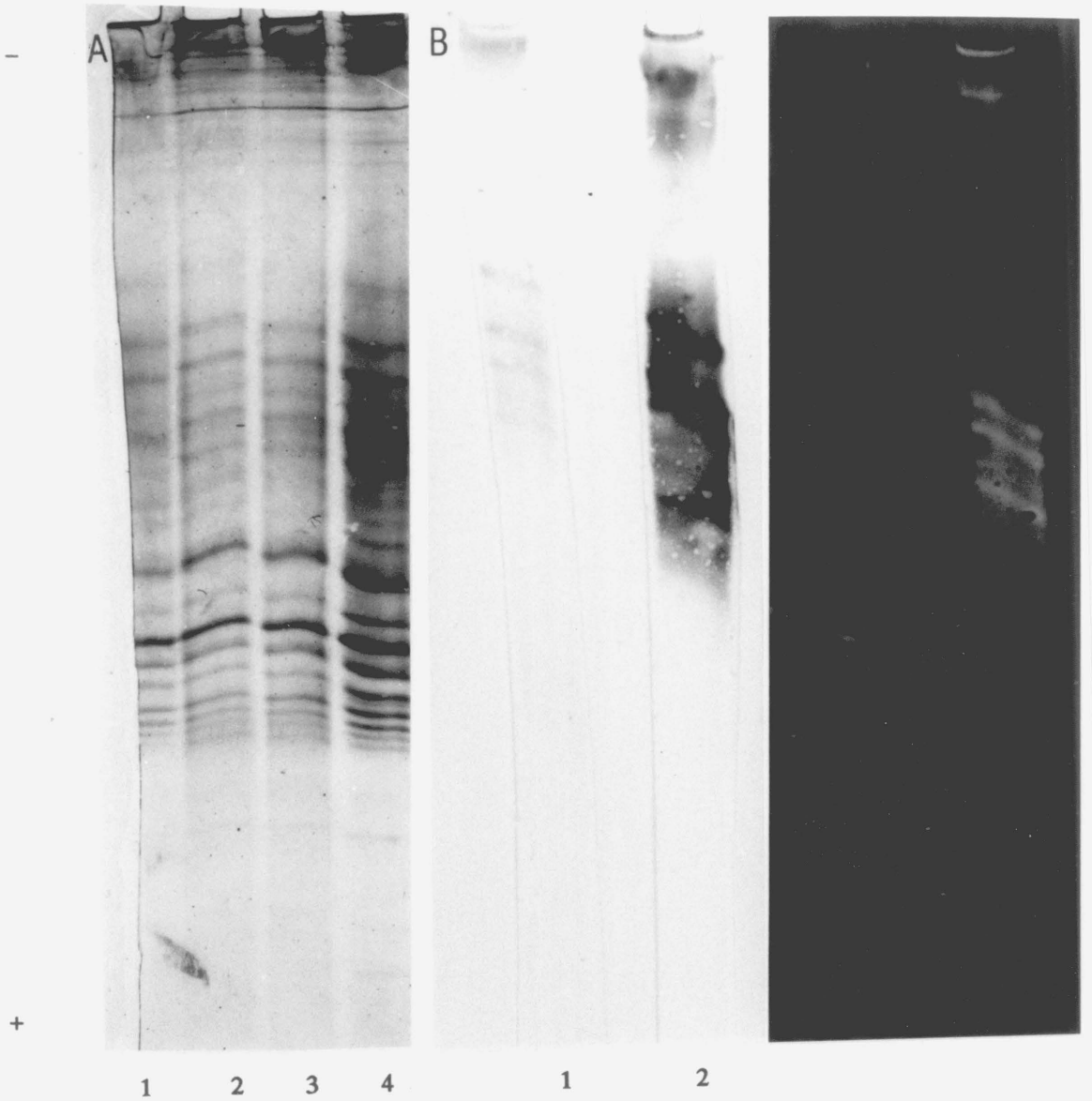

Fig. 4.4:- IEF pattern of mtp fractionated on YL1/2 column. Chick mtp was tyrosinated and fractionated on YL1/2 column essentially as described in Chapter 2, with the exceptions of eluting non-specific binding to the column with 0.2 M KCl and eluting the bound fraction (Tyr-Tu) with 0.5 M KCl wash. (A) shows the IEF pattern of Tyr-Tu (lane 1), Glu-Tu [the non-bound mtp fraction (lanes 2 and 3)] and twice cycled chick mtp, observed by Coomassie staining. (B) shows the YL1/2 immunostaining of western blots of Glu-Tu (lane 1) and Tyr-Tu (lane 2). (C) is the corresponding autoradiogram of (B), exposed for three weeks. Protein loadings in (A) were 61 µg, 43 µg, 86 µg and 83 µg for lanes 1, 2, 3 and 4 respectively. Loadings in (B) were 86 µg and 61 µg for lanes 1 and 2 respectively.

Does Phosphatase Treatment of MTP Affect The Isoform Complexity of β-Tubulin

The number of the tubulin bands resolved by IEF and identified as β-tubulin by KMX-1 immunostaining [Fig. 4.2(b) lanes 4 & 5] far exceeds the number of β-tubulin isotypes identified in chick brain extracts (β_7, β_1/β_2, β_4 and β_3- D.W.Cleveland, personal communication). Thus, the IEF β-tubulin heterogeneity cannot be accounted for solely by the expression of multi-tubulin genes. A mechanism by which additional heterogeneity can be generated is post-translational modification. Phosphorylation, which has been demonstrated to occur on β-tubulin, is expected to cause an acid shift in the pI of the modified protein. To investigate whether β-tubulin phoshorylation contributes towards the isoform complexity observed, the IEF pattern of alkaline phosphatase digested mtp was compared to that of untreated mtp. To treat tubulin with alkaline phosphatase, mtp in MEM buffer pH 7.0. The eluted mtp (5 $mg.ml^{-1}$) was treated with alkaline phosphatase (Boehringer) at 37 °C for 40 min., at an enzyme to protein ratio of 0.05. The digested protein was then processed for IEF as described earlier.

Figure 4.5 shows that the β-tubulin complexity of non-treated (lane A), and alkaline phosphatase treated lane (B) differs in that the intensity of the bands β_7, β_9 and β_{10} and possibly β_1 and β_2 are diminished upon treatment of tubulin with the alkaline phosphatase. This would indicate that these bands are likely to be phosphorylated. There is also a variation in the pattern of α-tubulin complexity upon phosphatase digestion in that only three variants are clearly visible after treatment with the enzyme. However, further experiments will be required to determine whether the α-tubulin isotypes are actually phosphorylated.

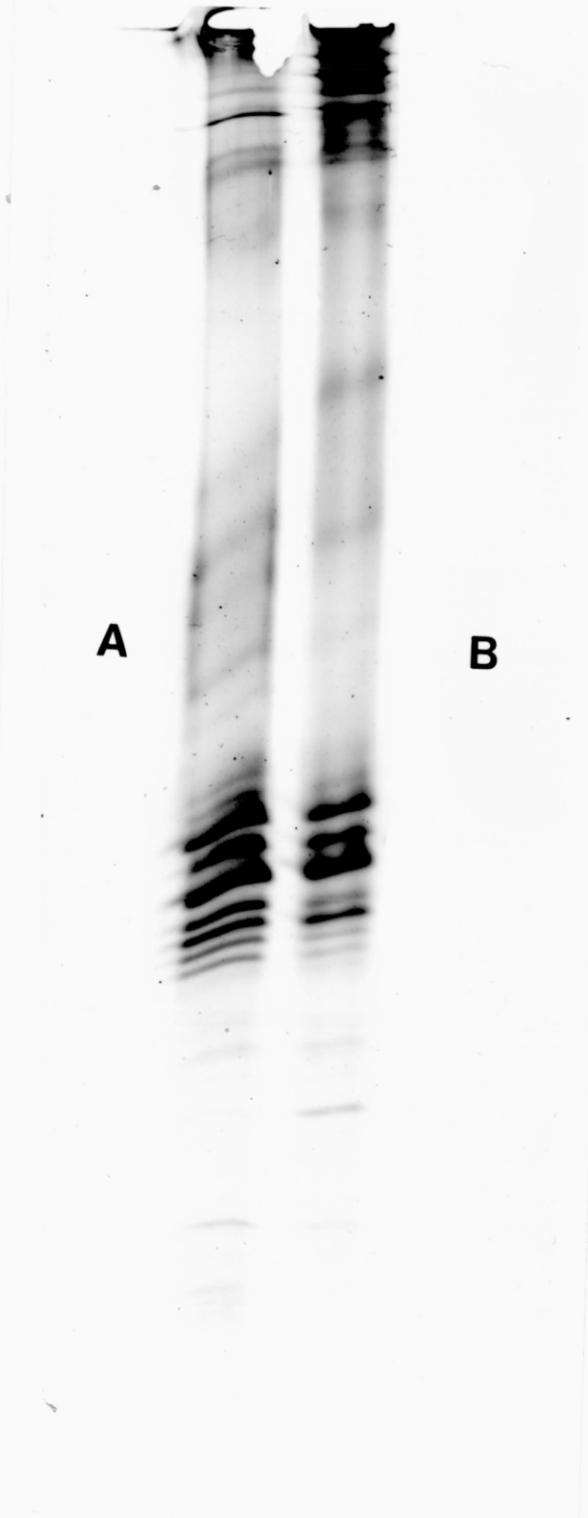

Fig. 4.5:- ***Tubulin IEF pattern after digestion with alkaline phosphatase.*** *Tubulin was incubated with the enzyme, prior to processing for IEF as described earlier. Lane (1) non-treated tubulin, Lane (2) phosphatase digested tubulin.*

Discussion and Conclusions:

This chapter described experiments aimed at characterising twice-cycled chick tubulin using a high resolution IEF system. The results showed that tubulin focuses into a minimum of 8 α-tubulin and 12 β-tubulin isoforms in a pattern similar to that previously reported utilising a lower resolution IEF regime[134]. The tubulin variants termed α_7 and α_8 were not observed on occasions and one possible reason accounting for this is that they might have co-migrated in certain instances with the most basic β-tubulins. Co-migration of the most acidic α-tubulin variants with the most basic β-tubulin variants is known to occur. Edde *et al* have reported the resolution of mouse neuronal tubulin into 8 α and 10 β variants, with the most acidic α-tubulins (which they also term α_7 and α_8) co-migrating with the most basic β-tubulins (termed β_1 and β_2)[40]. Co-migration of α-tubulin variants into the β-tubulin region has also been reported for mtp isolated from chick brain[134]. It is unlikely that α_7 and α_8 are artifactual as they were observed on numerous occasions and as α-tubulin from vertebrate brain is known to separate into 8 variants on IEF gels[134]. The separation pattern of β-tubulin on IEF gels was the same in all instances.

Can this heterogeneity be traced back to the multi-tubulin genes and the polypeptides they encode? Seven genes encode six distinct isotypic classes of β-tubulin in chick (Chapter 1), of which cβ5 and cβ6 are undetectable in adult chick brain extracts, cβ7 represents 50 %, cβ1 and cβ2 25 %, cβ4 25 % and cβ3 only 0.1 % (D.W. Cleveland-personal communication). The major β-tubulin variant observed by IEF is that designated β_6 [Fig. 4.2(a)] and this possibly represents the gene product of cβ7. Furthermore, the second major IEF variant, β_4, probably corresponds to the gene product of cβ1/cβ2 or cβ4. Some or all of the β-tubulin isotypes are probably represented by more than one variant on IEF gels resulting from modifications of these isotypes.

The α-tubulin bands, designated α_1-α_8 were found to be all tyrosinated apart from α_7 and α_8, as demonstrated by immunostaining with YL1/2. The variants α_7 and α_8 were however, shown to be potentially tyrosinable, indicating that all of the α-tubulin IEF isoforms can act as TTL substrates. The fraction of total tubulin (40-50 %, Chapter 3), which cannot be tyrosinated *in vitro* cannot therefore be attributed to specific isoforms.

As previously mentioned (Chapter 1), the α-tubulin gene family in the chick is a set of seven genes encoding six distinct polypeptides. The cα2 gene expression is restricted to testis and should not contribute to the observed IEF complexity[107]. Furthermore, expression of cα4 has not been detected so far, and it is not established yet whether it is expressed at all[108]. This leaves four genes: cα1, the major brain tubulin and cα8 both of which encode polypeptides with a C-terminus tyrosine; and cα3 and cα5/cα6 encoding two polypeptides lacking a C-terminus tyrosine[108,131].

The eight α-tubulin variants observed by IEF most likely represent post-translational modifications of some or all of these gene products. For instance, α_7 and α_8 which were found to be potentially tyrosinable could represent products of the genes cα5/cα6 and/or cα3. Both of these genes encode tubulin lacking a C-terminal tyrosine (the last encoded residue being glutamate)[108], but this does not preclude their tyrosination. Alternatively, they could represent products of cα1 and/or cα8 that have been detyrosinated *in vivo* by the enzyme Tubulin Tyrosine Carboxypeptidase (TTCP) and have an altered pI due to an additional post-translational modification (see below). This would imply that cα5/cα6 and cα3 encode tubulins that do not participate in the usual tyrosination/detyrosination cycle and that the products of these genes have the same pI as other isoelectric variants and hence, would be identified as being able to be tyrosinated. However, when tubulin was tyrosinated *in vitro* with TTL and then fractionationated on a YL1/2 immunoaffinity column the bound (Tyr-Tu) and void (Glu-Tu) protein had an

identical IEF pattern. If the two genes do encode polypeptides that cannot be tyrosinated then the IEF complexity of the Glu fraction should have been less than the Tyr-fraction, which was not the case.

The most probable source for α-tubulin heterogeneity by IEF therefore, is that α_7 and α_8 are products of cα1 and/or cα8 and that they have altered pIs due to an additional post-translational modification. The most probable modification is acetylation as these bands are reactive with 6-11-B-1 (Fig. 4.2). Exactly how much acetylation of α-tubulin contributes towards the IEF heterogeneity is not clear. For the chick tubulin variants α_3, α_5-α_8 to be derived from α_1, α_2 and α_4 by acetylation some or all of the these three variants have to be acetylated at multiple sites to generate species acidic enough to migrate to the region of α_3 and α_5-α_8 on IEF gels. For example, addition of a single acetate moiety to α_4 might generate the variant α_5 but the incorporation of two or more acetates is needed to generate α_6-α_8. The stoichiometry of α-tubulin acetylation is currently unknown, since although it is known to occur on the ε-amino group of Lys-40 in *Chlamydomonas* and this residue is conserved in many α-tubulins[78], incorporation of acetate can also occur at a site near the C-terminus of a mouse α-tubulin[40]. Therefore, α-tubulin can potentially incorporate acetate at more than one site. The fact that tubulin is acetylated with a stoichiometry of 1.1 mole.mole^{-1} does not necessarily indicate that α-tubulin is acetylated at a single site as for example, half of the α-tubulin subunits could be acetylated at two sites. Indeed, examples of chick α-tubulin lacking a Lys at position 40 are known. For instance, the testis specific α-tubulin gene cα2 encodes a polypeptide with a proline rather than lysine at position 40[107]. As for the α-tubulin genes expressed in brain, the complete protein coding sequence is available for two genes only, cα1 and cα5, both of which encode a Lys-40[108].

If acetylation does not occur on multiple sites on α-tubulin, then this modification cannot account on its own for all of the IEF heterogeneity observed and other uncharacterised modifications might be involved.

One cannot rule out that some of the observed heterogeneity might be artifactual, representing chemical modifications of some of the protein during the processing for IEF, even though previous studies have discarded this possibility. Proteolysis is unlikely to have contributed to the observed IEF complexity for several reasons. Firstly, the observed IEF pattern was more or less the same in all experiments performed and experience has shown that this pattern is not dependent on the 'history' of the protein. Furthermore, experiments whereby the supernatant obtained from homogenised calf brain, was left at room temperature for 6, 24 hours and 10 days prior to tubulin preparation showed that in all cases the IEF pattern was identical to tubulin prepared from supernatant in the presence of protease inhibitors[117].

It is therefore unlikely that the observed α-tubulin IEF complexity is artefactual, yet it is difficult to fully assign the heterogeneity to acetylation. It is therefore possible that there is additional source of *in vivo* heterogeneity, either at the transcriptional or the post-translational level. Alternate splicing of tubulin mRNA is a possible but unlikely source of major tubulin microheterogeneity, primarily because one mRNA species has been identified for most of the known tubulin genes. Furthermore, in mouse brain, where four β-tubulin genes have been shown to be expressed, only six translatable β-tubulin mRNAs have been identified.

One modification that might generate IEF complexity is the *in vivo* deamidation of aspargine and glutamine residues[140]. Hydrolysis of the amide groups of these residues to yield aspartic acid and glutamic acid residues is expected to decrease the overall pI of the protein and therefore, alter its mobility on IEF gels. A correlative relationship has been found between the *in vivo* half life of a protein and the amount of amidated residues it possesses[113]. Deamidation of Asn and Gln has been proposed to function as a molecular clock signalling the turnover of a protein and it is possible that some of the tubulin variants observed by IEF represent tubulins

which have been deamidated and therefore, were about to be degraded by the cell's proteolytic machinery. This fits well with recent observations by Lee *et al*, demonstrating that in adult rat, the brain specific β-tubulin isoform is extensively modified in neurons, causing an acid shift in some of the isoforms[79]. Most if not all of this variation has been allocated to the C-terminus, a region which is rich in glutamine residues.

As for β-tubulin, phosphorylation is the only known post-translational modification. However, pre-digestion of mtp with alkaline and acid phosphatase did not result in reduction of IEF isoform complexity, either indicating that phosphorylation does not play a role in yielding extra β-tubulin heterogeneity, or that tubulin is a poor substrate for the above enzymes. It is interesting to note, however that *in vitro* phosphorylation of alkaline phosphatase digested pig tubulin with Casein Kinase II using γ-^{32}P-ATP, showed that the labelled phosphate was incorporated into a single β-tubulin IEF variant[120]. This experiment also demonstrated that pig tubulin can act as a substrate for alkaline phosphatase (enzyme to substrate ratio of 0.05) removing the phosphate moiety from a serine residue. Moreover, experiments whereby cultured mouse neuronal cells were incubated with ^{32}Pi for 9 hours, prior to tubulin extraction showed that only one β-tubulin IEF variant was capable of being phosphorylated[40]. This tubulin variant identified as β_2 has been shown to be derived from a more basic variant termed as β_1 and is said to correspond to the neuron specific isotype cβ4[40]. Although the two studies described with mouse and pig tubulin suggest that at least one β-tubulin variant is generated by phosphorylation, no such variant was identified in the chick by phosphatase treatment. One possibility to account for this could be that dephosphorylation of chick β-tubulin with alkaline phosphatase results in a small undetectable shift in the pI such that no significant alteration in the mobility of the de-phosphorylated species is noticed on the IEF gels. Alternatively, the β-tubulin variant that is phoshorylated might co-migrate with another variant such that upon phosphatase digestion no alteration in the IEF pattern would be observed. Finally,

tubulin phosphorylation in the chick might be different than in pig or mouse. Nevertheless, the main conclusion that can be drawn from these experiments is that β-tubulin is not a major source of tubulin IEF heterogeneity. Clearly, other non-identified post-translational modifications must be involved, similar to those already discussed for α-tubulin

CHAPTER 5

Dynamics Of Tyrosinated And Detyrosinated Microtubules *In Vitro.*

INTRODUCTION:

Cells are known to possess subsets of microtubules that are differentially stable[122]. The mechanism generating such subsets of microtubules is unknown, but one possibility could be the assembly of kinetically heterogeneous dimers into distinct microtubule classes. Covalent modification of tubulin is a potential mechanism through which kinetic heterogeneity could be attained. Amongst all known tubulin chemical modifications, most attention has been focused on the tyrosination of α-tubulin, which is the most understood so far and which affects the C-terminus of the subunit, a region that has been implicated in the binding of MAPs[51,87].

Mammalian cells have been demonstrated to possess subsets of microtubules that are chemically distinct as judged by immunofluoresence[49] and ultrastructural[56] studies: a major Tyr-Tu rich population and a minor, sinous microtubule subset rich in Glu-Tu. The Glu microtubule population has been shown to be generated by post-polymerisation detyrosination of Tyr-Tu[57]. Turnover dynamics of Glu-Tu rich and Tyr-Tu rich microtubules *in vivo* has been investigated in cultured mammalian cells, by monitoring the incorporation of microinjected tubulin, tagged with a fluorescent derivative, onto pre-existing microtubules[20,68,75,112,145]. In one such study[145], TC-7 epithelial cells were microinjected with tagged tubulin, the incorporation of which, onto the ends of pre-existing microtubules, was monitored by double immunofluoresence. Results showed that Tyr-Tu rich microtubules incorporated the hapten-labelled tubulin within 2 min. of microinjection, whilst only few Glu-Tu rich microtubules had done so. Indeed, some Glu-Tu rich microtubules did not turnover even 16 hour after microinjection. Similar results were obtained with cultured Vero cells micro-injected with rhodamine tagged tubulin, whereby the

half-time for microtubule turnover was found to be 10 min. for Tyr microtubules and 1 hour for Glu ones[75]. Therefore, it appears that detyrosinated microtubules *in vivo* are more stable than tyrosinated ones, as they turnover more slowly, with some Glu microtubules not turning over for a whole cell cycle[145]. Glu microtubules were also demonstrated to have greater resistance against depolymerisation by anti-mitotic drugs such as Nocadozole and against dilution induced disassembly, while both populations were equally susceptible to cold induced disassembly[68].

Examination of the effect of tubulin tyrosination on the assembly capability of tubulin *in vitro*, showed that fully detyrosinated protein had the same assembly competency as tubulin that has been tyrosinated to about 37 %[111]. Further *in vitro* investigation of the effect of this modification on tubulin assembly failed to detect any difference in the assembly kinetics of detyrosinated and tyrosinated tubulin (Glu and Tyr-Tu respectively)[77]. *In vitro* assays of assembly showed that Glu-Tu and Tyr-Tu (prepared by exogeneous TTL treatment), assembled to the same extent in the presence of sub-saturating levels of MAPs and with identical rates of polymerisation. When assembly of these tubulins was induced with saturating levels of MAP-2, microtubules formed from both species incorporated the same proportion of the associated proteins[77]. However, small differences were observed between microtubules assembled from pure Glu and Tyr-Tu and sub-saturating levels of MAPs: more high molecular weight MAPs co-assembled with Tyr-Tu rich microtubules than Glu-Tu rich ones[77]. Furthermore, when Glu and Tyr-Tu were assembled with saturating levels of MAP-2 and then pulsed for 60 min. with MAP-2 that had been phosphorylated with ^{32}P-ATP, there was more phosphorylated MAP-2 associated with the Glu microtubules[77]. Moreover, *in vitro* assays of tubulin assembly in the presence of YL 1/2 showed that the antibody had no effect on the rate of nucleation or Co, indicating that tyrosination does not influence either of the two processes[124].

This chapter will describe experiments designed to compare the turnover rate of Glu and Tyr-Tu rich microtubules *in vitro*. Unlike previous *in vitro* work, which relied mainly on bulk turbidimetric measurements[77], the work described here utilises a sensitive test to compare the turnover kinetics of the two microtubule populations. Basically, the turnover dynamics of Glu and Tyr microtubules was studied by monitoring the length re-distribution of sheared microtubules after assembly to steady state. Length redistribution can result from re-annealing[115] or dynamic instability[96]. End to end annealing of microtubules is not a major factor causing length re-distribution, under the conditions used since the chick MAP-2:tubulin microtubules do not anneal and that all of the length re-distribution is a consequence of dynamic instability[22]. The extent of dynamic instability is dependent on the rate constants for subunit addition and loss to microtubules in elongating and shortening phases and the frequency of interconversion between these two phases[96]. As length re-distribution is dependent on numerous kinetic constants, then any difference in these parameters between Glu and Tyr microtubules will be reflected in the rate of re-elongation of sheared microtubules, thereby facilitating direct comparison of the dynamics of the two populations.

Twice cycled mtp is normally tyrosinated at the C-terminus end of α-tubulin to 20 %, primarily because of the loss of tyrosine by the recycling TTCP activity during the warm incubations of the mtp preparation. For the length redistribution experiments, microtubules assembled from non-treated, detyrosinated and tyrosinated mtp were compared for re-elongation after shearing.

Turnover Dynamics of Detyrosinated and Non-treated Mtp:

Twice cycled chick mtp in MEM buffer was detyrosinated by incubation with exogeneous CPA treatment (2.5 $\mu g.ml^{-1}$), for 20 min. at 37 °C, to generate Glu-Tu. CPA was inhibited by further 10 min. incubation with 20 mM DTT. A control sample was incubated without CPA and this represented control-Tu. Both samples were run on a G-50 Sephadex column equilibrated with MEM buffer containing 67 mM NaCl and assembled to steady state at 37 °C with 100 μM GTP, 1 mM PEP and 1 U/ml Pyruvate Kinase. At steady state, microtubules were sheared by 10 passages through a 100 μl Hamilton Syringe and immediately incubated at 37 °C. Aliquots (10 μl) were then taken out at various time intervals and fixed immediately in 90 μl of 0.1 % glutaraldehyde (Chapter 2). Fields of view on the copper grid were chosen solely on the basis of suitability for photography. Microtubules were measured with a ruler on a light box. Microtubules with one end apparent were doubled in length, whilst those with both ends not apparent were ignored.

Digestion of tubulin with CPA removed the α-tubulin tyrosine as it abolished the binding of YL1/2 to tubulin (Fig. 5.4). Assembly profiles of Glu and Tyr microtubules were shown in fig. 5.1 (A), whilst mean length of the microtubule populations at various time intervals are given in table V.I and are represented graphically in Fig. 5.1 (B). Distribution of the microtubule length at times 0,1,2,3,4 and 10 min. post-shearing for both Glu and Tyr microtubules are given in Fig. 5.2 and Fig. 5.3 shows sheared microtubules at 0 - 10 min. post-shearing. Results of this experiment showed that both Glu and Tyr MAP-2 rich tubulin assemble at the same initial rate and to the same extent [Fig. 5.1 (A)]. The identical extent of assembly for both samples indicate that both Glu and Tyr microtubules have the same steady state Co. Furthermore, analysis of the kinetics using a pseudo-first order plot (Chapter 1) showed that both populations have identical values for $k_{+1}[M]$. Moreover, as both samples were assembled from tubulin that has been

subjected to identical treatments and that had similar concentration, then the number of concentration of ends [M], should be identical indicating that the association rate constant (k_{+1}), for both populations is the same. As Co and k_{+1} are the same, it follows that k_{-1} should be identical for both tyrosinated and detyrosinated species. Therefore, turbidimetric analysis of tubulin assembly show that tyrosination does not influence the bulk kinetic parameters measured by such analysis.

The length re-distribution for sheared Tyr and Glu microtubules are virtually the same with the growing microtubules elongating at rates of 0.56 $\mu m.min^{-1}$ and 0.47 $\mu m.min^{-1}$ respectively [Fig. 5.1 (B)]. As length redistribution occurs through dynamic instability and as this is dependent on numerous kinetic parameters (Chapter 1), it follows that these parameters must be the same for both sets of microtubules. Therefore, fully detyrosinated and 20 % tyrosinated microtubules appear to turnover with similar kinetics. It is worth noting that the curve of Fig.5.1 (B) plateaus out after 4 min. which is probably due to the attainment of a balance between the net rates of shrinkage and elongation.

Table V.I:- Mean Length of Sheared Glu and Tyr (20 %) microtubule at 0-10 min. post -shearing.

Time Post-Shearing (min)	Mean Length (Glu MTs) (μm)	Mean Length (Tyr MTs) (μm)
0	0.81	0.62
1	1.21	1.29
2	1.64	1.85
3	2.20	2.20
4	2.97	2.83
10	3.79	3.58

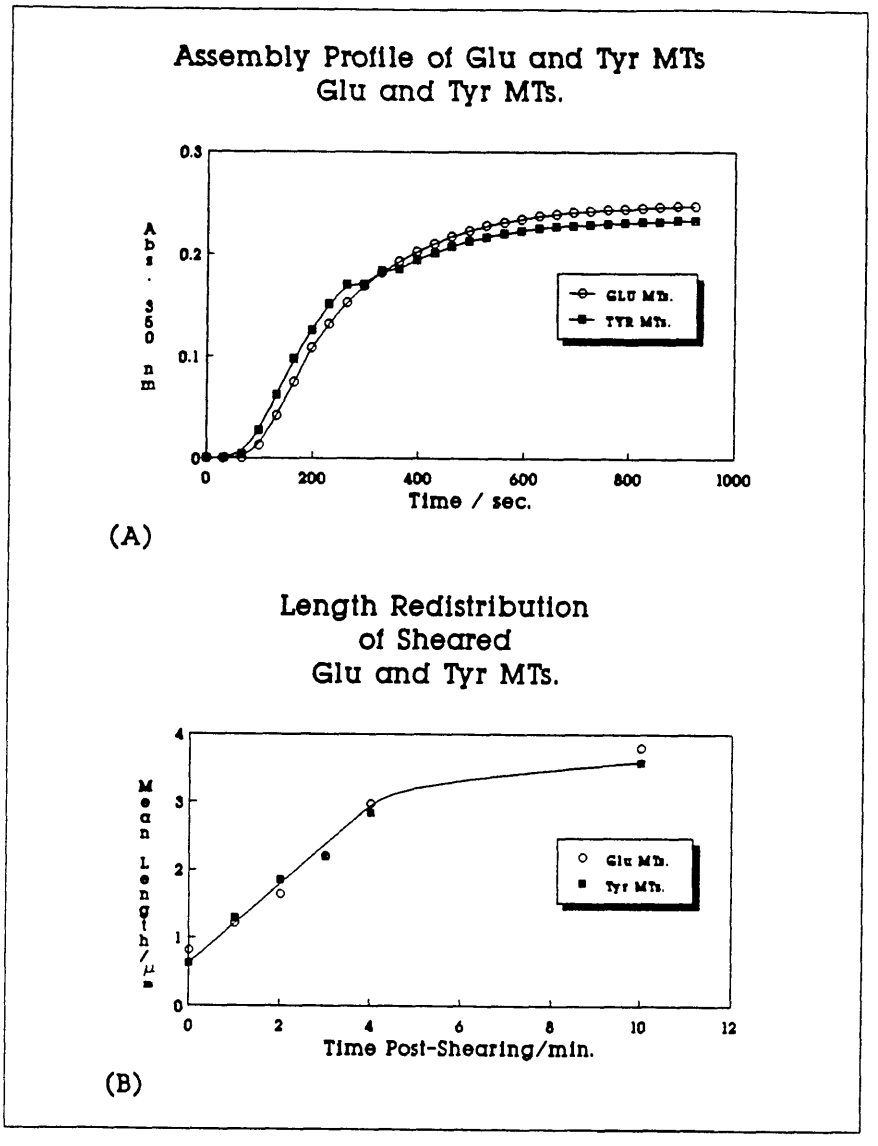

Fig. 5.1:- Assembly and Length Redistribution of Glu and Tyr Microtubules. Microtubules were assembeled from non-treated (20 %) tyrosinated and CPA digested mtp as described in the text, prior to shearing and monitoring length redistribution of sheared the microtubules. (A) assembly profile of microtubules. (B) Mean length variation of sheared microtubules with time.

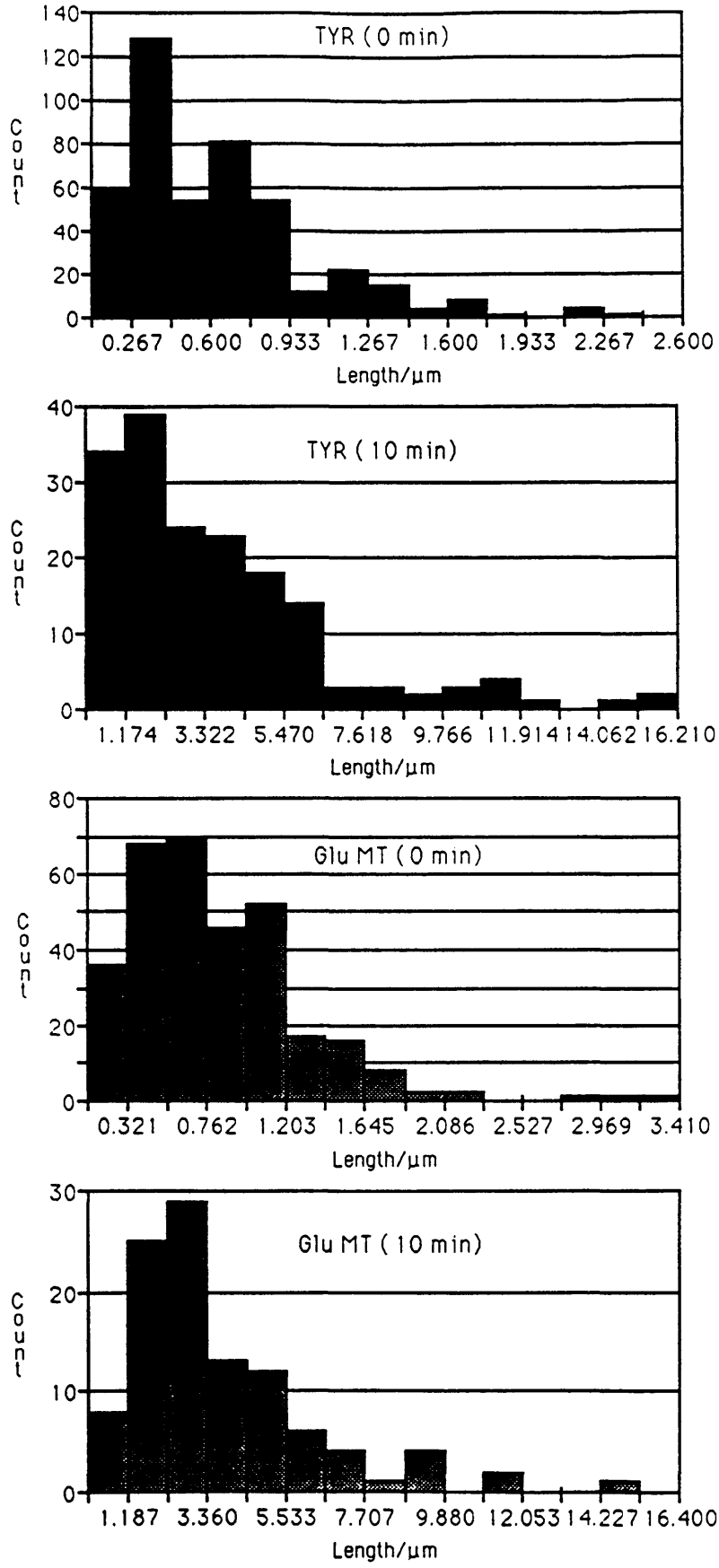

Fig. 5.2:- Length Distribution of Sheared Microtubules at 0–10 min. post shearing. (A) Glu Microtubules, (B) Tyr Microtubules.

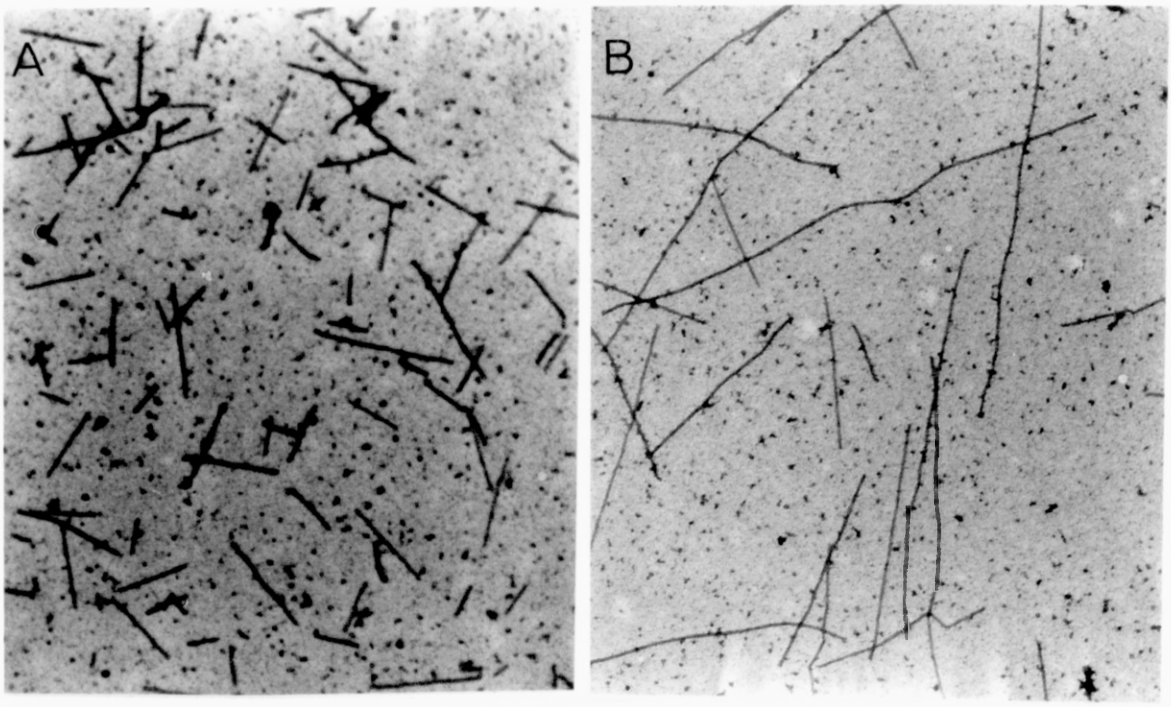

Fig. 5.3:- Electron Micrograph of Microtubules Sheared 10 Times Through A Hamilton Syringe. (A) Microtubules immediately after shearing, (B) Microtubules 10 min. after shearing.

Fig. 5.4:- YL 1/2 Immunostaining of Non-treated and CPA Digested Mtp. Treated (A) or non-treated (B) mtp was run on SDS-PAGE gels, followed by blotting to nitrocellulose and immunostaining with YL 1/2 (1:1000 dilution) and a peroxidase conjugated anti-rat secondary antibody (1:300 dilution) as in Chapter 2.

Turnover Dynamics of Partially and Maximally Tyrosinated Microtubules:

Mtp was maximally tyrosinated by incubation with exogeneous TTL (6 U/ml) at 37 °C for 30 min. as described in Chapter 2. A control sample was subjected to the same treatment omitting tyrosine from the incubation sample. It is important to have TTL in the control sample, as to make sure that any inhibition of assembly by TTL will occur in both samples. The samples were left on ice for 10 min. prior to desalting on a Sephadex G-25 column (Pharmacia PD-10), pre-equilibrated with MEM buffer containing 67 mM NaCl. Whenever tubulin was tyrosinated by TTL, it was found that seeding was required for assembly, as TTL seems to inhibit nucleation. Assembly was initiated in this experiment by the addition of seeds, composed of 10 μl of steady state sheared microtubules, assembled from 5 mg.ml^{-1} mtp for 10 min. with 100 μM GTP at 37 °C. After assembling to steady state, the microtubules were sheared and length re-distribution monitored as described earlier.

Assembly profiles [Fig. 5.5 (A)] show that both microtubule populations assemble to the same extent and at the same rate, although in this experiment there was some 'creep' in the absorbance at steady state for Tyr-microtubules (and later observed for Glu microtubules), which is probably due to some aggregation. Nevertheless, comparison of the two curves prior to creep suggests that both Co, k_{+1} and k_{-1} are the same for both populations.

The mean length of the sheared tyrosinated and maximally tyrosinated microtubules at 0-5 min. are given in table V.II and represented graphically in Fig. 5.5 (B). Length distribution of the microtubules is shown in Fig.5.6 and the rates of microtubule elongation were estimated from fig. 5.5 (B) and these were 0.90 μm.min^{-1} and 0.99 μm.min^{-1} for tyrosinated and maximally tyrosinated microtubules respectively, again indicating that tyrosination has no effect on the kinetic parameters governing dynamic instability and therefore, has no effect on the dynamics of microtubule turnover, in agreement with the results of the previous experiment.

Table V.II:- Mean Length of Sheared Tyr and Tyr-Rich microtubules at 0-5 min. post-shearing.

Time Post-Shearing (min)	Mean Length (Tyr MTs) (μm)	Mean Length(Tyr-rich MTs) (μm)
0	0.75	0.79
1	1.58	1.77
2	2.21	2.82
3	3.33	3.84
4	4.24	4.35
5	4.26	5.10

Table V.III:- Mean Length of Sheared Glu and Tyr (30 %) microtubules at 0-5 min. post -shearing.

Time Post-Shearing (min)	Mean Length (Glu MTs) (μm)	Mean Length (Tyr MTs) (μm)
0	0.81	0.62
1	1.21	1.29
2	1.64	1.85
3	2.20	2.19
4	2.97	2.83
5	3.79	3.58

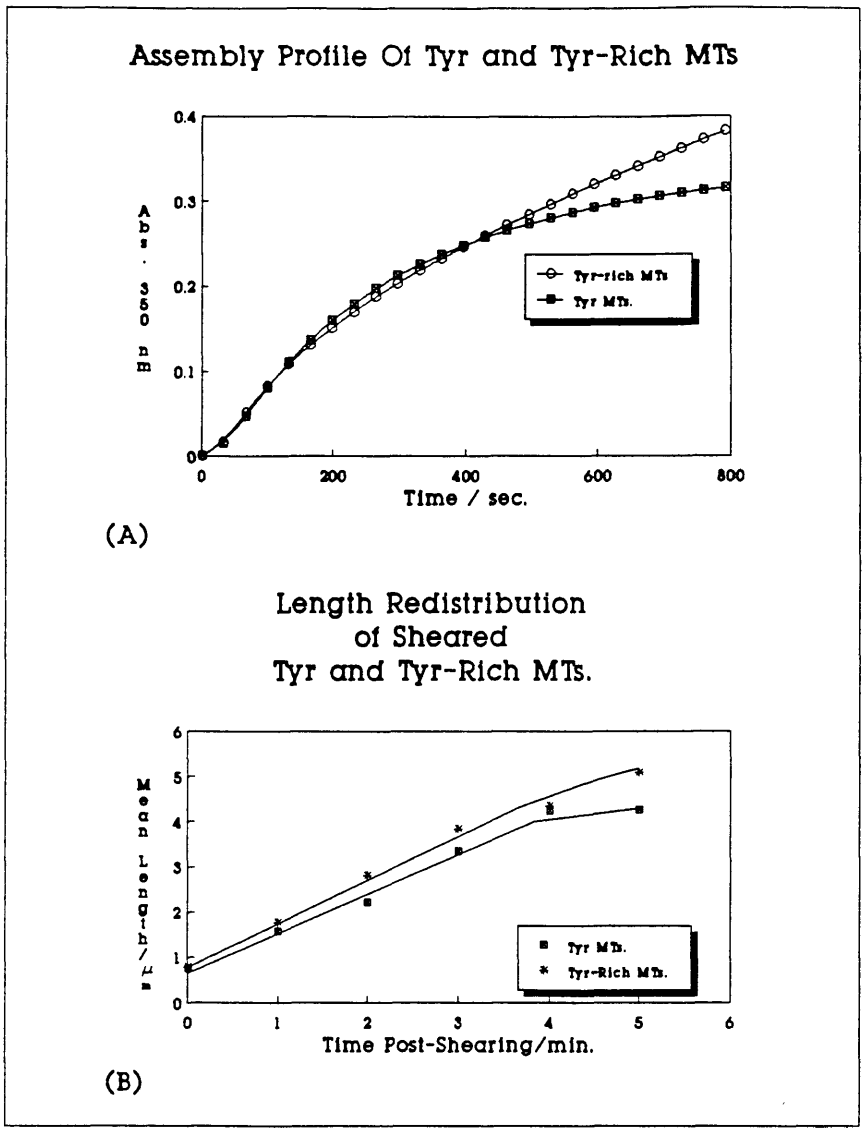

Fig. 5.5:- Assembly and Length Redistribution of Tyr and Tyr-rich microtubules. Microtubules were assembled *from non-treated and maximally tyrosinated mtp as described in the text prior to shearing and monitoring length re-distribution of the sheared microtubules. (A) Assembly profile of the microtubules. Note the continued increase in turbidity of Tyr-rich microtubules even after Tyr microtubules attained steady state, which probably is due to protein aggregation. (B) Mean length variation of sheared microtubules with time.*

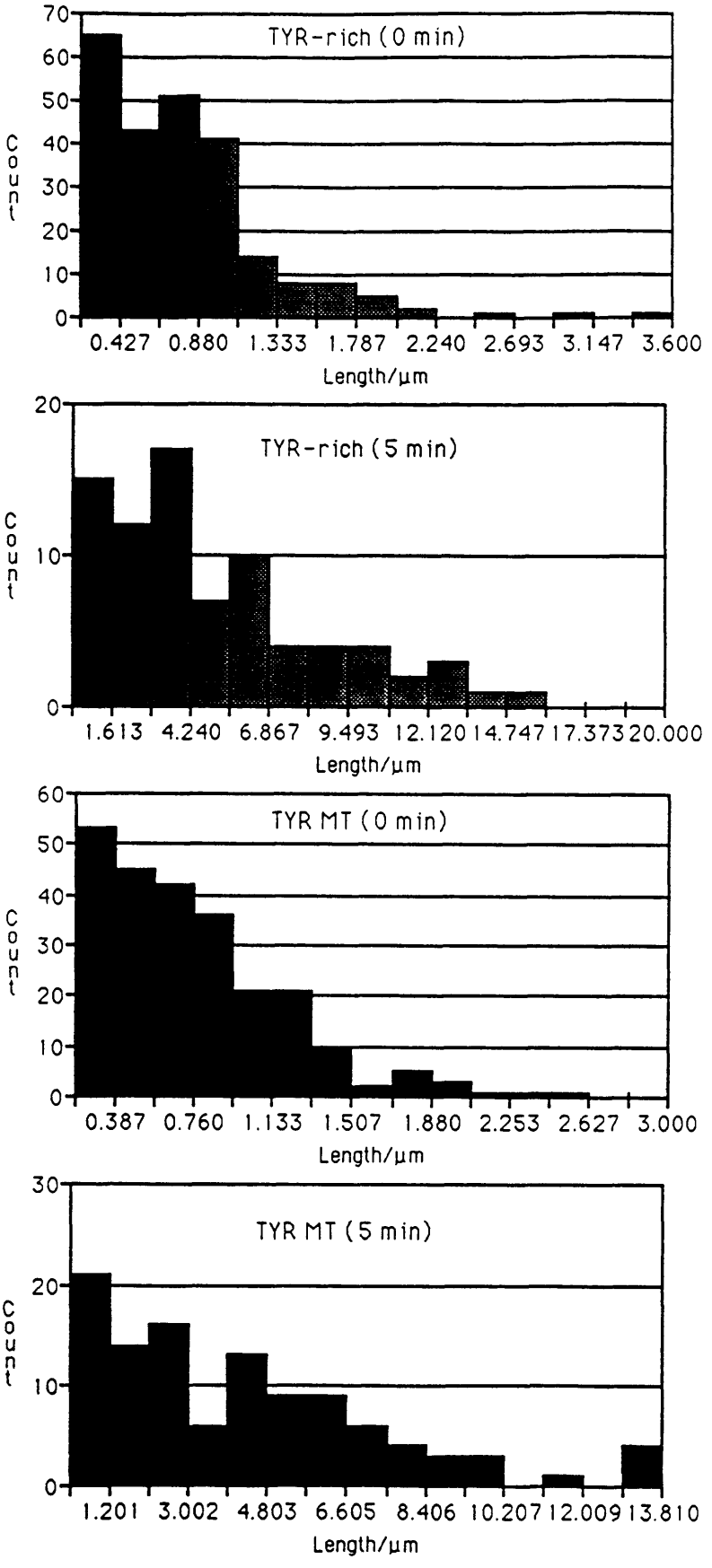

Fig. 5.6:- ***Length Distribution of Sheared Tyr and Tyr-rich microtubules at times 0-5 min. post-shearing.*** *(A) Tyr microtubules (20 % tyrosinated), (B) Tyr-rich microtubules (50 % tyrosinated).*

Turnover Dynamics of Detyrosinated and Tyrosinated Mtp:

Detyrosinated mtp prepared as in Chapter 2 was re-tyrosinated by incubation with exogeneous TTL (6 U/ml), ATP and tyrosine for 30 min. (Chapter 2). A control sample was subjected to the same treatment omitting TTL. After cooling on ice for 10 min. the mtp was desalted on a Sephadex G-25 column pre-equilibrated with MEM buffer containing 67 mM NaCl and then assembled in the presence of seeds and sheared as described earlier. The tyrosination level of TTL treated mtp was estimated to be 30 %. Although the level of tyrosination could have been increased to above 30 % by increasing the incubation time or by using higher TTL levels, this was not practical as increasing the incubation time to above 30 min. reduced the assembly competency of the protein. Furthermore, using TTL at a level higher than the one already used, was found to cause inhibition of assembly, even when the assembly was seeded. Therefore, 30 % tyrosination was the maximal level attained, whilst keeping the mtp assembly competent.

Fig. 5.7 (A) shows the assembly profiles of Glu and Tyr-rich microtubules, indicating that they assemble to the same extent and at the same rate, indicating similar Co, k_{+1} and k_{-1}. The mean length of the sheared microtubules are given in table V.III and are represented graphically in Fig. 5.7 (B). From this graph, the elongation rate of growing microtubules was estimated to be 0.52 and 0.60 $\mu m.min^{-1}$ for Glu and Tyr-Tu rich microtubules respectively, indicating that both populations turnover with similar dynamics. Length re-distribution of both populations at times 0 and 10 min are shown in Fig. 5.8 confirming that sheared microtubules undergo length redistribution with time. This particular experiment is important as it offers direct comparison of dynamics of fully detyrosinated microtubules with those enriched in tyrosinated tubulin.

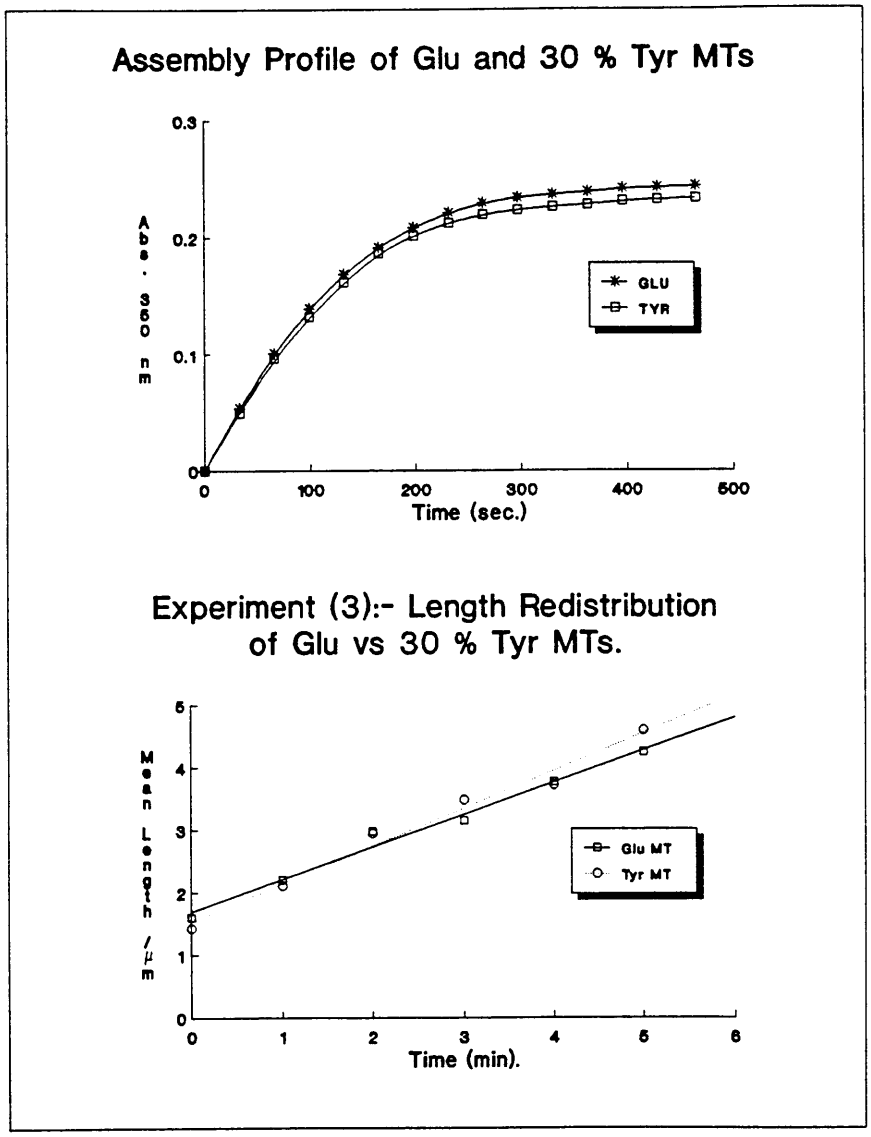

Fig. 5.7:- Assembly and Length Re-distribution of Glu and Tyr (30 %) Microtubules. (A) assembly profile of the two sets of microtubules. (B) variation of the mean length with time.

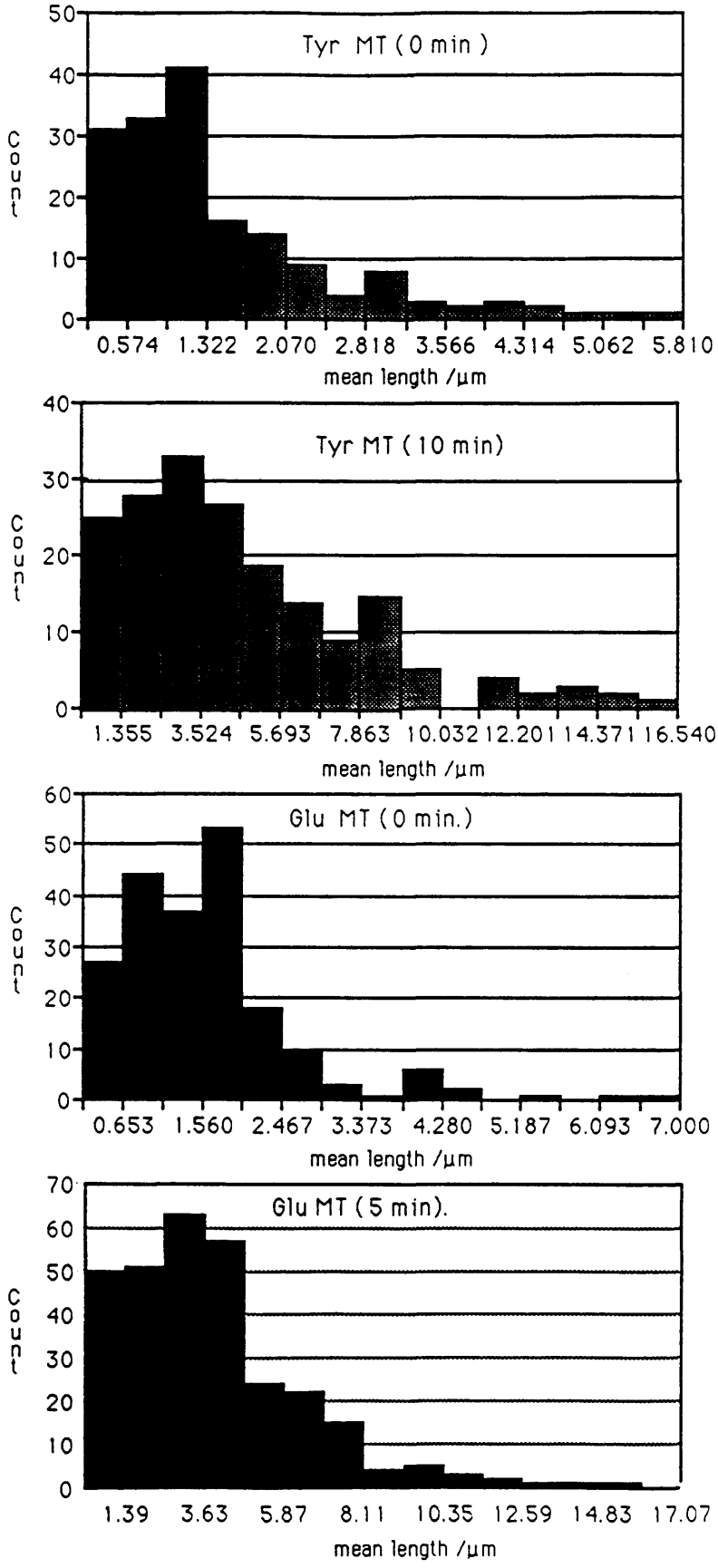

Fig. 5.8:- Length Distribution of Sheared Glu 30 % Tyr microtubules at 0 and 10 min. Post-Shearing. (A) Glu microtubules, (B) Tyr microtubules.

Discussion and Conclusions:

Previous *in vitro* studies have suggested that Tyr and Glu tubulin are kinetically homogeneous[76,113]. However, most of this work was based on turbidimetric analysis of polymer formation, and might not have detected any subtle effect of detyrosination. Indeed, these earlier studies reported some minor differences between Tyr- and Glu-Tu microtubules, particularly at low MAP stoichiometries[76]. One important effect of the MAPs is to suppress dynamic instability[42,62], a behaviour of microtubules at steady state which assumes the co-existence of two microtubule populations, a major population consisting of slowly growing microtubules and a minor population of rapidly shrinking ones, which interchange infrequently[96]. The growing population have been postulated to represent microtubules with a terminal cap of tubulin subunits that have not hydrolysed their GTP and hence, such a 'GTP Cap' was said to stabilise the microtubules[96,70]. Detyrosination could therefore stabilise microtubules by lowering either Co^{GTP}, Co^{GDP} or the transition frequencies for catastrophe or by elevating rescue transition frequency.

If tubulin tyrosination affects the kinetics of microtubule assembly and if this effect is on $_{k+1}{}^{GTP}$ then this should become apparent from the turbidimetric assembly graph. By contrast, it is often difficult to detect effects on either Co^{GTP} or Co^{GDP}, as there is often a certain amount of "creep" at steady state (see fig 5.5) and would be unlikely to detect any effect on GTP hydrolysis or the transition frequencies between the growing and shrinking phases. A more sensitive method for comparing the kinetics is therefore needed and monitoring length redistribution of sheared microtubules was found to be suitable for this purpose. Microtubules assembled to steady state and then sheared will show length redistribution through dynamic instability, with the consequence of increasing the mean length of the population and decreasing the number concentration of ends. As dynamic instability is governed by numerous kinetic parameters (Chapter 1), then any variation in the rate of length redistribution of two different microtubule populations will be a

reflection of a variation of some or all of the kinetic constants involved in dynamic instability, suggesting differential turnover rate of microtubules.

Sheared MAP-2 rich steady state microtubules in MEM buffer do not normally show length redistribution as MAPs suppress dynamic instability[42,62]. However, the inclusion of NaCl to 67 mM in the assembly buffer partially facilitates length re-distribution of sheared microtubules, presumably by weakening the ionic MAP-2:tubulin interaction. Mtp was used in these experiments rather than pure tubulin for two main reasons. Firstly, pure chick tubulin cannot be induced to assemble even in the presence of glycerol and high $MgCl_2$ concentration. Secondly, as re-annealing is a potential mechanism through which length re-distribution can take place[115] and since re-annealing depends on the sidewise alignment of microtubule ends, which is hindered in the presence of MAPs due to the projection of the MAP-2 lateral arms, then the contribution from end to end annealing of microtubules to length redistribution will be negligible. Furthermore, the fact that length redistribution does not occur when microtubules are assmbled with GMPPNP, further suggests that GTP hydrolysis dependent subunit addition is required for length re-distribution[22]. Moreover, the number concentration of microtubule ends employed to observed annealing[115] (6×10^{-8} M), exceeds that used in this study ($\simeq 8.9 \times 10^{-9}$ M).

Results from this chapter showed that detyrosinated and about 20 % tyrosinated sheared microtubules turnover with similar dynamics [Fig. 5.1 (B)], and a mean regrowth rate of 0.47 μm.min^{-1} and 0.56 μm.min^{-1} respectively. Furthermore, fully tyrosinated and 20 % tyrosinated microtubules turnover with regrowth rates of 0.90 and 0.99 μm.min^{-1} [Fig. 5.5 (B)], whilst fully detyrosinated and Tyr-Tu rich microtubules regrow at rates of 0.52 and 0.60 μm.min^{-1} respectively, [Fig. 5.7 (B)]. Several comments can be made at the above data:

Firstly, although there is a slight difference in the re-elongation rates of growing tyrosinated and detyrosinated microtubules after shearing, with tyrosinated microtubules having slightly higher rate, the difference is not considered significant, particularly when considering the marked difference in stability reported by the *in vivo* studies. Furthermore, in one experiment, tyrosinated microtubules re-elongated at a rate slower than detyrosinated ones (results not shown), suggesting that detyrosinated microtubules do not necessarily have a slower microtubule regrowth rate.

Secondly, comparison of the elongation rates for 20 % and fully tyrosinated microtubules from (0.90 and 0.99 μm.min^{-1} respectively) indicates that microtubules assembled from mtp subjected to *in vitro* tyrosination treatment has slower turnover dynamics than microtubules not subjected to such treatment (0.47 and 0.56 μm.min^{-1} for CPA digested and non-treated microtubules respectively). As the tyrosination mixture contains ATP and as twice cycled mtp contains a protein kinase activity associated with MAP-2[8], this difference in rate might be due to MAP-2 phosphorylation. Phosphorylation of MAP-2 increases k_{-1}, presumably through weaker MAP-2:microtubule interaction, and would therefore be expected to increase the extent of dynamic instability. The observed difference is also likely to be due to a difference in the initial mean length of sheared microtubules which is lower in the case of microtubules from non-treated mtp (0.62 μm compared with 0.79 μm), since the rate of length redistribution is probably affected by the initial mean length of microtubules.

These studies on the effect of detyrosination and of tyrosination therefore indicate that they have no effect on the kinetic parameters regulating dynamic instability, and provide definitive evidence against a direct role of detyrosination on the stabilisation of microtubules *in vitro*.

More extensive study of the effect of tyrosination on microtubules assembly *in vitro* has recently emerged through the work of Paturle *et al*[103]. Tubulin that has been maximally tyrosinated *in vitro* and then fractionated on a YL1/2 immunoaffinity column, generated tubulin species which was fully tyrosinated and which upon CPA treatment, yielded fully detyrosinated protein. *In vitro* assembly assays showed that both tubulins assemble at the same rate and to the same extent. Furthermore, the critical concentration for assembly (Co) was found to be the same for Glu and Tyr microtubules together with the steady state subunit incorporation. Moreover, oscillatory assembly behaviour of both Tyr and Glu microtubules was identical, together with their susceptibility to calcium induced disassembly. Finally, Glu and Tyr microtubules were stabilised to the same extent against dilution induced disassembly, by STOP, MAP-2 and tau.

In vivo studies correlated detyrosination with microtubule stability (see Chapter 1)and this led to the suggestion that Glu microtubules might be stabilised by capping of their ends, possibly with a protein, thereby preventing end wise disassembly such as that induced by drugs or dilution and this indicated that the enhanced stability of Glu microtubules *in vivo* appears not to be due to the mere removal of the C-terminus tyrosine[68]. Indeed, in cultured TC-7 cells, CPA digestion of the microtubule network of detergent extracted cells, prior to dilution to induce disassembly, did not generate increased resistance to depolymerisation[68]. Furthermore, complete disassembly of the microtubule network by nocodazole in cultured MDCK cells, followed by recovery from the drug, demonstrated that the re-appearance of Glu microtubules lagged 30 min. behind the appearance of Tyr microtubules[18]. However, microtubules stable against Nocadzole disassembly were observed only 3 min. after regrowth initiation, suggesting that microtubule stability is attainable without detyrosination[18]. Finally, microinjection of monoclonal antibodies raised against TTL, into cultured fibroblasts generated a fully detyrosinated microtubule network within 12 hour, demonstrating that despite the removal of the C-terminus tyrosine, the bulk of the microtubule array was dynamic, with 78 % of

the population incorporating hapten labelled tubulin within 2 min., further suggesting that it is not detyrosination *per se* that is responsible for microtubule stabilisation[146].

CHAPTER 6

Could There Be Proteins That Specifically Bind To And Stabilise Detyrosinated Microtubules?

The previous chapter demonstrated that the turnover kinetics of Glu and Tyr microtubules are similar and therefore, detyrosination on its own is not sufficient to incur microtubule stability. While tyrosination affects the C-terminus of α-tubulin, both the C-termini of α- and β-tubulin have been implicated in the regulation of microtubule assembly. Limited Subtilisin digestion of tubulin yields 1 Kd fragment from both the α- and β-tubulin C-termini which has been found to lower Co for tubulin assembly[119]. Furthermore, removal of 10 amino acid residues from the C-termini of both subunits by Carboxypeptidase Y treatment, has been shown to stabilise microtubules against Ca++ induced disassembly[138]. Moreover, the C-terminus has also been implicated in the binding of MAPs[51,87]. As *in vivo* observations suggest that detyrosination is correlated with microtubule stabilisation, one possibility is that certain stabilising agents might bind preferentially to Glu microtubules in the cell and suppress their turnover. Detyrosination therefore, might be an indirect cause of stabilisation.

So far, STOP and crude MAPs, have been tested as stabilisers of detyrosinated microtubules yet neither appear to confer enhanced stability[103]. As there is a spectrum of proteins in the cell that could potentially bind to microtubules, it was decided to look for proteins that specifically bind to and stabilise microtubules.

During the mtp preparation by temperature dependent cycles of assembly and disassembly a cold stable pellet of microtubules is obtained after the first assembly cycle. This cold pellet was shown to be enriched in acetylated[70] and detyrosinated

microtubules (R.Burgoyne-personal communication). If there are stabilising proteins that bind preferentially to detyrosinated microtubules, then the cold pellet would be an obvious candidate for searching for such proteins, which can then be tested for their stabilising effects on Glu microtubules *in vitro*.

Isolation of Cold Pellet Proteins:

Two methods have been used to extract proteins from the first cold pellet (CP). (A) The pellet was homogenised in 6 ml of MEM buffer containing 0.1 M $CaCl_2$ and 10 $\mu g.ml^{-1}$ Leupeptin. The homogenised suspension was left on ice overnight followed by centrifugation at 65,000 xg (MSE 8x8 ml rotor). The supernatant was then dialysed against several changes of MEM buffer to remove the calcium, recentrifuged at 180,000 xg for 1 hour and then stored in liquid nitrogen until use.

(B) The pellet was homogenised in 4 ml of MEM buffer containing 50 μM Taxol incubating at 37 $^{\circ}$C for 15 min. KCl was then added to 0.5 M and the suspension was centrifuged at 65,000 xg for 30 min. followed by overnight dialysis against MEM buffer. The dialysed supernatant was re-centrifuged at 180,000 xg for 1 hour and stored under liquid nitrogen.

Both methods of preparation gave identical results (Fig. 6.1 lanes C and D), although different proteins certain proteins were more enriched by the two procedures.

Binding of Cold Pellet Proteins to Microtubules:

Prior to examination for a stabilising effect, one needs first to demonstrate binding of extracted CP proteins to microtubules. Glu mtp (0.9 $mg.ml^{-1}$) prepared by YL1/2 immunochromatography and twice cycled mtp (0.9 $mg.ml^{-1}$) were

assembled with Taxol (13 μM) at 37 °C for 20 min. in the presence of 1 mM GTP. Extracted CP proteins were then added (4.7 $mg.ml^{-1}$) and incubated for 15 min. The microtubules were then pelleted by spinning in an Airfuge (Beckman) at 30 psi for 5 min. (at 100,000 xg). The pellets were analysed by SDS–PAGE (Fig.6.1). The Glu–Tu from the YL1/2 column is more enriched with MAP–2 and tau than twice cycled mtp (lanes A and B respectively), and this is typical of protein obtained by YL1/2 immunochromatography. The CP proteins (lanes C and D) consist of numerous bands covering a wide range of m.wt. and some of these bands are seen to associate with Glu microtubules (lanes E and F). The same proteins associate with Tyr microtubules (lanes G and H). Little self aggregation of CP proteins occurs as seen by incubating CP proteins in MEM buffer (Lane I). These results suggest that some proteins in the first cold pellet are capable of binding to microtubules. Similar results were obtained with pure tubulin obtained by phosphocellulose chromatography and assembled with Taxol.

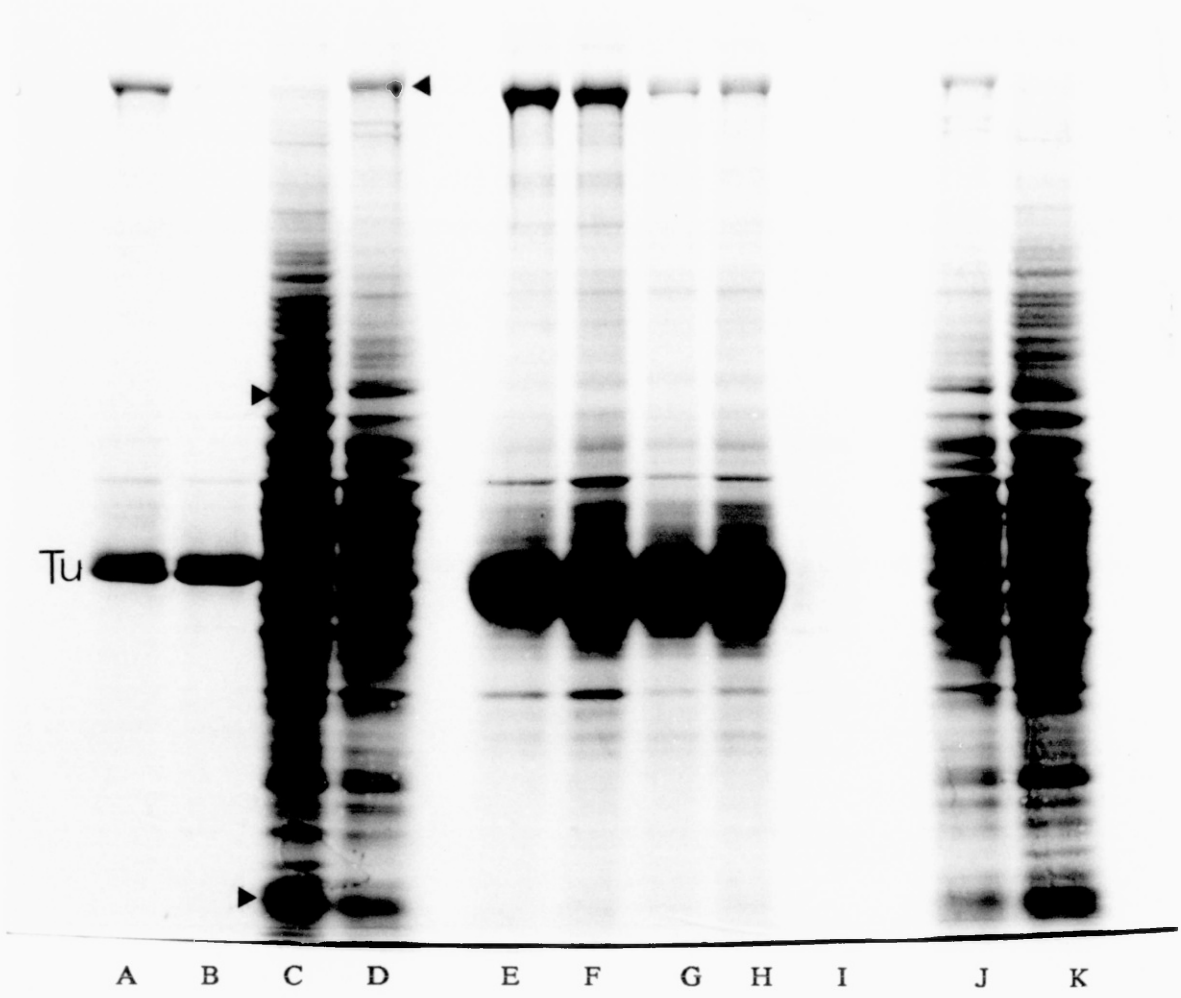

Fig. 6.1:- Binding of Calcium Extracted Cold Pellet Proteins by Pre-assembled Microtubules. Proteins were extracted from the cold pellet and incubated with pre-assembled microtubules as described in text, prior to fractionation by SDS-PAGE. Lanes:- A:-Glu mtp prepared by YL1/2 immunochromatography (85 μg), B:- twice cycled mtp (85 μg), C:- CP proteins extracted by Taxol and KCl (180 μg), D:- CP proteins extracted by the calcium procedure (180 μg), E & F:- Glu MT incubated with Calcium extracted CP proteins at a CP proteins:mtp ratio of 1.1 and 2.2 respectively, G & H:- Tyr MT incubated with CP Proteins as in E & F, I:- CP protein incubated at 1.4 mg.ml^{-1} incubated at 37 °C prior to centrifugation, J & K:- as in D & C (170 μg each). (▼) depict proteins more enriched by the isolation procedure used.

Turnover Dynamics of Detyrosinated Microtubules in the Presence of Cold Pellet Proteins:

The turnover dynamics of tyrosinated and detyrosinated microtubules with and without CP proteins has been examined in a variety of ways. One approach was to examine the length redistribution following shearing (Fig.6.2).

Twice cycled mtp was detyrosinated by exogeneous CPA treatment (2.5 $\mu g.ml^{-1}$) at 37 °C for 20 min. followed by further incubation for 10 min. in the presence of 15 mM DTT and cooling on ice for 10 min. Another mtp sample was subjected to the same treatment without the addition of CPA and this represented Tyr-Tu (with about 20 % tyrosination level). Both samples were desalted on a Sephadex G-50 column pre-equilibrated with MEM buffer containing 67 mM salt prior to assembly with 100 μM GTP, 1 mM PEP and 6 U/ml Pyruvate Kinase at 37 °C in a final assay volume of 500 μl. At steady state (17 min. later), 100 μl of CP proteins (4.73 $mg.ml^{-1}$), prepared by calcium extraction, were added to the microtubules (to give a CP protein:mtp ratio of 0.35), followed by further incubation for 11 min. An aliquot (100 μl) was taken out from each cuvette and microtubules were sheared by 10 passages through a Hamilton syringe. The microtubules were incubated at 37 °C, and aliquots (10 μl) were taken at various time intervals, using an automatic dispenser with the end of the plastic tip cut-off to prevent shearing of the microtubules. All samples were then fixed in glutaraldehyde and processed for electron microscopy as in Chapter 2. Microtubules were photographed at a magnification of x10,000 and measured with a ruler using a light box.

The mean length of the sheared microtubules at various time intervals are given in Table VI.I. The initial elongation rate (between 0 and 2 min.) 0.80 and 1.10 $\mu m.min^{-1}$ for Glu and Tyr microtubules respectively, suggesting that Glu microtubules, in the presence of CP proteins, turnover at a slower rate than those composed of about 20 % tyrosinated tubulin and that protein(s) from the cold pellet

may be stabilising these microtubules. This contrasts with the results of chapter 5 where detyrosinated and tyrosinated microtubules turned over with similar kinetics, indicating that the above results represent a specific property of CP proteins on detyrosinated microtubules.

To further investigate this phenomenon, the turnover rate of Glu microtubules was determined in the presence of varying amounts of CP proteins. In the experiment depicted in fig 6.3 (A), four samples of CPA digested mtp (section 2.x) that have been desalted on a Sephadex G-50 column pre-equilibrated with MEM/NaCl buffer were assembled to steady state (37 °C for 15 min.), at a concentration of 2.50 mg.ml^{-1}, after which varying amounts of CP proteins were added, followed by further incubation for 12 min. The microtubules were then sheared as described earlier and aliquots removed at 0-5 min. post-shearing, fixed in glutaraldehyde and processed for electron microscopy.

Results from the above experiment are given in table VI.II and are represented graphically in fig. 6.3 (A). The rate of re-elongation of the four samples (hereon referred to as S1-S4 with CP protein:mtp ratio of 0, 0.25, 0.50 and 0.74 respectively) was estimated to be 0.16, 0.16, 0.14 and 0.19 μM.min^{-1} for S1-S4 respectively. These rates were plotted against the CP proteins:mtp ratio and the obtained dose response graph [fig. 6.3 (B)] shows that there is no correlation between the amount of CP protein added and the turnover rate of Glu microtubules indicating that CP proteins do not stabilise these microtubules. The apparent stabilisation previously observed (Fig.6.2), was not demonstrated in this experiment, the reason for this discrepancy is unknown but might be related to factors such as the age of CP extract.

Table VI.I:- Variation of the mean length of sheared detyrosinated and tyrosinated microtubules in the presence and absence of calcium extracted cold pellet proteins. Data is represented graphically in Fig. 6.2.

Time Post-Shearing (Tyr MT) (min)	Mean Length (Glu MT) (μm)	Mean Length (μm)
0	1.22	1.58
1	2.11	2.97
2	2.90	3.56
3	2.82	3.44
4	3.50	4.11
5	3.60	4.82
10	4.97	5.12

Table VI.II:- Variation of the mean length of sheared detyrosinated microtubules in the presence of varying amounts of CP proteins. S1-S4 refer to the four samples tested and the values between brackets to the CP protein:mtp ratio.

Time post-shearing	Mean Length (μm)			
(min)	S1 (0)	S2 (0.25)	S3 (0.50)	S4 (0.75)
0	9.70	9.21	9.46	9.85
1	12.45	12.30	12.23	13.02
2	14.90	15.65	14.39	17.83
3	19.46	16.81	15.88	18.77
5	21.84	22.00	20.66	24.61

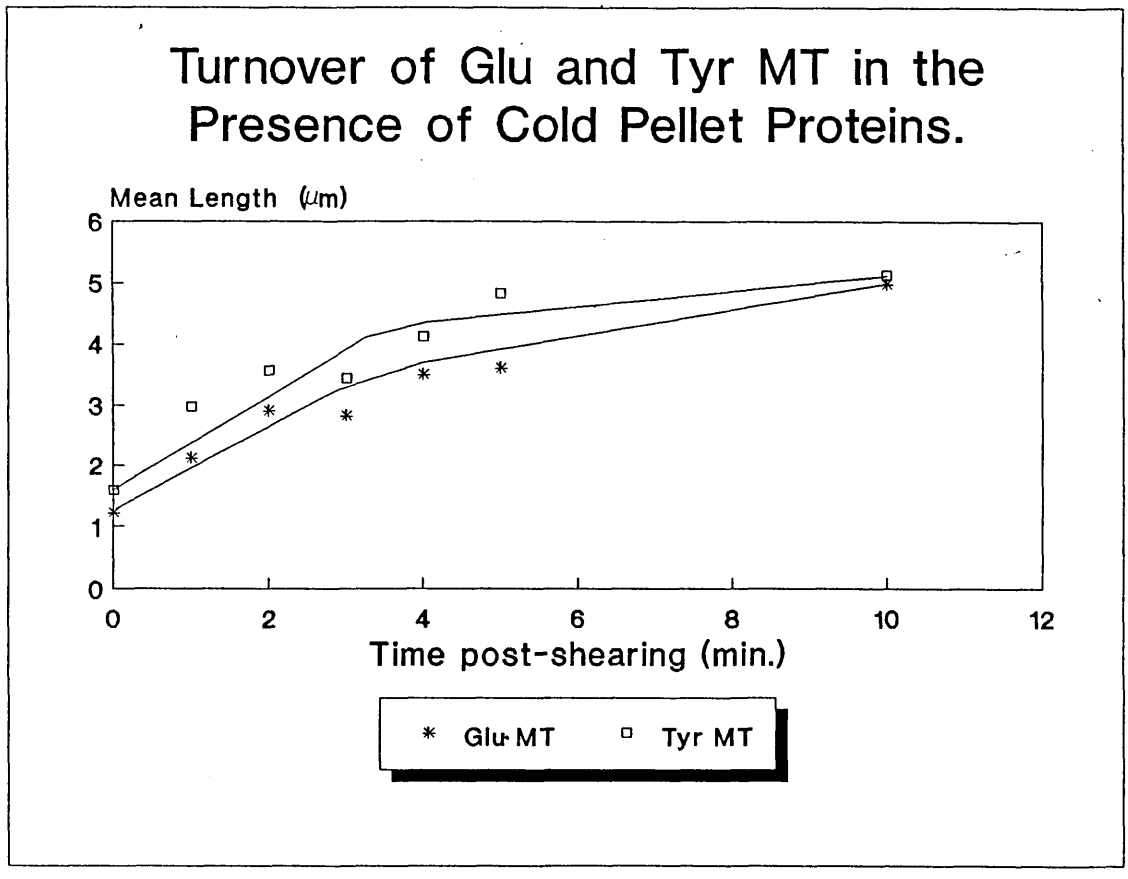

Fig. 6.2:- Length Redistribution of Sheared Glu and Tyr Microtubules in the presence of CP Proteins. CPA digested and non-treated mtp (20 % tyrosinated) were assembled to steady state, incubated with CP proteins, sheared and the length re-distribution monitored by electron microscopy. Microtubules were sheared again at 3 min. post initial shear.

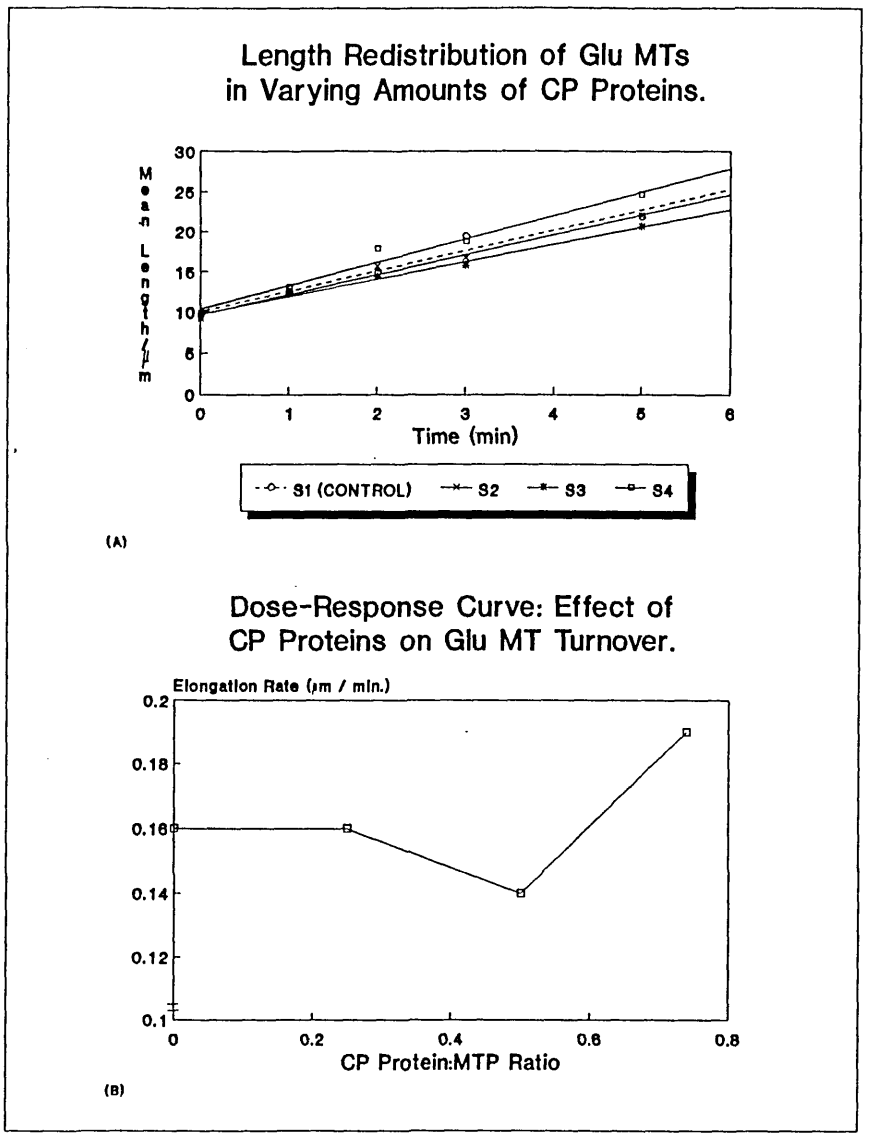

Fig. 6.3:- Length Redistribution of Sheared Glu Microtubule in the presence of Varying Amounts of CP proteins. Four samples of CPA digested mtp (S1-S4) were assembled to steady state prior to addition of varying amounts of calcium extracted CP proteins and shearing as described in text. Graph (A) is a plot of mean length vs time for the four samples, whilst graph (B) shows the variation of the re-elongation rate as a function of CP protein:mtp ratio.

The second approach for studying the stabilisation of detyrosinated microtubules by the CP proteins was to examine the disassembly kinetics induced by nocodazole, since detyrosinated microtubules were shown to be resistant to nocodazole induced disassembly *in vivo*.

To assay for stabilty against disassembly, microtubules assembled with ^{3}H-GTP and incubated with CP proteins, were depolymerised with nocodazole, monitoring the loss of polymer by the filter assay of Wilson[153] *et al.* In the experiment described in fig. 6.4 (A), two samples of detyrosinated mtp (2.45 mg.ml^{-1}) were assembled with 100 μM GTP, 1mM PEP, 6U/ml Pyruvate Kinase and 2.5 μCi of ^{3}H-GTP. After attaining steady state (30 min. at 37 °C), CP proteins were added to one sample to give a CP protein:mtp ratio of 0.17, whilst the other sample was mock treated with MEM/NaCl buffer. Both the CP proteins and buffer added contained 6% DMSO so that after addition to the assembled microtubules, the final DMSO level was 1%. This was necessary so as to prevent precipitation of nocodazole once added to the samples. Thirty minutes later, a 50 μl aliquot was taken from each sample, added to 1 ml of Stabilising Buffer (100 mM Mes, pH 6.4, 1 mM EGTA, 1mM $MgCl_2$, 25 % v/v glycerol, 10 % v/v DMSO and 5 mM ATP), and nocodazole was added to the samples to a final concentration of 5 μM. Aliquots (50 μl), were then removed from each sample at various time intervals, diluted into 1 ml of Stabilising Buffer (SB) and left at 37 °C until filtered. All diluted samples were filtered on Whatman GF/C filter discs, pre-wet with S.B., using negative pressure. Each filter was further washed with 15 ml of S.B., allowed to air dry, soaked in 1 ml of 0.1 M NaOH overnight and counted in 6 ml of "Ready Protein Scintillant".

Results from such an experiment are shown in Fig. 6.4 (A). The two curves are similar in shape and are reminiscent of a first-order decay reaction. Microtubule disassembly can in fact be regarded as a first-order decay process with respect to the disappearance of microtubule ends[64] and thus, the rate of disassembly is

dependent on the length distribution of microtubules and on the disassembly rate constant k_{-1}. Although the two curves are similar in shape, the half-life for decay is apparently different, in that Glu microtubules without CP proteins have a shorter half-life than those with CP proteins present. Accurate determination of the half-life from the curves is not possible due to the scatter of the points at early sampling time. However, analysis of the last four points on each curve [Fig.6(B)] yields an estimated rate constant for disassembly of 0.57 and 1.24 $hour^{-1}$, corresponding to a half-life of microtubule end disappearance of 73 and 34 min. for Glu microtubules with and without CP proteins respectively. These preliminary results therefore suggest that detyrosinated microtubules, in the presence of CP proteins are more stable against nocodazole induced disassembly.

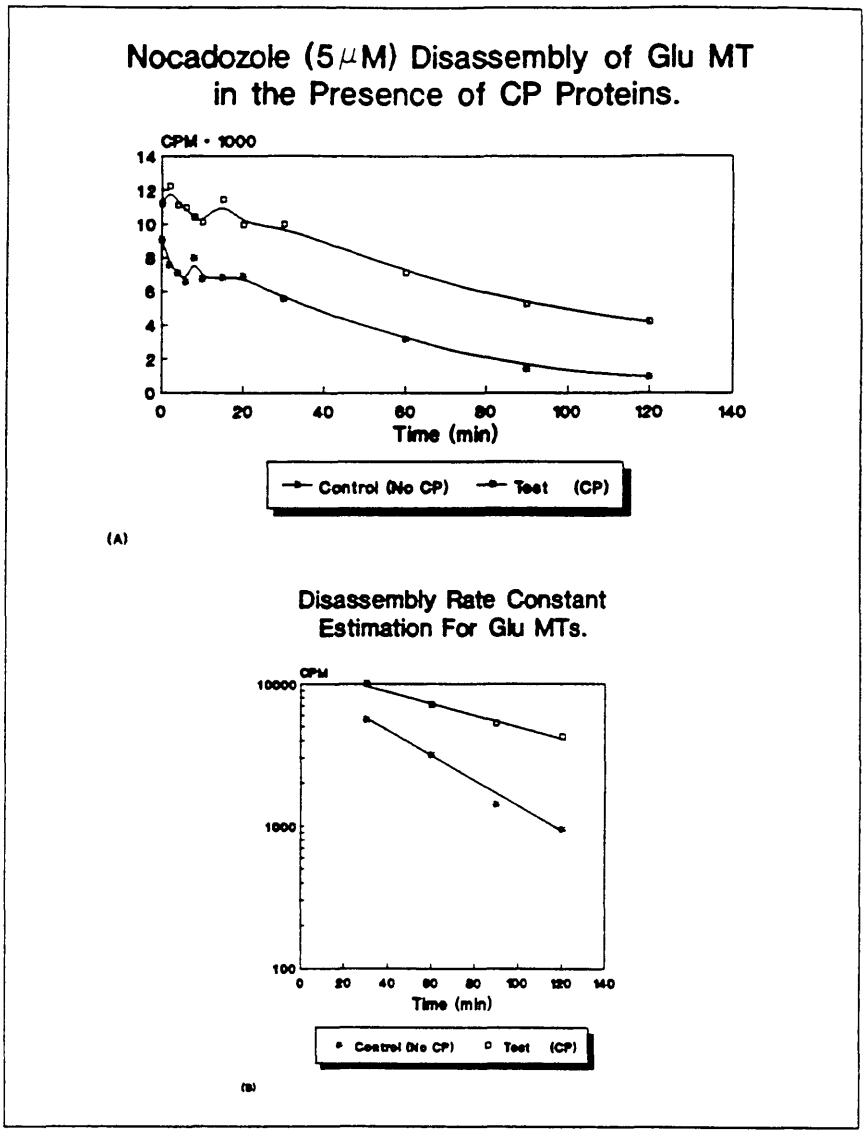

Fig. 6.4:- Nocodazole Induced Disassembly of Detyrosinated Microtubule in The Presence of Cold Pellet Proteins. Detyrosinated microtubules were assembled to steady state in the presence of ^3H-GTP, prior to disassembly with 5 μM nocodazole, either in the presence or absence of CP proteins. Disassembly was followed by monitoring the loss of ^3H-GTP activity. (A):- Disassembly profile of Glu microtubules in the presence and absence of CP proteins. (B):- Semi-log plot of the four data points of each disassembly curve to estimate the disassembly rate constant.

The disassembly profile of microtubules in the presence of the first cold supernatant, obtained after centrifugation of chick brain homogenate (Chapter 2), has also been examined.

Two samples of detyrosinated mtp (2.60 mg.ml^{-1}) were assembled to steady state (30 min. at 37 °C) with 100 μM GTP, 1 mM PEP, 6 U/ml Pyruvate Kinase and 2.5 μCi ^{3}H–GTP, after which 100 μl of cold supernatant (containing 6% DMSO) were added, followed by further incubation for 30 min. nocodazole was then added to 10 μM and aliquots (50 μl) were taken at various time intervals, and processed for filtration on GF/C discs as described previously.

The results from the above experiment are given in Fig. 6.5, and it can be seen that the disassembly profile for both populations, at 5 μM nocodazole, resembles a first–order decay process. Furthermore, similar stabilisation of the microtubules, to that observed with the CP proteins has been observed with the cold supernatant [Fig.6.5(A)]. The half–life for decay was about 30 min. and 20 min. in the presence and absence of the cold supernatant respectively [Fig. 6.5(B)], suggesting a small stabilisation effect at moderate nocodazole concentrations. By contrast, no difference could be detected when disassembly was induced by addition of 10 μM nocodazole. Results from such an experiment are shown in Fig. 6.5 (C) whereby the two disassembly curves are seen to be superimposable, indicating that the cold supernatant has no influence on the stability of microtubules at high concentrations of nocodazole.

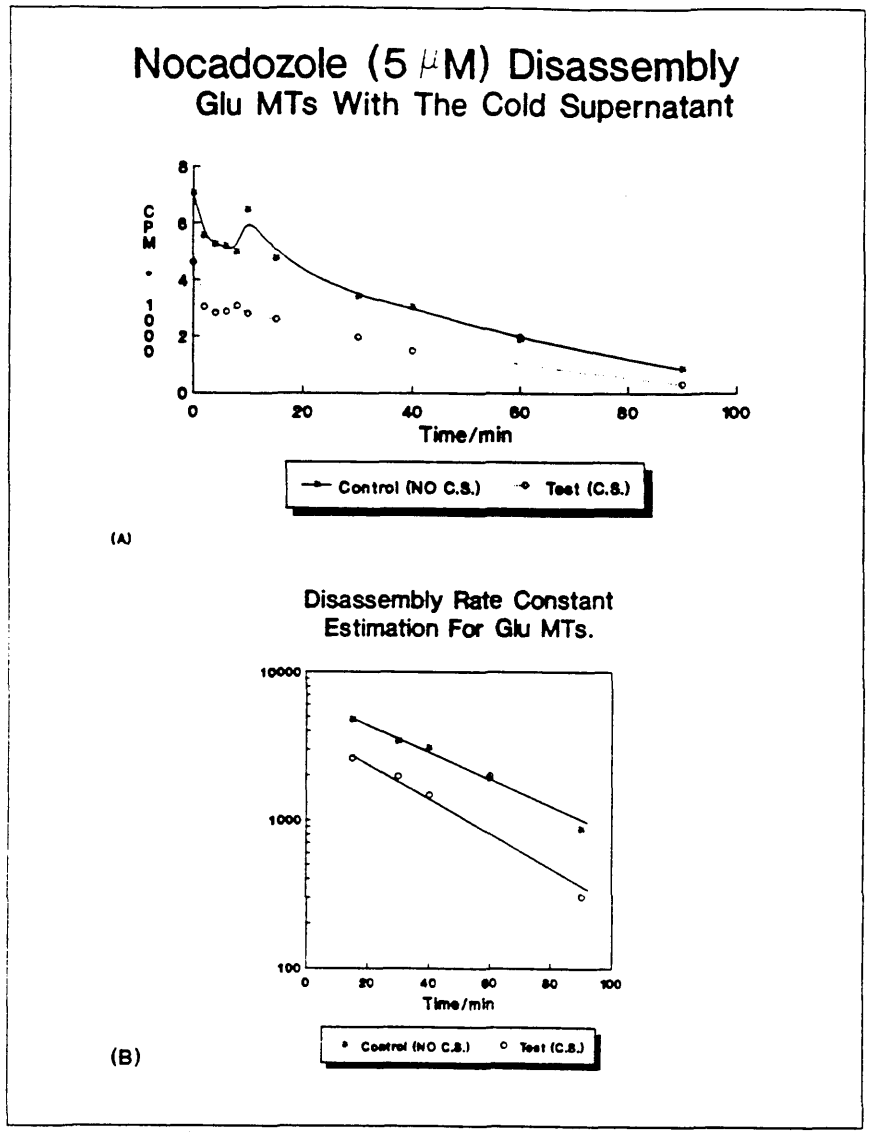

Fig. 6.5:- Nocodazole Induced Disassembly of Detyrosinated Microtubules in the Presence of the Cold Supernatant. Detyrosinated microtubules were assembled to steady state with ^3H-GTP, prior to disassembly with 5 μM nocodazole, in the presence and absence of added cold supernatant proteins. Disassembly was monitored by following the loss of ^3H-GTP, using the filter assay (A). The half-life for loss of microtubule ends was about 30 and 24 min. in the presence and absence of added supernatant respectively (B).

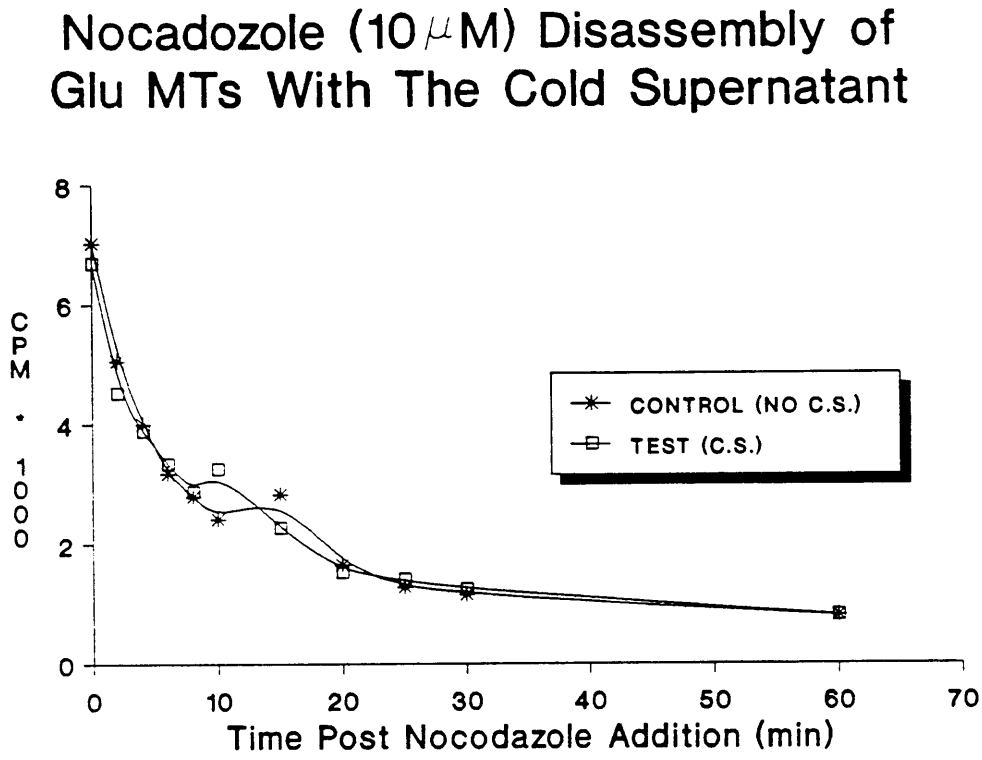

Fig. 6.6:- Nocadazole Induced Disassembly of Detyrosinated Microtubules in the Presence of the Cold Supernatant. Detyrosinated microtubules were assembled to steady state with ^{3}H-GTP, prior to disassembly with 10 μM nocodazole. Loss of polymer was followed by monitoring the loss of ^{3}H-GTP using the filter assay. The half-life for loss of microtubule ends was estimated to be 4 min. in the presence and absence of the cold supernatant.

Discussion and Conclusions:

The cold pellet, composed of cold stable microtubules and other proteins obtained after the first cycle of temperature dependent assembly, is enriched in acetylated and detyrosinated tubulin. Proteins were extracted from this cold pellet by calcium disassembly to obtain a spectrum of proteins of varying molecular weights some of which bind to pre-assembled microtubules as judged by SDS-PAGE (Fig. 6.1).

Two experiments suggested that the extracted CP proteins influence the dynamics of detyrosinated microtubules causing them to be more stable. In the first experiment, sheared Glu microtubules elongated with slower kinetics in the presence of CP proteins than sheared Tyr microtubules (Fig. 6.2) and in the second experiment, detyrosinated microtubules had a longer half-time for loss of microtubule ends by nocodazole induced disassembly, in the presence of CP proteins than in their absence [73 and 34 min. respectively Fig. 6.4 (A)].

But how much do these data suggest a causal effect of CP proteins on Glu microtubules stability? If the effect of CP proteins seen in Fig. 6.2 was genuine, then the more CP protein present the more enhanced the stabilising effect should be. However, the experiment whereby sheared Glu microtubules elongated in the presence of varying amounts of CP proteins [Fig. 6.3(A)] suggested that these proteins do not influence the turnover rate of sheared microtubules in a dose-dependent manner [Fig. 6.3(B)], contradictory to the results of Fig. 6.2. Although it is difficult to judge which result is more valid, if one considers the nocodazole disassembly experiments however, the balance tips towards a stabilising effect of CP proteins on Glu microtubules. Comparison of the two curves of Fig. 6.4 (hereafter referred to as the Test and Control curves depicting microtubule disassembly in the presence and absence of CP proteins respectively), it is obvious that the disassembly rate is different, with the half-time for microtubule end

disappearance being 73 and 34 min. for the Test and Control samples respectively. Yet, the count rate at 0 min. for the Test curve is much higher than the Control curve, which is surprising as both populations should have the same polymer mass. Two explanations could account for this.

Firstly, it is possible that CP proteins bind ^{3}H–GTP and therefore, generate a systematic overestimation in the count rate of all the data points. Indeed, if one subtracts the count rate at 120 min. for the Test curve (where most microtubules should disassembled as judged by the Control curve), from the rest of the data points, then both the Test and the Control curves can be essentially superimposed, suggesting that they disassemble at similar rates. If there are indeed GTP binding proteins in the cold pellet they should also be present in the cold supernatant, yet the experiment shown in Fig. 6.6 show that the presence of cold supernatant does not enhance the ^{3}H–GTP content of a sample as the Test and Control curves were more or less superimposable.

The difference between the initial count rate of the Test and Control samples of Fig. 6.4(A) could also arise from a difference in the initial length distribution of the two microtubule populations. If the Test microtubules were shorter, they will be expected to incorporate more ^{3}H–GTP than the Control ones as the number of ends will be higher, provided that the length of the microtubules exceeds the magnitude of the excursions at the ends. This is likely to occur after addition of the cold supernatant to the samples, where shearing of the microtubules probably occurs upon mixing.

If there are proteins in the cold pellet that stabilise Glu microtubules preferentially, then they should also be present in the cold supernatant and they should have some effect on the resistance of Glu microtubules to nocodazole induced disassembly. Furthermore, as any stabilising agent present in the cold pellet is expected to be present in lower concentration in the cold supernatant, then the

stabilising effect incured by the cold pellet should be greater than the cold supernatant. The cold supernatant, from which the cold pellet originated, was also tested for stabilisation of Glu microtubules. At 5 μM nocodazole, the half-time for disassembly was 20 and 30 min. for the Test and the Control samples respectively [Fig. 6.5(B)]. Therefore, the cold supernatant seems to stabilise Glu microtubules against Nocodozole disassembly, but to a lesser extent than the cold pellet (half-life of 73 min), in agreement with the argument presented above. The half-life for end disappearance in the absence of any added proteins was estimated to be 30 and 34 min. in two separate experiments (Fig. 6.4 and 6.5), confirming the reproducibility of such experiments. At 10 μM nocodazole, disassembly of microtubules occurred rapidly, with a half-life of about 5 min. both in the presence and absence of the cold supernatant. This *in vitro* observation is in concordance with *in vivo* ones, where complete disassembly of the microtubule network in cultured MDCK cells, including the more stable detyrosinated ones, occurs at 33 μM nocodazole[116]. However, one important difference that one should be aware of is that the susceptibility to nocodazole of microtubules from non-neuronal cells might differ from that of microtubules from neuronal ones.

As nocodazole is causing microtubule disassembly at substoichiometric concentrations, then it must be working via an "end poisoning" mechanism. If the cold pellet does contain stabilising proteins then these probably, but not necessarily work by capping the ends of Glu microtubules and thus, prevent endwise disassembly. Khawaja *et al*[68] demonstrated that detyrosinated microtubules from cultured cells were resistant to nocodazole and dilution induced disassembly (both of which are end-wise mediated processes), but not to cold induced depolymerisation, which probably involves fractionation of a microtubule along its length prior to its disintegration and this suggests that disassembly of the microtubules occurs via a capping mechanism[88]. If the results obtained with the cold pellet reflect the true situation, then detyrosination could be regarded as a cause of microtubule stabilisation. However, tyrosinated microtubules can also be stabilised *in vivo*. Bre *et al*[18] showed

that after the disassembly of the microtubule network in MDCK cells by high nocodazole concentration, the first microtubules to regrow after recovery from the drug were tyrosinated and some of these microtubules were stable against moderate levels of nocodazole. Therefore, the combined results of Khawaja *et al* and Bre *et al* suggest that stabilisation of detyrosinated microtubules must involve a different mechanism than that utilised to stabilise the tyrosinated ones.

The results of Webster *et al*[146] whereby anti-TTL antibodies were microinjected into cultured cells to generate a detyrosinated microtubule network, that incorporated biotinylated tubulin at a rate similar to the bulk array of tyrosinated microtubules; does not really exclude the possibility that detyrosination causes microtubule stabilisation. It is possible that the limiting factor in this case is the cellular concentration of the stabilising agent, which might not necessarily increase upon depletion of the TTL molecules. These results therefore, merely confirm that detyrosination *per se* does not incur microtubule stabilisation.

In summary, preliminary results suggest that the first cold pellet might contain a protein(s) that is capable of stabilising detyrosinated microtubules. The results in this study however, are still at an early stage. Nevertheless, the cold pellet warrants further investigation in the search for a Glu microtubule specific stabilising protein.

Chapter 7

General Discussion

The study described in this thesis was undertaken to further advance the understanding of the mechanism(s) controlling microtubule function and assembly. In particular, the involvement of α-tubulin tyrosination has been examined. There could be various levels of control:

1) The transcription of the multiple tubulin isoforms and their subsequent post-translational modification.
2) The expression of associated proteins and their preferential interaction with specific tubulin isoforms.
3) The binding of other ligands such as Ca^{++}, Mg^{++}, GTP and ATP.

The complexity of the transcribed tubulin from brain and their subsequent modifications has been documented using a combination of IEF and immunostaining of Western blots (Chapter 1). Like other reports e.g [134], this study shows that twice cycled chick brain tubulin resolves into 8 α- and 12 β-tubulin variants on IEF gels, which had been modified to enable maximal resolution of the the protein bands (chapter 4). Immunostaining with YL 1/2, a monoclonal antibody specific for tyrosinated α-tubulin and 6-11-B-1, a monoclonal antibody specific for acetylated α-tubulin, showed that the resolved α-tubulin variants vary in their post-translational modification status, some being tyrosinated and acetylated, whilst others being tyrosinated and de-acetylated while two are both detyrosinated and acetylated (Table IV.I, chapter 4).

The IEF complexity observed for tubulin confirmed earlier suggestions that this heterogeneity cannot be accounted for solely by the expression of multi-tubulin genes. This increased complexity is likely to be generated by post-transational

modifications[43,134,140]. Direct demonstration that post-translational modifications contribute towards the IEF heterogeneity of tubulin has recently been demonstrated by Denoulet *et al*[36], using mouse neuronal cells cultured for two weeks. These cells were pulsed for 30 min. with ^{35}S-methionine and then chased with unlabelled methionine for up to 48 hours. Tubulin extracted from the cultured cells during the pulse and at different intervals during the chase, was separated by IEF and Coomassie staining of the gels showed the extracted tubulin to resolve into 6 α (α_1-α_6) and 9 β-variants (β_1-β_9). However, autoradiography of these gels showed that only α_1 (and possibly α_3), β_1, β_3, β_4 and β_6 had incorporated ^{35}S-methionine during the pulse indicating that they were transcriptionally derived and represented primary gene products. Moreover, the variants α_2-α_6 and β_2, β_5, β_7-β_9 appeared over a period of 48 hours during the chase indicating that they were post-translationally derived by chemical modifications of the primary tubulin gene products.

Tyrosination of α-tubulin can be ruled out as a contributor towards this increased IEF complexity (Chapter 4). Phosphorylation of α-tubulin on the C-terminus tyrosine and acetylation are likely candidates. Results in Chapter 4 showed that α_1,α_2 and α_4-tubulin were not acetylated on or near Lys-40 as judged by 6-11-B-1 immunostaining. This has recently been confirmed by fluorography of IEF gels of tubulin extracted from cultured mouse primary neurones incubated for 4 hours with ^{3}H-acetate, under conditions inhibiting protein synthesis, showed that only the variants α_3-α_8 incorporated the radiolabelled acetate, and that only these variants were reactive with 6-11-B-1[40]. Similarly, α_1,α_2 and α_4 were not modified when mouse tubulin was acetylated *in vitro* using ^{3}H-acetyl-CoA[40]. The similarity of the pattern of acetylation from chick and mouse tubulin, both *in vivo* and *in vitro*, further substantiates the remarkable conservation of tubulin and strongly indicates that acetylation is functionally important.

Finally, the recently characterised sequential glutamylation of α-tubulin at residue Glu-450 is a possible source of α-tubulin heterogeneity[41]. Progressive addition of glutamyl residues to α-tubulin will lead to progressive increase in the negatively charged residues of the tubulin, causing an acid shift of the modified protein during IEF.

The source of β-tubulin heterogeneity is more difficult to predict. Phosphorylation is the most obvious candidate for generating some of the observed isoform complexity and pre-digestion of tubulin with alkaline phosphatase prior to IEF showed a decrease in the complexity of β-tubulin and possibly of α-tubulin variants (chapter 4), indicating a possible contribution of this modification towards tubulin microheterogeneity.

It is difficult to establish whether this tubulin microheterogeneity is involved in the control of microtubule function or assembly. The arguments for and against a regulatory functional role have been presented in Chapter 1. The demonstration that the tubulin microheterogeneity is the same following two cycles of assembly (Chapter 4) confirms the previous report that all of the tubulin IEF variants can be utilised for polymerisation into microtubules[134]. This indicates that the microheterogeneity is either not involved in regulating microtubule assembly or that its effects are too subtle to be detected by such an assay.

One aspect of the α-tubulin heterogeneity phenomenon that was of particular interest is the tyrosination status of the α-tubulin isoforms. As presented in Chapter 3, α-tubulin was tyrosinated with a stoichiometry of about 0.5 mole.mole^{-1}, indicating that a fraction of α-tubulin did not act as a substrate for the *in vitro* purified TTL, in agreement to previous reports[10,113,114]. This sub-stoichiometric labelling by TTL was not due to the selective utilisation of specific α-tubulin IEF variants since IEF and immunostaining with YL1/2 demonstrated that all of the resolved α-tubulin isoforms were potentially tyrosinable (Chapter 4). This precluded the primary sequence of α-tubulin as the sole determinant of catalysis by TTL. A possible mechanism that might generate a TTL tubulin non-substrate is the existence

of certain β-isoform(s) incapable of binding to the enzyme. As the formation of a TTL/β-tubulin complex has been shown to be part of the α-tubulin tyrosination reaction mechanism[149], then clearly any β-tubulin isoform lacking the capability to bind TTL will result in the associated α-tubulin to be a non-substrate. Hence, certain α-/β-tubulin isoform combinations might be necessary for participation in the tyrosination reaction. It is interesting to note that about 50 % chick brain tubulin is non-tyrosinable and that the β-tubulin isotype cβ7 defines 50 % of the chick brain β-tubulin composition (D. Cleveland- personal communication). Furthermore, the reported magnitude of the non-tyrosinable fraction varies from as little as 15 % to as high as 55 % depending on developmental stage and differentiation (Chapter 3). This variation could be related to change in the complexity of the tubulin isoforms during development and differentiation. For example, in the chick brain mtp, the TTL non-substrate changes from 23 % in embryos to 55 % in adults. Moreover, the relative amounts of the IEF variants designated β4 and β6 (Fig. 4.2) have been shown to vary during development with β6 (which is less abundant than β4 in embryos) increasing in quantity (and becoming more abundant than β4) in adults[134]. The increased magnitude of the tubulin non-substrate during adulthood could therefore, be related to variation in the relative abundance of β4 and β6 or any of the other β-tubulin variants. Alternatively, a post-translational modification of β-tubulin on a site required for interaction with TTL might hinder the formation of a productive enzyme-substrate complex. Similarly, a post-translational modification on α-tubulin might serve a similar purpose. It will be particularly interesting to see whether detyrosinated but potentially tyrosinable tubulin that have been acetylated with TAT, could still be tyrosinated by TTL. It will also be interesting to see the effect of mutations in the β-tubulin genes on the magnitude of the TTL tubulin non-substrate pool.

It is interesting to note that a thorough examination of the chick β-tubulin amino acid sequences enables the classification of the encoded peptides into two classes, based on the identity of the amino acid residue at position 35, 57 and 124

(R.G.Burns, unpublished observation). The major brain β-tubulin isoform, cβ7, which comprises 50 % of the tubulin in whole brain extracts, has TGA as the amino acid residues at positions 35/57/124. Moreover, the other β-tubulin isoforms present in brain cβ1/cβ2 and cβ4 which comprise 25 % each of the tubulin in whole brain extracts have SNS and NHC as the residues at position 35/57/124 respectively. Therefore, a distinct class of β-tubulin exist in brain (cβ7) which comprises about 50 % of the β-tubulin, a value similar to the magnitude of tyrosinable α-tubulin in brain. There is no evidence that these three residues are involved in the binding of TTL, but if they are, then they offer a mechanism through which substoichiometric tyrosination could occur, in that only the α-tubulin(s) associated with cβ7 would get tyrosinated.

The dissociation constant for tubulin as measured at 4 °C is 0.8 x 10^{-6} M[39]. If the above argument is correct, then repeated cycles of *in vitro* tyrosination at 37 °C and cold dissociation on ice should enable an increase in the magnitude of the tyrosinable α-tubulin fraction through "shuffling" of the α- and β-tubulin isoforms at 4 °C. However, preliminary experiments whereby tubulin has been subjected to three cycles of tyrosination at 37 °C using TTL, with two cold incubations (at 4 °C) of the tyrosination mixture between the cycles of warm incubations, showed that no increase in the extent of tyrosination was observed. Therefore, under conditions which might permit "shuffling" of the α- and β-tubulin isoforms, no increase in the extent of α-tubulin tyrosination was obtained, possibly indicating that the β-tubulin primary sequence might not be related to the extent of α-tubulin tyrosination.

The question then emerges, is the observed stoichiometry of α-tubulin tyrosination by TTL an *in vitro* phenomenon or does it also occur *in vivo*. Certainly, estimates of the tubulin composition in mammalian cultured cells indicated that tyrosinated tubulin is the major constituent of α-tubulin in the free dimer pool[57]. Furthermore, microinjection of detyrosinated tubulin, tagged with a fluorescein derivative, into cultured mammalian cells, revealed that the tubulin was

fully tyrosinated prior to incorporation onto pre-existing microtubules[144]. This would suggest that the tyrosinating machinery in the cell is non-discriminatory, capable of modifying all of the available α-tubulin. This would indicate that the substoichiometric tyrosination of α-tubulin might be an *in vitro* phenomenon only, but how would such a phenomenon arise? One possibility is that the modifying enzyme TTL exists in two isoforms, each capable of tyrosinating a fraction (say 50 %) of α-tubulin *in vitro*, and one of these isoforms is lost or de-activated during the *in vitro* purification procedure. Indeed, in each TTL preparation performed in this study, a fraction comprising about half of the TTL activity eluted in the void of the Q-sepharose column (Chapter 3) and this was not due to the saturation of the column which has an available capacity of 110 mg.ml^{-1} at pH 8.0 (Ref. Ion Exchange Chromatography: principles and methods-Pharmacia publications). Similar observations were made when DEAE-cellulose was used instead of Q-sepharose. It is possible that the activity lost in the void during the TTL preparation represents a TTL isoform different than that binding to the column, and which is capable of tyrosinating the *in vitro* tubulin non-substrate fraction. Although the TTL preparation utilised by Schroder *et al*, which is prepared by one step immunoaffinity is also incapable of tyrosinating the whole of the α-tubulin pool *in vitro*[125], it does not invalidate the presented argument as the monoclonal antibody used in the immunoaffinity purification was raised against a protein purified in a similar procedure to the one described in Chapter 3 and therefore, would have only generated a single TTL isoform used for raising the monoclonal antibody. Whatever the source of the α-tubulin non-tyrosinable fraction *in vitro* is, no obvious function could be assigned to it.

Several *in vitro*[134] and *in vivo*[81] studies have shown that all of the tubulin isoforms available in a cell are assembly competent. However, there are no indications as to kinetics through which the individual tubulin variants assemble. Kinetic heterogeneity can be very important for the construction of functionally distinct microtubules. One particular variant of tubulin for which the assembly

kinetics have been examined both *in vitro* and *in vivo*, is the tyrosinated form of α-tubulin. *In vitro* studies showed that tyrosination has no effect on the assembly kinetics of twice cycled brain tubulin[77,111,103,112]. However, such studies relied mainly on bulk measurements of the microtubule population using turbidimetry and could only account for obvious differences in some of the kinetic parameters involved in the assembly of microtubules. The most extensive work on the effect of tyrosination on the *in vitro* kinetics of tubulin polymerisation, done by Kumar and Flavin, utilised three times polymerised tubulin that had been tyrosinated *in vitro* prior to chromatography on sephadex G-50 and phosphocellulose and ammonium sulphate precipitation[77]. Clearly, such a protein that has been subjected to so many purification steps might have lost its capacity for self-assembly. The core experiment in Kumar and Flavin's work which suggested similarity in the rate and extent of assembly of tyrosinated and detyrosinated tubulin was through the use of protein prepared as described above and induction of its assembly by the addition of purified MAPs. The results represented in their Fig. 2 show that no plateau in the turbidity was attained upon warming up the mixture for polymerisation, indicating that the increase in turbidity might be due to tubulin or MAP aggregation rather than tubulin polymerisation and therefore, any conclusions based on this experiment will always be questionable.

The aim of the experiments described in Chapter 5 was to settle the dilemma of kinetic differences between detyrosinated and tyrosinated α-tubulin. For this purpose, an *in vitro* test sensitive to variations in the assembly kinetic constants measured by turbidimetric analysis, and which are also sensitive to the kinetic parameters governed by dynamic instability was utilised. By monitoring the length re-distribution of detyrosinated and tyrosinated microtubules sheared at steady state, it was concluded that both populations of microtubules turnover with similar dynamics and that tyrosination has no influence on the assembly kinetics. But what kind of kinetic parameters were these experiments aimed at detecting? Like all proteins, the function of the tubulin subunit is dependent on the conformation it

adopts. Postingl *et al* suggested that a tyrosine at the C-terminus of α-tubulin would have an effect on the predicted secondary structure of that region, in that the helix potential of the C-terminus is decreased upon addition of the tyrosine[106]. Structural alteration in the C-terminus region might influence the conformation of the nearby N-terminal region of the β-tubulin subunit, the domain where the exchangeable GTP site is found[84]. This might then have an effect on the GTPase activity of the tubulin subunit. Hence, tyrosination might speed up the decapping of a tyrosinated microtubule, by speeding up GTP hydrolysis, causing it to be more dynamic than a detyrosinated one, thereby increasing the transition frequency between growing and shrinking phases.

The similar rates of length redistribution following shearing of microtubules tyrosinated to differing extents (Chapter 5), does not support the above possibility. The lack of any consistent difference strongly indicates that there is no substantial effect on the kinetics of GTP hydrolysis. The conclusions reached in chapter 5 are in agreement with previous *in vitro* work by Kumar and Flavin and also in agreement with recent work by Paturle *et al* whereby detyrosinated and tyrosinated tubulin were found to be kinetically equivalent[103]. These results are also in agreement with those of Skoufias *et al*[129] whereby the dynamic behaviour of the two microtubule populations was similar as judged by video enhanced dark field microscopy. Therefore, the work described in chapter 5 combined with previous and recent *in vitro* evidence, enables one to conclude that tyrosination of the α-tubulin does not alter the intrinsic assembly kinetics of tubulin and hence, does not offer any kinetic route through which microtubule assembly might be regulated. If tyrosination influences the behaviour of microtubules, it must do so through regulating the binding of MAPs or other ligands to the microtubule.

In vivo studies examining the dynamics of Glu and Tyr microtubules have generated results that conflict with those obtained *in vitro*. Glu tubulin was often found to be associated with stable assemblies of microtubules[54]. Furthermore,

microinjection of tagged tubulin into cultured cells has shown that the sinuous cytoplasmic Glu microtubule array was more resistant to tubulin incorporation, turning over with a half-life far greater than that observed for the bulk population[75,128,145]. Moreover, several studies have shown that the Glu microtubule array was more resistant to depolymerisation by anti-mitotic drugs and by dilution, than the bulk tyr microtubule network[17,20,55,68,75]. Furthermore, it was demonstrated that such enhanced stability was not an intrinsic property of the detyrosinated tubulin subunit itself[68].

To reconcile the kinetic results obtained *in vitro* with those obtained *in vivo*, one can argue that the enhanced stability of Glu microtubules *in vivo* is due to the binding of a stabiliser of these microtubules, conferring stability on them. Indeed, *in vitro* studies by Kumar and Flavin showed that microtubules assembled from tyrosinated tubulin, bound more MAP-2 (when added in sub-stoichiometric amounts) than those constructed from detyrosinated ones, while phosphorylated MAP2 was selectively excluded from binding to Tyr microtubules[77]. Therefore, preferential association of certain MAPs to a particular class of microtubules is known.

Search for a Glu-microtubule specific stabilising MAP was done using the cold stable pellet, rich in detyrosinated (R. Burgoyne-personal communication)and acetylated tubulin[70]. This pellet was extracted with calcium and the obtained proteins were used for an *in vitro* assay developed to test the susceptibility of detyrosinated microtubules against depolymerisation by nocodazole in the presence and absence of the extracted proteins. Results in Chapter 6 showed that stability of Glu microtubules could be induced *in vitro* in the presence of CP proteins and similar results were obtained with the cold supernatant although the stabilising effect was lower than that observed with the CP proteins. Therefore, it is possible that a Glu-microtubule specific MAP(s) might be present in the cold pellet.

How might such stabilising MAPs bind to Glu microtubules? First, they could bind uniformly along the length of the Glu microtubules and so stabilise them. This possibility is unlikely however, as it would require such stabilising proteins to be present in stoichiometric amounts to the tubulin. No protein was present on an SDS-PAGE gel in a proportion close to the intensity of the tubulin band (Fig. 6.1, Chapter 6). The second possibility is that a MAP might bind to the two ends of a microtubule, preventing endwise disassembly by nocodazole, with the "caps" preventing any loss or addition of subunits. One possible capping protein is that termed STOP (stable tubule only polypeptide) which has been shown to prevent subunit loss from microtubules due to cold temperature[89]. This protein stabilises microtubules against disassembly when present in extremely low concentrations, indicating that it might stabilise the microtubules by capping the ends. Capping structures have been visualised at the tips of most ciliary and flagellar microtubules, with the distal tips of both the central pair and outer doublet being attached to the flagellar membrane of *Chlamydomonas* and to ciliary membrane of *Tetrahymena* by the so-called central microtubule cap and the distal filaments, respectively[37]. Distal filaments, linked to ciliary membranes at their distal end, form at their proximal end a carrot-shaped structure which inserts into the lumen of the A-microtubule. This structure has been termed the distal filament plug, has been purified, and shown to consist of several polypeptides[135]. Capped cilia from bovine trachea do not nucleate microtubule assembly *in vitro* from their distal ends eventhough assembly was nucleated by uncapped or broken ones[38]. Recently, homology between kinetochore proteins and ciliary capping structures of *Tetrahymena thermophila* have been demonstrated based on cross-reactivity with CREST antisera, specific for kinetochore proteins[92]. Results from such study demonstrated the presence of at least one major kinetochore antigen in the ciliary microtubule capping structures, suggesting structural and functional homology between the two structures that bind to the plus end of microtubules.

Glu microtubules are often bent and have a curly morphology in the cytoplasm. One mechanism through which curled microtubules can be obtained is by subjecting a force along a straight microtubule attached at both ends to fixed structures. Hence, a Glu microtubule might be centrosomally capped at its (-) end and say capped by a membrane protein at its (+) end. Ankyrin, is one protein that might be involved in such a capping mechanism. This membrane protein has been previously shown to associate with microtubules *in vitro*[14] and it is possible that it might bind preferentially to detyrosinated microtubules. However, preliminary experiments performed during the course of this study (not shown) failed to detect any preferential association of ankyrin with detyrosinated microtubules as judged by SDS-PAGE. Nevertheless, conclusive evidence can only be obtained after determination of the binding constants of ankyrin to Glu and Tyr microtubules.

One argument against a capping mechanism specific for detyrosinated microtubules is that it would be "inefficient" or "metabolically wasteful" to detyrosinate a whole microtubule, while only the end subunits need to be modified in order to cap it. Furthermore, a capping protein such as distal filament plugs are generally inserted into the lumen of microtubules[37], whilst the C-terminus of α-tubulin protrudes from the wall of the microtubule.

Is detyrosination a cause or consequence of microtubule stabilisation? Many *in vivo* studies have correlated stability with detyrosination, but several examples of a stable subset of cytoplasmic microtubules that are tyrosinated are known[18,55]. However, this could be to an alternative mechanism for microtubule stabilisation such as binding of stabilising MAPs different from the Glu-tubulin specific ones.

Double immunofluorescence studies with 6-11-B-1 and a general anti-α-tubulin monoclonal antibody showed that a subset of microtubules in cultured mammalian cells, such as the 3T3 cell line, are acetylated and some of these microtubules, similar to detyrosinated ones have curly morphology[105]. Moreover, acetylation was

demonstrated to be a post-assembly process and acetylated microtubules were on the whole more resistant to depolymerisation by anti-mitotic drugs than the bulk array of cytoplasmic microtubules[105,20]. In contrast to detyrosinated microtubules, acetylated ones were also stable against cold disassembly[26]. Moreover, the staining pattern of acetylated microtubules with 6-11-B-1 was patchy, indicating that acetylation occurs only at distinct sites along a microtubule.

Cultured human fibroblasts, which contain little or no Glu microtubules, have regions of acetylated tubulin, which they term acetylated domains, at the ends (terminal domains) or along the length of acetylated microtubules[143]. Injection of biotinylated tubulin have shown that such domains are more resistant to incorporation of the tagged tubulin indicating that the acetylated regions turned over slowly. This compares with the finding in interphase TC-7 cells, that microtubules enriched in Glu tubulin coincide with those enriched with acetylated tubulin[20]. Similar results were reported by Schulze *et al* in human retinoblastoma cells[122]. Examination of the kinetics of reappearance of these two post-translational modifications, after release from nocodazole disassembly demonstrated that both modifications re-appeared post-assembly[20]. However, re-appearance of acetylated microtubules preceded that of detyrosinated ones, and the pattern of accumulation of each modification was distinct in that acetylation appeared in distinct sites along the length of microtubules, whilst detyrosination appeared uniformly along the length of the microtubules. This fits well with the recent demonstration that detyrosination in the cytoplasmic array of *T.brucei* occurs vectorially along the length of microtubules[123].

Having established the coincidence of acetylation and detyrosiantion in some cultured mammalian cells, one can envisage that two kinds of microtubule stability occur. Bre *et al* have shown that in cultured mammalian cells, after release from nocodazole disassembly, the first microtubules to regrow were tyrosinated and some of these were stable[18]. Therefore, if these growing Tyr microtubules were acetylated at certain domains (which might define TAT binding sites on a microtubule), and

certain acetyl tubulin specific MAPs were bound to these sites with the consequence of stabilising the microtubules long enough for the tubulin tyrosine carboxypeptidase to detyrosinate the microtubules, then any Glu-tubulin specific MAPs might then bind to provide for example long term stability for this microtubules.

An alternative possibility is that, detyrosination may not be related to stability, but that stabilisation by acetylation allows detyrosination which might be needed for another purpose. For instance, it was argued previously that microtubules with curly morphology might arise by subjecting a microtubule attached to fixed structures at its two ends to a force along their length. This could happen for instance during organelle transport along the length of a microtubule by a microtubule motor. Indeed, movement of kinesin along centrosomally nucleated microtubules *in vitro* produces kinks[61]. It is interesting to note that after wounding of a 3T3 cultured monolayer, the cell rapidly generates a stable array of detyrosinated (and some tyrosinated) microtubules oriented towards the direction of cell migration (*ie* the direction of applied wound)[55]. The presence of tyrosinated stable microtubules is indicative of a recent stabilisation event and the orientation of the bulk stable microtubule array, which is mainly detyrosinated, might indicate active transport of organelles/vesicles towards the leading edge of migrating cells (corresponding to anterograde movement). Furthermore, co-localisation of acetylated microtubules with detyrosinated ones has been demonstrated in axons of rat cerebellum[25], a region where much transport activity is expected to take place.

Finally, both acetylation and detyrosination might be involved in microtubule stabilisation through a cross-linking mechanism. If one for instance considers a MAP that binds to a tubule and projects an arm-like process upon binding, and if one assumes that the arm like projection can bind preferentially to acetylated tubulin, then such a MAP can cross-link two acetylated/detyrosinated microtubules by attaching its main body to detyrosinated subunits of one microtubule and its arm like projections to the acetylated sites of the other microtubule. This fits well with the

observed patch pattern of acetylation along a microtubule where the acetylated regions might represent specific attachment sites for a MAP projection. Co-localisation of acetylated and detyrosinated microtubules has not been demonstrated in chick neurones. However, the immunostaining results described in Chapter 4 show co-localisation of detyrosination and acetylation in two of the α-tubulin isoforms and whether this is a reflection on the specificity of the enzyme tubulin acetylase remains to be determined.

If detyrosination is not involved in regulating microtubule assembly or stability what other regulatory aspects could it be involved in? Tyrosination could regulate microtubule assembly via a second post-translational modification which would not have been detected by the current experiments. For instance, Wandosell *et al* have shown that tyrosinated α-tubulin can be phosphorylated on the C-terminus tyrosine moeity, by the insulin receptor kinase and such modification resulted in the blockage of polymerisation of the modified moiety[141]. Certainly, if such modification was operational *in vivo*, it would account for some of the observed heterogeneity of the α-tubulin isoforms, and would offer a regulatory mechanism controlling the assembly of tyrosinated tubulin *in vivo*.

Calcium ions regulate the assembly of microtubules by causing depolymerisation of the assembled polymer[155]. The calcium binding site has been allocated to the C-terminus of tubulin as removal of 1 Kd (6-8 residues) of the C-terminus of the α- and β-tubulin subunits by carboxypeptidase Y treatment relieves the calcium inhibitory effect. It is possible that the mere removal of the C-terminus tyrosine might influence the calcium induced disassembly[138]. However, results by Paturle *et al*, comparing the calcium disassembly of detyrosinated and tyrosinated microtubules *in vitro* and preliminary results obtained in this study show that tyrosination has no influence on the rate or extent of calcium induced depolymerisation[103].

Tyrosination could also be responsible for regulation of microtubule assembly with nucleotides other than GTP. Tubulin has a weak binding site for ATP on the α–subunit[156,157]. Burns and Islam have shown that tubulin can assemble *in vitro* with ATP into microtubules and filaments that are not seen with GTP induced assembly[24]. The assembly induced by ATP was not due to the regeneration of depleted GTP by the NDP kinase activity. Furthermore, the fraction of tubulin that is assembly competent with ATP, was only about 20–35 % of that obtained with GTP and this is of the same magnitude of the tyrosinated tubulin fraction obtained upon preparation of twice cycled mtp from chick brain by cycles of temperature dependent polymerisation and depolymerisation. Moreover, CPA digestion of the mtp prior to assembly with ATP prevents the formation of any microtubules. This would suggest that tyrosination might serve as a mechanism for selective assembly with ATP *in vivo*. In fact, the intracellular ATP concentration in neuronal tissue (1–2 mM) is sufficient to assemble the estimated 50 % tyrosinated tubulin present in chick brain as the *in vitro* ATP concentration needed to induce the assembly of the 20–35 % tyrosinated fraction was 20 μM[24]. If such assembly occurs *in vivo*, then it would provide a mechanism, other than post-polymerisation detyrosination, for the construction of tyrosinated and detyrosinated microtubules. It should be noted that the detyrosinating enzyme can act on dimeric tubulin as well as polymeric form of tubulin[3].

In summary, *in vitro* and *in vivo* experiments have demonstrated that both Glu and Tyr tubulin are assembly competent. However, *in vitro* experiments have demonstrated that detyrosination (and acetylation) is correlated but not required for microtubule stability. This study has confirmed the lack of any effect of tyrosination on the *in vitro* kinetics of microtubules and has shown that Glu microtubule stability can be enhanced by the addition of cold supernatant or extracted cold pellet proteins.

What kind of *in vitro* work could further the understanding of the role of the role of α–tubulin tyrosination on the function of microtubules?

Certainly, the results obtained with the CP proteins are worth further investigation. One could for instance try and isolate the stabilising agent present in the cold pellet and characterise it. One approach would be to fractionate the extracted CP proteins by gel filtration and characterise the protein peak containing the stabilising activity. Moreover, now that it is possible to obtain fully tyrosinated and detyrosinated tubulin by YL 1/2 immunochromatography, such tubulin can be used to construct microtubules (at least by taxol assembly), which can then be used for the isolation of any MAPs specific for the tyrosinated or detyrosinated forms. One approach would be to use microtubule affinity chromatography using Glu and Tyr microtubules to isolate any MAPs specific for either form from crude brain extracts. Such an approach has been successfully used recently by Kellogg *et al*[67] to isolate MAPs from cytoplasmic extracts of *Drosophilla* embryos and to raise individual polyclonal antibodies that specifically recognise 25 of these proteins. If Glu tubulin specific MAPs were found using such an approach, then one could raise antibodies against such MAPs and investigate their distribution *in vitro*.

Microtubule binding proteins such as ankyrin and other MAPs probably warrant further investigation. Particularly, the strength of binding of such proteins to Glu and Tyr microtubules would enable deductions about specific associations of any of these MAPs with a particular subset of microtubules. Methods such as the one recently developed by Azhar *et al*[9] utilising iodinated MAPs to determine the dissociation constant for MAP–2–microtubule interaction, can be used for such analysis.

Moreover, it is probably worth estimating the strength of ATP binding to Tyr and Glu tubulin to determine whether detyrosination induces a conformational change that prevents the binding of ATP to the α–tubulin subunit. Finally, it will be interesting to monitor the kinetics of assembly of tubulin samples with various proportions of

acetylation and detyrosination to determine the combined effect of both modifications on the *in vitro* dynamics of microtubules.

We are still far from understanding the role of the tyrosination/detyrosination cycle in the functional regulation of microtubules. However, the scope for future work should further advance our understanding of the role of this modification.

References

1) Alonso, C.A., Arce, C.A. & Barra, H.S. (1988) **Eur. J. Biochem.** 177, 517-522.

2) Arai, T. & Matsumoto, G. (1988) J. **Neurochem.** 51, 1825-1838.

3) Arce, C.A. & Barra, H.S. (1985) **Biochem. J.** 226, 311-317.

4) Arce, C.A. & Barra, H.S. (1983) **FEBS Lett.** 157, 75-78.

5) Arce, C.A., Hallak, M.E., Rodriguez, J.A., Barra, H.S. & Caputto, R. (1977) J. Neurochem. 31, 205-210.

6) Argarana, C.E., Barra, H.S and Caputto, R. (1980) J. **Neurochem,** 34, 114-118.

7) Argarana, C.E., Barra, H.S. and Caputto, R. (1981) J. **Biol. Chem.** 236, 827-830.

8) Avila, J., Diaz-Nido, J., Wandosell, F., Hargreaves, A., Hernandez, M.A. & Serrano, L. (1988) in **Structure and Functions of the Cytoskeleton, Rousset, B.A.F. editor,** 171, 439-445.

9) Azhar, S., Rho, M.B., Wallis, K.T & Murphy, D.B. (1988) J. **Cell. Biol.** 107, 460 a.

10) Barra, H.S., Arce, C.A. & Argarana, C.E. (1988) **Molec. Neurobiol.** 2, 133-153.

11) Barra, H.S., Arce, C.A., Rodriguez, J.A. & Caputo,R. J. Neurochem. 21: 1241-1251.

12) Barra, H.S. & Argarana, C.E. (1982) Biochem. Biophys. Res. Comm. 108, 654-657.

13) Barra, H.S., Rodriguez, J.A., Arce, C.A. & Caputto, R. (1973a) J. Neurochem. 20 97-108.

14) Bennet, V., Davis, J. and Fowler, W.E. (1982) Phil. Trans. Roy. Soc. Lon. 299, 301-312.

15) Berhadsky, A.D. & Vasiliev, J.M. (1988) Cytoskeleton, Plenum Press.

16) Borisy, G.G. & Burgen, L.G. (1982) Methods in Cell Biol. 24 A, 171-187.

17) Bre, M.H. & Karsenti, E. (1988), Cell Motil. & the Cytoskel. (in press).

18) Bre, M.H., Kreis, T.H. & Karsenti, E. (1987) J. Cell Biol. 105, 1283-1296.

19) Brinkley, B.R., Cox, S.H., Pepper, D.A., Wible, L., Brenner, S.L. & Pardue, R.L. (1981) J. Cell Biol. 90, 554-562.

20) Bulinski, J.C., Richards, J.E. & Pipperno, G. (1988) J. Cell Biol. 106, 1213-1220.

21) Burgoyne, R.D., Cambray-Deakin, M.A., Lewis, S.A., Sarker, S. & Cowan, N.J. (1988) EMBO J. 7, 2311-2319.

22) Burns, R.G., ChownSmith, L. & McInnes, C. (1986) J. Cell Biol. 103, 131a.

23) Burns, R.G. & Islam, K. (1984) **Eur. Journal Biochem.** 141, 599–608.

24) Burns, R.G. & Islam, K. (1986) **Annal. New York Acad. of Sci.** 466, 340–356.

25) Cambray–Deakin, M.A. and Burgoyne, R.D. (1987), J. Cell Biol. 104, 1569–1574.

26) Cambray–Deakin, M.A., Robson, S.J. & Burgoyne, R.D. (1988) **Cell Motil. and the Cytoskel.** 10 438–449.

27) Carlier, M.F. & Pantaloni, D. (1981) **Biochem.** 20, 1918–1924.

28) Chang, S. & Flavin, M. (1988) **Cell Motil. and the Cytoskel.**, 10, 400–409.

29) Cleveland, D.W. (1987) **J. Cell Biol.**, 381–383.

30) Cleveland, D.W. & Sullivan, K.F. (1988) **Ann. Rev. Biochem** 54, 331–365.

31) Correia, J.J, Baty, L.T., Williams, R.C. (1987) J. Biol. Chem. 262, 17278–17284.

32) Cowan, N.J., Lewis, S.A, Gu, W. & Burgoyne, R.D. (1988) **Protoplasma** 145, 106–111.

33) Creigton, T.E. **Proteins: Structure and Molecular Properties.**

34) Dahl, J.L. & Weibel, V.J. (1979) **Biochem. & Biophys. Res. Comm.** 86, 822–828.

35) De-Brabander, M.J., Van de Veire, R.M.L., Aerts, F.E.M., Borgers, M. & Jansen, P.A.J. (1976) **Cancer Research** 36, **905-916.**

36) Denoulet, Ph., Edde, B., Pinto-Henrique, D., Koulakoff, A., Berwald-Netter, Y. & Gros, F. (1988) **in Structure and Functions of the Cytoskeleton** (Rousset, B.A.F editor) **Colloque Inserm** 171, **231-237.**

37) Dentler, W.L. (1980) **J. Cell Sci.** 42, **207-220.**

38) Dentler, W.L. (1986) **J. Cell Biol.** 103, **279 a.**

39) Detrich, W.H. & Williams, R.C. (1978) **Biochemistry** 17 **3900-3906.**

40) Edde, B., Denoulet, P., de-Nechaud, B, Koulakoff, A., Berwald-Netter, Y. & Gross, F. (1988) **Biology of the Cell** 65, **109-117.**

41) Edde, B., Rossier, J., Le Caer, J.P., Desbruyeres, E., Gross, F. & Denoulet, P. **Science** 247, **83-85** (1989).

42) Farrell, K.W., Jordan, M.A., Miller, H.P. & Wilson, L. (1987) **J. Cell Biol.** 104, **1035-1046.**

43) Field, D.J., Collins, R.A. & Lee, J.C. (1984) **Proc. Natl. Acad. Sci. USA** 81, **4041-4045.**

44) Flavin, M. & Murofushi, H. (1984) **Methods in Enzymol.** 106, **223-237.**

45) Fulton, C. & Simpson, A. (1976) **Cell motility** Book C (Goldman/Pollard/Rosenbaum editors) **Cold Spring Harbour, 987-1005.**

46) Gard, D.L. & Kirschner, M.W. (1985) J. Cell Biol. 100, 764-774.

47) Gaskin, F. (1982) Methods in Enzymol. 85, 433-439.

48) George, H.J., Misra, L., Field, D., & Lee, J.C. (1981) Proc. Natl. Acad. Sci. USA 20, 2402-2409.

49) Geunes, G., Gundersen, G., Nuydens, R., Cornelissen, F., Bulinski, J.C. & DeBrabender, M. (1986) J. Cell Biol. 103, 1883-1893.

50) Gibbons, I.R. (1989) J. Biol. Chem. 263, 15837-15840.

51) Ginzburg, I & Littauer, U.Z. (1988) Protoplasma 145, 140-144.

52) Gozes, I & Littauer, U.Z. (1978) Nature 276, 411-413.

53) Gull, K., Wilcox, M., Birkett, C.R. (1987) FEBS Lett. 219, 31-36.

54) Gundersen, G.G. & Bulinski, J.C. (1986) Eur. J. Cell Biol. 42, 288-294.

55) Gundersen, G.G. & Bulinski, J.C. (1988) Proc. Nat. Acad. Sci. USA 85, 5946-5950.

56) Gundersen, G.G., Kalnoski, M.H. & Bulinski, J.C. (1984) Cell 38, 779-789.

57) Gundersen, G.G., Khawaja, S. & Bulinski, J.C. (1987) J. Cell Biol. 105, 251-264.

58) Hartree, E.F. (1972) Anal. Biochem. 48, 422-427.

59) Havercroft, J.C. & Cleveland, D.W. (1984) J. Cell Biol. 99, 1927-1935.

60) Hirokawa, N., Shiomura, Y. & Okabe, S. (1988) J. Cell Biol. 107, 1449-1459.

61) Hollenbeck, P.J. (1988) Protoplasma 145, 145-152.

62) Horio, T. & Hotani, H. (1986) Nature 321, 605-607.

63) Horwitz, S.B., Lothstein, L., Manfredi, J.J., Mellado, W., Parness, J., Roy, S.N., Schiff, P.B., Sorbara, L. & Zeheb, R. (1986) Dynamic Aspects of Microtubule Biology (David Soiffer editor), Annal. of the New York Acad. of Sci. 466, 733-744.

64) Johnson, K.A. & Borisy, G.G. (1977) J. Mol. Biol. 117 1-31.

65) Joshi, H.C., De Brabander, M., Geuens, G. & Cleveland, D.W. (1989) J. Cell Biol. 109, 337 a.

66) Karsenti, E., Kobayashi, S., Mitchison, T. & Kirschner, M. (1984) J. Cell Biol. 98, 1763-1776.

67) Kellogg, D.R., Field, C.M. & Alberts, B.M. (1989) J. Cell Biol. 109, 2977-2992.

68) Khawaja, S., Gundersen, G.G. & Bulinski, J.C. (1988) J. Cell Biol. 106, 141-149.

69) Kilmartin, J.V., Wright, B. & Milstein, C. (1982) J. Cell Biol. 93, 576-582.

70) Kim, H. & Binder, L.I. (1988) J. Cell Biol. 107, 24 a.

71) Kimmel, B.E., Samson, S., Wu, J., Hirschberg, R. & Yarbrough, L.R. (1985) Gene 35, 237-248.

72) Kirschner, K. & Mandelkow, E.M. (1985) EMBO Journal 4, 2397-2402.

73) Kirschner, M. & Mitchison, T. (1986) Cell 45, 329-342.

74) Kobayashi, T. & Flavin, M. (1981) Comp. Biochem. Physiol. 69 B, 387-392.

75) Kreis, T.E. (1987) EMBO J. 6, 2597-2606.

76) Kumar, N. & Flavin, M. (1981) J. Biological Chem. 256, 7678-7686.

77) Kumar, N. & Flavin, M. (1982) Eur. J. Biochem. 128, 215-222.

78) Le Dizet, M , Piperno, G. (1987) Proc. Nat. Acad. Sci. USA 84, 5720-5724.

79) Lee, M.K., Rebhun, L.I. & Frankfurter, A. (1989) J. Cell Biol. 109, 338 a.

80) Lee, J., Field, D.J. & Lee, Y.L.L (1980) Biochem. 19, 6209-6215.

81) Lewis, S.A., Gu, W. & Cowan, N.J. (1987) Cell 49, 539-548.

82) Lewis, S.A., Wang, D. & Cowan, N.J. (1988) Science 242 936-939.

83) L'Hernault, S.W. & Rosenbaum, J.L. (1983) J. Cell Biol. 97, 258-263.

84) Linse, K. & Mandelkow, E.M. (1988) J. Biol. Chem. 263, 15205-15210.

85) Lueduena, R.F. (1979) in Microtubules (Roberts, K. & Hyams J.S. editors) 65-116.

86) Luduena, R.F., Anderson, W.H., Prasad, V, Jordan, M.A. & Fellous, A. (1986) Dynamic Aspects of Microtubule Biology (David Soiffer editor), Annal. of the New York Acad. of Sci. 466, 718-732.

87) Maccioni, R.B., Rivas, C.I. & Vera, C.J. (1988) EMBO Journal 7, 1957-1963.

88) Mandelkow, E.M. & Mandelkow, E.R. (1985) J. Molec. Biol. 181, 123-125.

89) Margolis, R.L., Job, D., Pabion, M., Rauch, C.T. (1986) Dynamic Aspects of Microtubule Biology (David Soiffer editor), Annal. of the New York Acad. of Sci. 466, 306-321.

90) Margolis, R.L. & Wilson, L. (1981) Nature 293, 705-711.

91) Maruta, H., Greer, K. & Rosenbaum, J.L. (1986) J.Cell Biol 103 571-579.

92) Miller, J.M., Wang, W. & Dentler, W.L. (1987) J. Cell Biol. 107 29 a.

93) Mitchison, T.J. (1988) Ann. Rev. Cell Biol. 4, 527-549.

94) Mitchison, T.J. (1989) J. Cell Biol. 109, 637-652.

95) Mitchison, T.J. & Kirschner, M. (1984) Nature 312, 232-237.

96) Mitchison, T.J. & Kirschner, M. (1984) Nature 312, 237-241.

97) Moura-Neto, V., Mallet, M., Jeantet, C. & Prochiantz, A. (1983), EMBO J. 2, 1243-1248.

98) Murphy, D.B. (1987) Protoplasma 145, 176-181.

99) Murphy, D.B., Wallis, K.T. & Grasser, W.A. (1984) in Molecular Biology of the Cytoskeleton (Borisy, G.G., Cleveland, D.W. & Murphy, D.B. edditors) 59-70.

100) Murofushi, H. (1980) J. Biochem. 87, 979-984.

101) Oakley, C.E. & Oakley, B.R. (1989) Nature 338, 662-664.

102) Otey, C.A., Kalonski, M.H. & Bulinski, J.C. (1986) Anal. Biochem. 157, 71-76.

103) Paturle, L., Wehland, J., Margolis, R.L. & Job, D. (1989) Biochemistry 28, 2698-2704.

104) Piperno, G. & Fuller, M.T. (1985) J. Cell Biol. 101, 2085-2094.

105) Piperno, G., Le Dizet, M. & Chang, X. J. (1987) J. Cell Biol. 104, 289-302.

106) Postingl, H., Little, M., Krauhs, E. & Kampf, T. (1979), Nature 282, 423-424.

107) Pratt, L.F., Okamura, S. & Cleveland, D.W. (1987) Molec. and Cell. Biol. (1987) 7, 552-555.

108) Pratt, L.F. & Cleveland, D.W. (1988) EMBO Journal 7, 931-940.

109) Prescott, A., Foster, K.E., Warn, R.M. & Gull, K. (1989) J. Cell Sci. 92, 595–605.

110) Raff, E. C. (1984) J. Cell Biol. 99, 1–10.

111) Raybin, D. & Flavin, M. (1975) Biochem. Biophys. Res. Comm. 65, 1088–1095.

112) Raybin, D. & Flavin, M. (1977) J. Cell Biol. 73, 492–504.

113) Robinson, A.R. (1974) Proc. Nat. Acad. Sci. USA 71, 885–887.

114) Rodriguez, A.J. & Borisy, G.G. (1978) Biochem. Biophys. Res. Comm. 83, 579–586.

115) Rothwell, S.W., Grasser, W.A. & Murphy, D.B. (1985) J. Cell Biol. 102, 619–627.

116) Sackett, D.L. & Wolff, J. (1986) J. Biol Chem. 261, 9070–9076.

117) Sasse, R., Glyn, N.C.P., Birkett, C.R. & Gull, K. (1987) J. Cell Biol. 104, 41–49.

118) Sasse, R. & Gull, K. (1988) J. Cell Sci. 90, 577–589.

119) Serrano, L., De La-Torre, J., Maccioni, R.B. & Avila, J. (1984) Proc. nat. Acad. Sci. USA 81, 5989–5993.

120) Serrano, L., Diaz-Nido, J., Wandosell, F. & Avila, J. (1987) J. Cell Biol. 105, 1731–1739.

121) Schneider, A., Sherwin, T., Sasse, R., Russel, G. & Gull, K. (1987) J. Cell Biol. 104, 431–438.

122) Schulze, E., Asai, D.J., Bulinski, J.C. & Kirschner, M. (1987) J. Cell Biol. 105, 2167–2177.

123) Sherwin, T. & Gull, K. (1989) Cell 57, 211–221.

124) Sherwin, T., Schneider, A., Sasse, R., Seebeck, T. & Gull, K. (1987) J. Cell Biol. 104, 439–446.

125) Schroder, H.C., Wehland, J. & Weber, K. (1985) J. Cell Biol. 100, 276–281.

126) Schulze, E. & Kirschner, M. (1987) J. Cell Biol. 104, 277–288.

127) Schulze, E. & Kirschner, M. (1986) J. Cell Biol. 102, 1020–1031.

128) Silflow, C.D. & Rosenbaum, J.L. (1985) Molec. and Cell. Biol. 5, 2389–2397.

129) Skoufias, D.A., Farrell, K., Matsumoto, B. & Wilson, L. (1989) J. Cell Biol. 109, 342 a.

130) L'Hernault, S.W. & Rosenbaum, J.L. (1985) J. Cell Biol. 100, 457–462.

131) Sullivan, K.F. (1988) Ann. Rev. Cell Biol. 4, 687–716.

132) Sullivan, K.F. & Cleveland, D.W. (1986) Proc. Nat. Acad. Sci. USA 83, 4327–4331.

133) Sullivan, K.F., Machlin, P.S., Ratrie, H. & Cleveland, D.W. (1986) J. Biol. Chem. 261, 13317-13322.

134) Sullivan, K.F. & Wilson, L. (1984) J. Neurochem. 42, 1363-1371.

135) Supernant, K.A. & Dentler, W.L. (1986) J. Cell Biol. 103, 133 a.

136) Thompson, W.C. (1980) Methods in Cell Biol. 24 A, 235-253.

137) Thompson, W.C., Deanin, G.G. & Gordon, M.W. (1979) Proc. Nat. Acad. Sci. USA 76, 1318-1322.

138) Towbin, H., Staehlin, T. & Gordon, J. (1979) Proc. Nat. Acad. Sci. USA 76,4350-4354.

139) Vera, J.C., Rivas, C.I. & Maccioni, R.B. (1989) Biochemistry 28, 333-339.

140) von Hungen, K.V. Chin, R.C. & Baxter, C.F. (1981) J. Neurochem. 37, 511-514.

141) Wandosell, F., Serrano, L. & Avila, J. (1987) J. Biol. Chem. 262, 8268-8273.

142) Wandosell, F., Serrano, L., Hernandez, M.A. & Avila, J. (1986) J. Biol. Chem. 261, 10332-10339.

143) Webster, D.R. & Borisy, G.G. (1989) J. Cell Sci. 92, 57-65.

144) Webster, D.R., Gundersen, G.G., Bulinski, J.C. & Borisy, G.G. (1987) J. Cell Biol. 105, 265-276.

145) Webster, D.R., Gundersen, G.G., Bulinski, J.C. & Borisy, G.G. (1987) Proc. Nat. Acad. Sci. USA 84, 9040–9044.

146) Webster, D.R., Wehland, J., Weber, K. & Borisy, G.G. (1988) J. Cell Biol. 107, 24 a.

147) Wehland, J., Schroder, H.C. & Weber, K. (1986) Annal. New York Acad. Sci. USA 466, 609–621.

148) Wehland, J. & Weber, K. (1987) J. Cell Biol. 88, 185–203.

149) Wehland, J. & Weber, K. (1987) J. Cell Biol. 104, 1059–1067.

150) Wehland, J., Willingham, M.C. & Sandovell, I.V. (1983) J. Cell Biol. 97, 1467–1475.

151) Weisenberg, R.C. (1986) Dynamic Aspects of Microtubule Biology (David Soiffer editor), Annal. of the New York Acad. of Sci. 466, 543–551.

152) Wiche, G. (1989) Biochem. Journal 259, 1–12.

153) Wilson, L., Bradford–Snyder, K. & Thompson, W.C. (1980) Methods in Cell Biol. 24 A, 160–169.

154) Wilson, L. & Farrell, K.W. (1986) Dynamic Aspects of Microtubule Biology (David Soiffer editor), Annal. of the New York Acad. of Sci. 466, 690–708.

155) Wolff, J. (1988) in Structure and Function of the Cytoskeleton (Rousset, B.A.F editor) Colloque Inserm 171, 477–490.

156) Zabrecky, J.R. & Cole, R.D. (1982) **Nature** 296, 757-759.

157) Zabrecky, J.R. & Cole, R.D. (1983) **Arch. Biochem. Biophys.** 225, 475-481.

Abbreviations

MEM buffer: see Chapter 2

MM buffer: see Chapter 2

RB buffer : Runing Buffer (see Chapter 3)

SDS-PAGE : Sodium Dodecyl Sulphate PolyAcrylamide Gel Electrophoresis

IEF : Iso-electric Focusing.

MES : (2[N-morpholino]ethanesulphonic acid)

DTT : DL- Dithiothreitol

TEMED : N,N,N',N'- Tetramethyl-ethylenediamine

PEP : phosphoenol pyruvate

ATP : Adenosine triphosphate

GTP : Guanosine triphosphate

CP : Cold Pellet (see Chapter 6)

TTL : Tubulin Tyrosine Ligase

STOP : Stable Tubule only polypeptide.